Madelung deformity

Peymani, A.

Publication date
2021
Document Version
Final published version

ISBN 978-94-93197-68-8

MADELUNG DEFORMITY

ABBAS PEYMANI

MADELUNG DEFORMITY

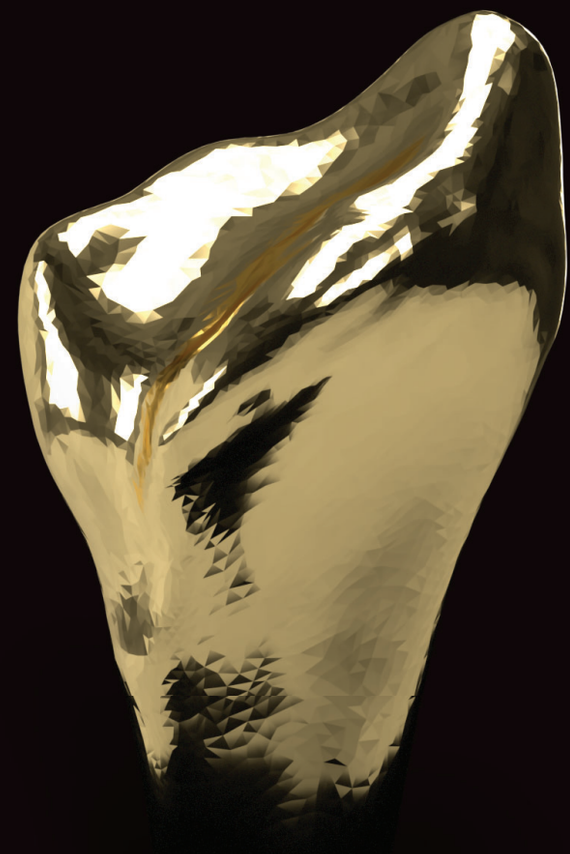

ABBAS PEYMANI

MADELUNG DEFORMITY

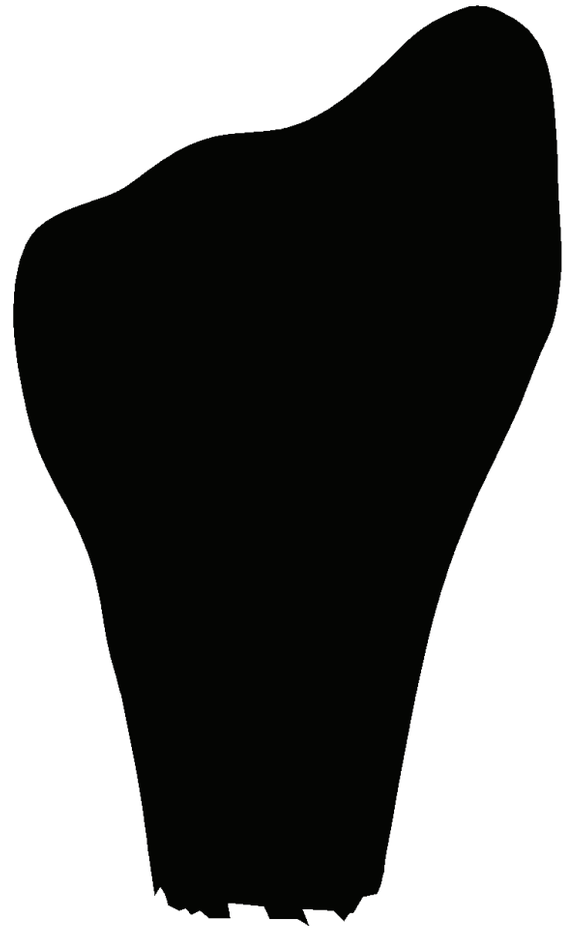

ABBAS PEYMANI

MADELUNG DEFORMITY

Abbas Peymani

This thesis was prepared at the Amsterdam University Medical Center, University of Amsterdam, Amsterdam, The Netherlands. The author received the AMC PhD Scholarship 2017 from the Amsterdam University Medical Center supporting this research.

ISBN
978-94-93197-68-8

WEBSITE
www.madelungdeformity.com

COVER DESIGN AND THESIS LAY-OUT
Abbas Peymani

PRINTED BY
Off Page, Amsterdam

MADELUNG DEFORMITY

ACADEMISCH PROEFSCHRIFT

ter verkrijging van de graad van doctor
aan de Universiteit van Amsterdam
op gezag van de Rector Magnificus
prof. dr. ir. K.I.J. Maex

ten overstaan van een door het College voor Promoties ingestelde commissie,
in het openbaar te verdedigen in de Agnietenkapel
op donderdag 27 mei 2021, te 10.00 uur

door

Abbas Peymani
geboren te Gouda

PROMOTIECOMMISSIE

Promotor:	prof. dr. C.M.A.M. van der Horst	AMC-UvA
Copromotores:	dr. S.D. Strackee	AMC-UvA
	dr. ir. G.J. Streekstra	AMC-UvA
Overige leden:	prof. dr. M. Maas	AMC-UvA
	prof. dr. G.M.M.J. Kerkhoffs	AMC-UvA
	dr. M.H.M. van Doesburg	AMC-UvA
	dr. M. Foumani	Martiniziekenhuis Groningen
	prof. dr. F. Nollet	AMC-UvA
	prof. dr. H.E.J. Veeger	TU Delft
	dr. J.W. Colaris	Erasmus MC

Faculteit der Geneeskunde

"You must love and be kind to everybody,
care for the poor,
protect the weak,
heal the sick,
teach and educate the ignorant."

- 'Abdu'l-Bahá

TABLE OF CONTENTS

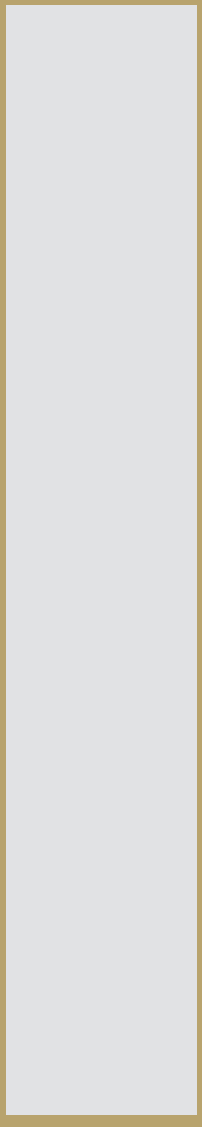

GENERAL INTRODUCTION

1

INTRODUCTION AND SCOPE OF THIS THESIS

The hand is one of the most sophisticated pieces of natural engineering in the human body. Refined through millennia of evolution, it is our most crucial anatomical apparatus, with no other species on this earth having such a vast portion of the brain dedicated to its control.[1] From the time we first grip the fingers of our delivering obstetrician or loving parent, our hands are used for exploration and control. As we progress through life, its purpose beyond mere survival becomes evident, contributing to our thriving as a species through the generation of art, literature, music, and as a versatile tool to convey our most inner thoughts and emotions.[2,3] From within, the interplay of anatomical structures is both intricate and fascinating. Unfortunately, as with any complex system, sometimes, something goes wrong.

SKELETAL ANATOMY

The skeletal anatomy of the hand can be divided into three anatomical regions: the phalanges on the distal end, the metacarpals in the middle, and the wrist on the proximal side. While the phalanges and metacarpals allow for precision grasping and translocation of objects, the wrist augments their freedom of movement along three axes. The wrist consists of the carpus and the forearm's distal bones (Figure 1), which give rise to various joints in-between. In turn, the carpus consists of eight carpal bones, roughly aligned in two rows: (1) the proximal carpal row, encompassing the scaphoid, lunate, triquetral and pisiform bones; and (2) the distal carpal row, encompassing the trapezium, trapezoid, capitate, and hamate bones.[4,5]

The two bones of the forearm, the radius and the ulna, form two fundamentally crucial wrist joints on the distal end: (1) the radiocarpal joint, capacitating the articulation between the distal forearm and the proximal carpal row; and (2) the radioulnar joint, capacitating the articulation between the radius and the ulna.[6] The radiocarpal joint contributes to the performance of various wrist movements: flexion, extension, radial deviation, ulnar deviation, and dart-throwing motion.[7,8] The radioulnar joint expands on this by enabling the radius to rotate around the ulna, providing a pivot for the underarm's pronation and supination.[9,10] In addition to the osteology and joints as described here, the skeletal anatomy of the wrist is heavily supported by its ligamentous counterpart, often divided into the extrinsic wrist ligaments, intrinsic wrist ligaments, and the triangular fibrocartilagenous complex (TFCC).[11-13] It is the biomechanical interaction between

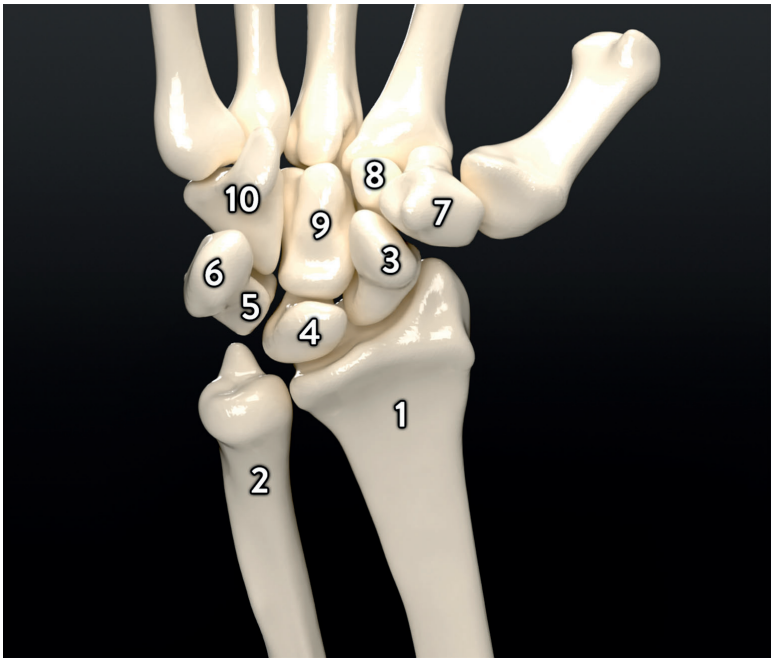

Figure 1. Wrist bones: (1) radius, (2) ulna, (3) scaphoid, (4) lunate, (5) triquetral, (6) pisiform, (7) trapezium, (8) trapezoid, (9) capitate, and (10) hamate.

the aforementioned anatomical structures that not only enables the comprehensive functionality as seen in the human hand, but allows us to do so in an optimized fashion by augmenting the balance between strength, stability, and mobility.

EMBRYOLOGY

Before the unfolding of the structures as described in the previous paragraph, the upper limb undergoes a perplexing developmental process. From a molecular point-of-view, the stakeholders of this embryological process include a mix of proteins, receptors, and transcription factors, which, to this day, are subject to extensive scientific research in regard to both morphogenesis and timing.[14] As will be evident from the next paragraphs, upper limb development in human embryogenesis mainly occurs between weeks four and eight. These weeks define a critical period, where any deviations from the normal developmental pattern could have devastating consequences and result in congenital upper limb anomalies.[15]

Around three weeks after initial embryonic fertilization, the notochord expresses the sonic hedgehog (SHH) protein, which on day 26 initiates upper limb development through the formation of the limb bud: an outgrowth of lateral plate and somatic mesoderm into the overlying ectoderm.[16] Lateral plate mesoderm gives rise to the bones, cartilage, and tendons; somatic mesodermal cells form the vessels, nerves, and muscles.[17] Mesenchymal cells that originate from this mesoderm differentiate into either chondrocytes that form cartilage in endochondral skeletal elements or osteoblasts that form bone in membranous skeletal elements. All bones in the upper limb are endochondral except the distal phalanges, which are membranous.[16]

On day 31, the first axial blood vessels appear, starting with the marginal vein and giving rise to the subclavian-axillary-brachial axis's arterial vessels with lymphatic vessels following closely.[18] On day 36, upper limb chondrification ensues, nerve trunks start entering the arm, and joint development commences through the repression of chondrogenesis at future joint sites; the first joints form proximally at the shoulder and the last joints develop distally at the hand.[19] Around eight weeks, the development of joints, muscles, nerves, and the vascular system finally comes to an end. During this same period, the humerus and the tips of the distal phalanges are ossified, with ossification of other bones occurring in a later stage from a proximal to distal direction.[19] In addition to this step-wise chronological approach, wrist development can be classified using patterning mechanisms through the three spatial axes of development: proximodistal, anteroposterior, and dorsoventral; with their key regulators being fibroblast growth factor (FGF), SHH, and the Engrailed-1 (EN-1) genes respectively.[20]

ANOMALOUS DEVELOPMENT

Alterations in developmental pathways, genes, or gene regulators can produce a variety of upper limb anomalies. These congenital anomalies can be categorized to distinguish malformations, deformations, and dysplasia. A malformation is an abnormal formation, a deformation is an abnormality caused after normal formation, and dysplasia is an abnormality in the size, shape, and organization of cells within a tissue.[21] In turn, malformations can and are increasingly being

subclassified based on their respective axis of formation and differentiation, using the well-adopted Oberg-Manske-Tonkin (OMT) classification framework.[22,23] Nevertheless, this 'demarcation' is not flawless as the axes of limb development are dependent on each other, with a failure in one axis often leading to multiaxial pathologies.[16]

Several population and registry database studies have aimed to shine light on the epidemiology of congenital upper limb anomalies.[24-26] It has been estimated that over 2000 children per year are born in the United States with congenital hand differences, resulting in lifelong impacts on patients' physical functioning, mental health, and social wellbeing.[27] Therefore, it is of paramount importance to maximize our scientific research efforts, not only to increase our arsenal of medical knowledge to provide viable solutions to affected children but also to understand the impact on patients' lives. This is a challenging endeavor due to both the nature of congenital hand differences and the complexities of collaborative data collection, especially for rare conditions where low patient numbers have severely hindered the potential for conclusive research. One of these extremely rare congenital hand differences is known as the enigmatic 'Madelung deformity'.

MADELUNG DEFORMITY

Madelung deformity is named after the distinguished German surgeon Otto Wilhelm Madelung, who was the first to present and publish his findings in 1878.[28,29] Since x-ray imaging would not be discovered until years later, the first published images of the deformity were drawn by hand (Figure 2).[28,30] Madelung deformity's incidence and prevalence are unknown, and our most recent estimate is from a 1994 study that investigated 1476 pediatric hand patients, estimating the subgroup prevalence of Madelung deformity to be around 1.7% in the context of congenital hand anomalies.[31] This rarity is also reflected in the scarcity of published medical literature, with the overwhelming majority of studies including less than 20 patients.[29]

Classically, the skeletal deformity is characterized by a bowing of the radius, an ulnar and volar tilt of the distal radius, a triangular arrangement of the proximal carpal bones, and a relatively long ulna (Figure 3).[29,32] It is hypothesized that a distal radial epiphyseal growth arrest causes these abnormalities.[33] Interestingly, each patient's anatomical configuration can be unique since the deformity is increasingly progressive, and the skeletal abnormalities can present on a broad spectrum.[34] Clinical and imaging studies have also highlighted the existence of two soft-tissue anomalies: an anomalously thickened radiolunate ligament (also known as Vickers ligament) and the recently discovered radiotriquetral ligament.[35-38] However, it is still unclear whether these ligaments are present in all Madelung deformity cases or only in a specific subset. Often, the deformity is caused by mutations of the short stature homeobox (SHOX) gene,[34,39,40] coding for a transcription factor that plays an important role in bone growth and maturation. Madelung deformity typically presents bilaterally with a female predominance, and genetic associations have been found particularly with Leri-Weill dyschondrosteosis and Turner syndrome.[41-43] Although initially asymptomatic, its progressive symptoms become evident in early adolescence and could include pain, limited range of motion, decreased grip strength, and aesthetic hindrances.[44,45] In the diagnostic workup, the progressive symptomatology is normally combined with x-ray

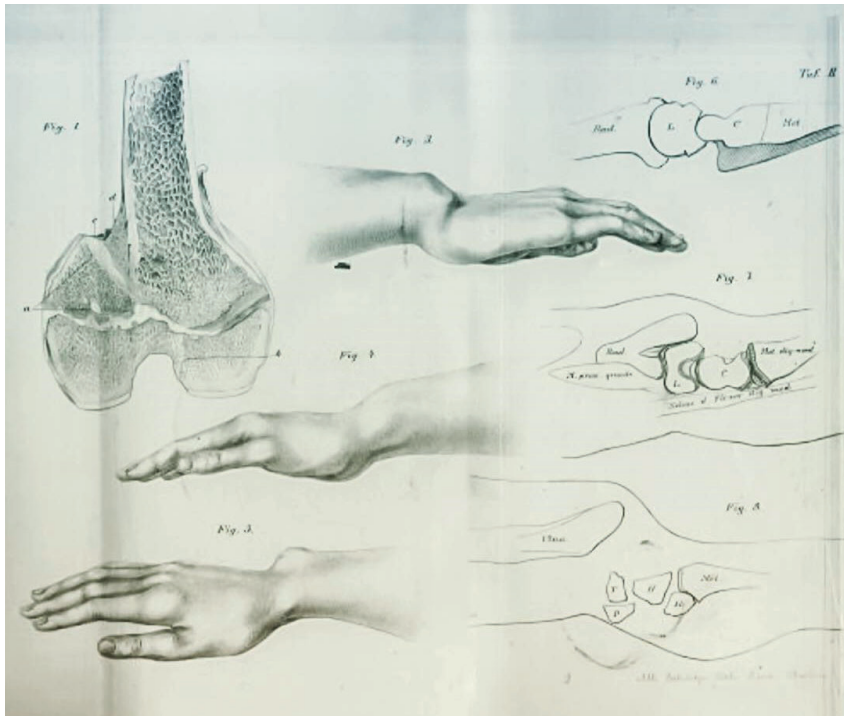

Figure 2. The first hand-drawn images of Madelung deformity, published in 1878 by Otto Wilhelm Madelung.

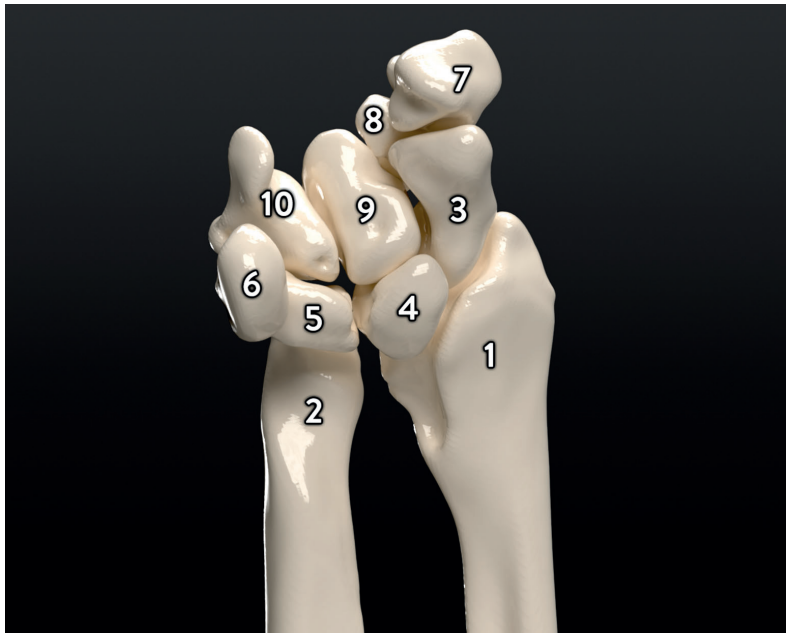

Figure 3. Wrist bones of a Madelung deformity patient: (1) radius, (2) ulna, (3) scaphoid, (4) lunate, (5) triquetrum, (6) pisiform, (7) trapezium, (8) trapezoideum, (9) capitatum, and (10) hamatum.

imaging, on which several parameters are quantified based on radiographic criteria.[46] Despite these criteria having revolutionized our diagnostic assessment, the process remains suboptimal due to considerable overlap between measurement results of patient wrists and healthy wrists[47] and our inability to accurately and reliably diagnose mildly deformed cases.[48] This is unfortunate since the conditions progressive nature is not only with respect to the degree of skeletal deformity but also with the associated life-altering symptomatology.[49] Detecting the condition at its early stages would allow for prompt surgical intervention, limiting the progression to more severe levels of deformity. Classically, surgical treatment is centered around osteotomies of the radius and/or ulna, the aim being to restore the deformed distal radius angles and to harmonize the lengths of radius and ulna.[49,50] In parallel, surgeons often perform a release of the anomalous ligaments as these are thought to contribute to the pathophysiological process and symptoms.[36,38] While Madelung deformity surgeries have been performed since the mid-1800s, a gold standard for treatment has yet to be determined.[29]

IMAGING MODALITIES

After the invaluable first steps of thorough history taking and an extensive hand and wrist examination, clinicians regularly utilize medical imaging to advance their understanding of a patient's problem. Since the first radiograph, the hand and wrist have been the subject of medical imaging, with one of the first published images by Wilhelm Conrad Roentgen being an image of his wife's hand.[51] The diagnostic process usually starts (and often ends) with conventional x-ray imaging, producing two-dimensional (2D) representations of three-dimensional (3D) anatomy to visualize the situation within. The classic 'hand series' radiographs consist of three projections: posteroanterior (PA), oblique, and the lateral view (Figure 4).

As the density of bones allows the absorption of relatively large amounts of high energy electromagnetic radiation, x-rays are well suited to view and assess bone fractures, bone injuries, and joint abnormalities. However, since the 2D information resulting from x-ray imaging is prone to the overlapping of anatomical features, its diagnostic accuracy in regard to sensitivity and specificity can be limited for certain wrist conditions.[52,53] Clinicians can, therefore, request computed tomography (CT) imaging, generating cross-sectional images reconstructed from x-ray attenuation measurements. This enables a 3D assessment of the wrist and, after segmentation, a visualization of bone models in 3D space (Figure 5).

While x-ray and CT imaging are mostly utilized to assess skeletal anatomy, magnetic resonance imaging (MRI) is generally applied to visualize relevant soft tissues in the wrist.[54] Using magnetic fields and radio waves instead of ionizing radiation, MRI can be used to accurately evaluate the pathology of tendons, ligaments, and cartilage (Figure 6).[55] Through the visualization of internal structures, these imaging modalities can help the clinician understand a patient's problem and determine a diagnosis. Wrist imaging is also being increasingly used in the pre-operative surgical planning process, peri-operative assessment, and as a way to track the post-operative course. Especially CT imaging has proven to be useful in pre-operative planning, not only aiding the surgeon in the decision-making process but also to personalize the surgery to a patient's anatomy by the design and 3D-printing of cutting guides, reduction guides, and most recently

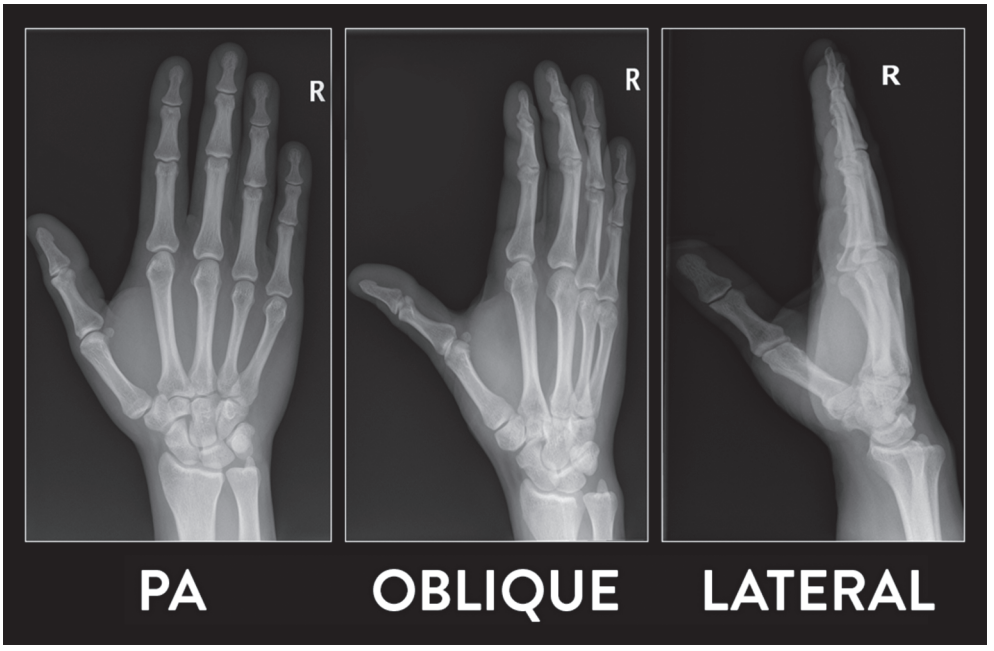

Figure 4. Routine radiographic hand series showing the posteroanterior (PA), oblique, and the lateral view. Case courtesy of Dr. Craig Hacking, Radiopaedia.org.

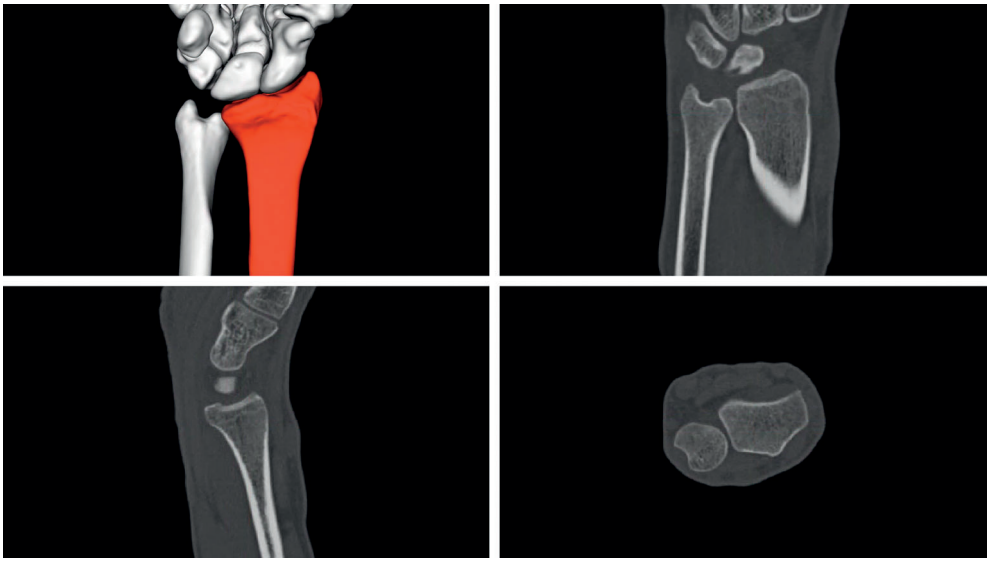

Figure 5. CT scan of the wrist showing slices in the coronal (top right), sagittal (bottom left), and axial (bottom right) planes. A 3D representation can be visualized after segmentation (top left).

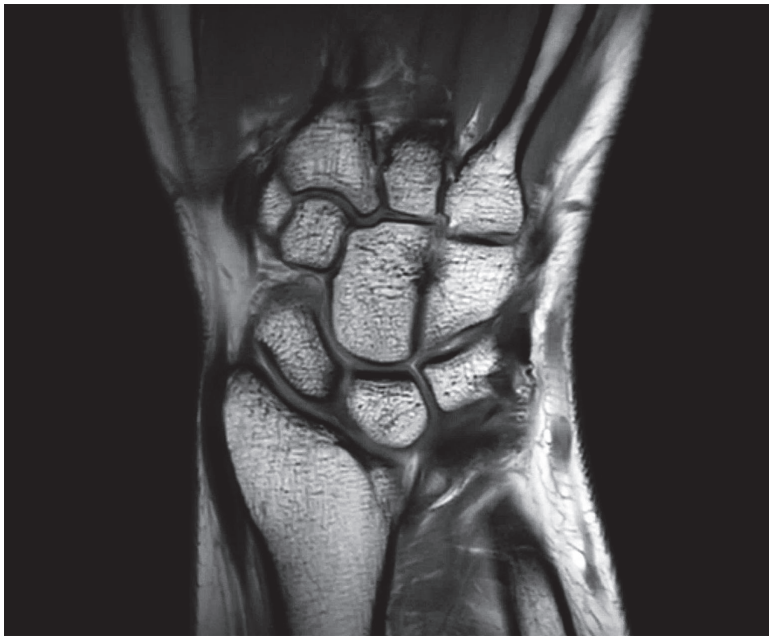

Figure 6. MRI imaging of the wrist.

even the custom plate used for fixation of bony segments.[56-58] Through further evolvement of our imaging modalities and software tools, it is now possible to track wrist movement by performing continuous CT scans of the wrist during motion using four-dimensional (4D) CT imaging.[59-61] The latter technique has proven to be feasible in assessing both joint cartilage thickness and carpal bone kinematics.[62,63]

THE SCOPE OF THIS THESIS

Nearly 200 years after Otto Wilhelm Madelung first published his findings, many questions have remained unanswered in regard to definition, anatomical findings, symptomatology, etiology, diagnostics, and optimal surgical approach of Madelung deformity. Is it because our current knowledge sources are based on small-powered studies? Or the fact that an overwhelming majority of clinical studies still resort to primitive 2D imaging methods to analyze a complex 3D problem? In medicine, it has been the field of medical imaging that has most prominently reaped the benefits of technological advancements.[64] Therefore, it might be advantageous to apply our modern and updated arsenal of imaging modalities to remove some of the mysteries surrounding Madelung deformity.

We start this journey in **Chapter 2** by evaluating the current body of literature on Madelung deformity to identify all diagnostic criteria, indication criteria, available surgical treatment options, and clinical outcomes. Based on our findings, we propose a reporting protocol for the workup

of new patients and prospective studies, hopefully increasing the quality of evidence in future research to compensate for the small patient numbers.

Given the rarity of the condition and little known about the patient perspective, we present a study design in **Chapter 3** to evaluate patient outcomes by harnessing the global reach of social media. Using the universal Patient-Reported Outcomes Measure Information System (PROMIS), a cross-sectional survey is conducted to assess Madelung deformity's clinical spectrum and its impact on physical, mental, and social health aspects.

After gaining insights into the current state of affairs, we aim to evolve our approach by engaging three innovative methodologies in Madelung deformity imaging: 3D quantifications, 4D kinematics, and statistical analyses of shape. **Chapter 4** describes our very first experiences with these three concepts. An in-depth overview is provided of our methodology and calculations for determining cartilage thickness and articular surface area of the wrist joints. In addition, a relatively simple and reproducible method is introduced for the quantification of 3D anatomical shapes. Each of these newly introduced concepts will be further developed and applied to wrists of Madelung deformity patients, serving as the foundation of the next three chapters.

In **Chapter 5**, we implement a 3D approach to Madelung deformity. The applicability of current 2D criteria is investigated, and multiple new 3D parameters are developed to automatically quantify the wrist, removing inter- and intra-rater differences in the process. We speculate that these new parameters could expand our anatomical understanding.

Both skeletal and soft tissue abnormalities have been described in Madelung deformity. To understand the effects of these changes on the radiocarpal joint, we biomechanically assess patients' wrists using 4D CT imaging in **Chapter 6**. Carpal kinematics are visualized and quantified, articular surface areas are determined, and radiocarpal cartilage thickness levels are calculated. These computations are done in both patients and healthy volunteers to assess any relevant differences.

In **Chapter 7**, we develop a 3D statistical shape model, a computer-generated model that encodes all anatomical shape information, to investigate shape characteristics and variations in the distal radius of patients. Based on shape differences, we attempt to develop a classification and investigate the efficacy of shape information for use in diagnostic predictive models.

Combining our findings from the previous three chapters, we introduce a novel surgical approach in **Chapter 8**. This corrective surgical technique is explained and compared to the 'classic' osteotomy. Utilizing the protocol introduced in the 2nd chapter, we report and compare clinical and functional outcomes.

In summary, this thesis has the following specific aims:

- Chapter 2: evaluate our current knowledge of Madelung deformity and reveal the steps used in the patient workup.
- Chapter 3: provide insights into patient characteristics and gain an understanding of the burden that patients carry.
- Chapter 4: develop computational quantifications of the wrist through 3D imaging, 4D imaging, and shape analysis.
- Chapter 5: perform a 3D analysis of Madelung deformity's anatomy by re-evaluating previous 2D-based parameters and developing new 3D-based parameters.
- Chapter 6: investigate the biomechanical effects of the abnormal anatomy on carpal bone mobility and wrist joints.
- Chapter 7: analyze all the information in the distal radial shape using a computer-generated model and use the ensuing quantifications in diagnostics.
- Chapter 8: describe a new surgical technique and compare outcomes with the 'classic' treatment option.

REFERENCES

1. Catani M. A little man of some importance. ***Brain.*** 2017;140(11):3055-3061.
2. Morgan MH, Carrier DR. Protective buttressing of the human fist and the evolution of hominin hands. ***J Exp Biol.*** 2013;216(Pt 2):236-244.
3. Schwarz RJ, Taylor C. The anatomy and mechanics of the human hand. ***Artificial limbs.*** 1955;2(2):22-35.
4. Behnke RS. ***Kinetic anatomy.*** Human Kinetics 1; 2006.
5. Lewis OJ, Hamshere RJ, Bucknill TM. The anatomy of the wrist joint. ***J Anat.*** 1970;106(Pt 3):539-552.
6. Milch H. So-Called Dislocation of the Lower End of the Ulna. ***Ann Surg.*** 1942;116(2):282-292.
7. Sarrafian SK, Melamed JL, Goshgarian GM. Study of wrist motion in flexion and extension. ***Clin Orthop Relat Res.*** 1977(126):153-159.
8. Wolfe SW, Crisco JJ, Orr CM, Marzke MW. The dart-throwing motion of the wrist: is it unique to humans? ***J Hand Surg Am.*** 2006;31(9):1429-1437.
9. Almquist EE. Evolution of the distal radioulnar joint. ***Clin Orthop Relat Res.*** 1992(275):5-13.
10. Wolfe SW, Pederson WC, Hotchkiss RN, Kozin SH, Cohen MS. ***Green's operative hand surgery: the pediatric hand E-book.*** Elsevier Health Sciences; 2010.
11. Taleisnik J. The ligaments of the wrist. ***J Hand Surg Am.*** 1976;1(2):110-118.
12. Berger RA. The anatomy of the ligaments of the wrist and distal radioulnar joints. ***Clin Orthop Relat Res.*** 2001(383):32-40.
13. Leversedge FJ, Goldfarb CA, Boyer MI. ***A pocketbook Manual of hand and upper extremity anatomy: Primus manus.*** Lippincott Williams & Wilkins; 2010.
14. Hita-Contreras F, Martinez-Amat A, Ortiz R, et al. Development and morphogenesis of human wrist joint during embryonic and early fetal period. ***J Anat.*** 2012;220(6):580-590.
15. Seiler JG, Hurley R, Lazar T, Wang T. ***Essentials of hand surgery.*** Lippincott Williams & Wilkins; 2002.
16. Al-Qattan MM, Yang Y, Kozin SH. Embryology of the upper limb. ***J Hand Surg Am.*** 2009;34(7):1340-1350.
17. Daluiski A, Yi SE, Lyons KM. The molecular control of upper extremity development: implications for congenital hand anomalies. ***J Hand Surg Am.*** 2001;26(1):8-22.
18. Zaleske DJ. Development of the upper limb. ***Hand Clin.*** 1985;1(3):383-390.
19. Al-Qattan MM, Kozin SH. Update on embryology of the upper limb. ***J Hand Surg Am.*** 2013;38(9):1835-1844.
20. Cole P, Kaufman Y, Hatef DA, Hollier LH, Jr. Embryology of the hand and upper extremity. ***J Craniofac Surg.*** 2009;20(4):992-995.
21. Oberg KC, Feenstra JM, Manske PR, Tonkin MA. Developmental biology and classification of congenital anomalies of the hand and upper extremity. ***J Hand Surg Am.*** 2010;35(12):2066-2076.
22. Tonkin MA, Tolerton SK, Quick TJ, et al. Classification of congenital anomalies of the hand and upper limb: development and assessment of a new system. ***J Hand Surg Am.*** 2013;38(9):1845-1853.
23. Goldfarb CA, Ezaki M, Wall LB, Lam WL, Oberg KC. The Oberg-Manske-Tonkin (OMT) Classification of Congenital Upper Extremities: Update for 2020. ***J Hand Surg Am.*** 2020.

24. Goldfarb CA, Wall LB, Bohn DC, Moen P, Van Heest AE. Epidemiology of congenital upper limb anomalies in a midwest United States population: an assessment using the Oberg, Manske, and Tonkin classification. ***J Hand Surg Am.*** 2015;40(1):127-132 e121-122.

25. Giele H, Giele C, Bower C, Allison M. The incidence and epidemiology of congenital upper limb anomalies: a total population study. ***J Hand Surg Am.*** 2001;26(4):628-634.

26. Ekblom AG, Laurell T, Arner M. Epidemiology of congenital upper limb anomalies in 562 children born in 1997 to 2007: a total population study from stockholm, sweden. ***J Hand Surg Am.*** 2010;35(11):1742-1754.

27. Franzblau LE, Chung KC, Carlozzi N, Chin AY, Nellans KW, Waljee JF. Coping with congenital hand differences. ***Plast Reconstr Surg.*** 2015;135(4):1067-1075.

28. Madelung O. Die spontane Subluxation der Hand nach vorne. ***Verh Dtsch Ges Chir.*** 1878;7:259-276.

29. Arora AS, Chung KC. Otto W. Madelung and the recognition of Madelung's deformity. ***J Hand Surg Am.*** 2006;31(2):177-182.

30. Spiegel PK. The first clinical X-ray made in America--100 years. ***AJR Am J Roentgenol.*** 1995;164(1):241-243.

31. Flatt AE. ***The care of congenital hand anomalies.*** Quality Medical Publishing; 1994.

32. Harley BJ, Carter PR, Ezaki M. Volar surgical correction of Madelung's deformity. ***Tech Hand Up Extrem Surg.*** 2002;6(1):30-35.

33. Anton JI, Reitz GB, Spiegel MB. Madelung's Deformity. ***Ann Surg.*** 1938;108(3):411-439.

34. Zebala LP, Manske PR, Goldfarb CA. Madelung's deformity: a spectrum of presentation. ***J Hand Surg Am.*** 2007;32(9):1393-1401.

35. Cook PA, Yu JS, Wiand W, et al. Madelung deformity in skeletally immature patients: morphologic assessment using radiography, CT, and MRI. ***J Comput Assist Tomogr.*** 1996;20(4):505-511.

36. Vickers D, Nielsen G. Madelung deformity: surgical prophylaxis (physiolysis) during the late growth period by resection of the dyschondrosteosis lesion. ***J Hand Surg Br.*** 1992;17(4):401-407.

37. Stehling C, Langer M, Nassenstein I, Bachmann R, Heindel W, Vieth V. High resolution 3.0 Tesla MR imaging findings in patients with bilateral Madelung's deformity. ***Surg Radiol Anat.*** 2009;31(7):551-557.

38. Hanson TJ, Murthy NS, Shin AY, Kakar S, Collins MS. MRI appearance of the anomalous volar radiotriquetral ligament in true Madelung deformity. ***Skeletal Radiol.*** 2019;48(6):915-918.

39. Rappold GA, Fukami M, Niesler B, et al. Deletions of the homeobox gene SHOX (short stature homeobox) are an important cause of growth failure in children with short stature. ***J Clin Endocrinol Metab.*** 2002;87(3):1402-1406.

40. Herdman RC, Langer LO, Good RA. Dyschondrosteosis. The most common cause of Madelung's deformity. ***J Pediatr.*** 1966;68(3):432-441.

41. Nielsen JB. Madelung's deformity. A follow-up study of 26 cases and a review of the literature. ***Acta Orthop Scand.*** 1977;48(4):379-384.

42. Clement-Jones M, Schiller S, Rao E, et al. The short stature homeobox gene SHOX is involved in skeletal abnormalities in Turner syndrome. ***Hum Mol Genet.*** 2000;9(5):695-702.

43. Belin V, Cusin V, Viot G, et al. SHOX mutations in dyschondrosteosis (Leri-Weill syndrome). ***Nat Genet.*** 1998;19(1):67-69.

44. dos Reis FB, Katchburian MV, Faloppa F, Albertoni WM, Laredo Filho J, Jr. Osteotomy of the radius and ulna for the Madelung deformity. ***J Bone Joint Surg Br.*** 1998;80(5):817-824.

45. Houshian S, Schroder HA, Weeth R. Correction of Madelung's deformity by the Ilizarov technique. ***J Bone Joint Surg Br.*** 2004;86(4):536-540.

46. McCarroll HR, Jr., James MA, Newmeyer WL, 3rd, Molitor F, Manske PR. Madelung's deformity: quantitative assessment of x-ray deformity. ***J Hand Surg Am.*** 2005;30(6):1211-1220.

47. McCarroll HR, James MA, Newmeyer WL, 3rd, Manske PR. Madelung's deformity: quantitative radiographic comparison with normal wrists. ***J Hand Surg Eur Vol.*** 2008;33(5):632-635.

48. Farr S, Guitton TG, Ring D, Science of Variation G. How Reliable is the Radiographic Diagnosis of Mild Madelung Deformity? ***J Wrist Surg.*** 2018;7(3):227-231.

49. Kozin SH, Zlotolow DA. Madelung Deformity. ***J Hand Surg Am.*** 2015;40(10):2090-2098.

50. Ali S, Kaplan S, Kaufman T, Fenerty S, Kozin S, Zlotolow DA. Madelung deformity and Madelung-type deformities: a review of the clinical and radiological characteristics. ***Pediatr Radiol.*** 2015;45(12):1856-1863.

51. Wilson AJ, Mann FA, Gilula LA. Imaging the hand and wrist. ***J Hand Surg Br.*** 1990;15(2):153-167.

52. Balci A, Basara I, Cekdemir EY, et al. Wrist fractures: sensitivity of radiography, prevalence, and patterns in MDCT. ***Emerg Radiol.*** 2015;22(3):251-256.

53. Jorgsholm P, Thomsen NO, Besjakov J, Abrahamsson SO, Bjorkman A. The benefit of magnetic resonance imaging for patients with posttraumatic radial wrist tenderness. ***J Hand Surg Am.*** 2013;38(1):29-33.

54. Fotiadou A, Patel A, Morgan T, Karantanas AH. Wrist injuries in young adults: the diagnostic impact of CT and MRI. ***Eur J Radiol.*** 2011;77(2):235-239.

55. Berquist TH. Imaging of articular pathology: MRI, CT, arthrography. ***Clin Anat.*** 1997;10(1):1-13.

56. Dobbe JG, Kievit AJ, Schafroth MU, Blankevoort L, Streekstra GJ. Evaluation of a CT-based technique to measure the transfer accuracy of a virtually planned osteotomy. ***Med Eng Phys.*** 2014;36(8):1081-1087.

57. Dobbe JG, Vroemen JC, Strackee SD, Streekstra GJ. Patient-specific distal radius locking plate for fixation and accurate 3D positioning in corrective osteotomy. ***Strategies Trauma Limb Reconstr.*** 2014;9(3):179-183.

58. Dobbe JG, Vroemen JC, Strackee SD, Streekstra GJ. Patient-tailored plate for bone fixation and accurate 3D positioning in corrective osteotomy. ***Med Biol Eng Comput.*** 2013;51(1-2):19-27.

59. Leng S, Zhao K, Qu M, An KN, Berger R, McCollough CH. Dynamic CT technique for assessment of wrist joint instabilities. ***Med Phys.*** 2011;38 Suppl 1:S50.

60. Tay SC, Primak AN, Fletcher JG, et al. Four-dimensional computed tomographic imaging in the wrist: proof of feasibility in a cadaveric model. ***Skeletal Radiol.*** 2007;36(12):1163-1169.

61. Carelsen B, Bakker NH, Strackee SD, et al. 4D rotational x-ray imaging of wrist joint dynamic motion. ***Med Phys.*** 2005;32(9):2771-2776.

62. Foumani M, Strackee SD, Jonges R, et al. In-vivo three-dimensional carpal bone kinematics during flexion-extension and radio-ulnar deviation of the wrist: Dynamic motion versus step-wise static wrist positions. ***J Biomech.*** 2009;42(16):2664-2671.

63. Foumani M, Strackee SD, van de Giessen M, Jonges R, Blankevoort L, Streekstra GJ. In-vivo dynamic and static three-dimensional joint space distance maps for assessment of cartilage thickness in the radiocarpal joint. ***Clin Biomech (Bristol, Avon).*** 2013;28(2):151-156.

64. Laal M. Innovation process in medical imaging. ***Procedia-Social and Behavioral Sciences.*** 2013;81(0):60-64.

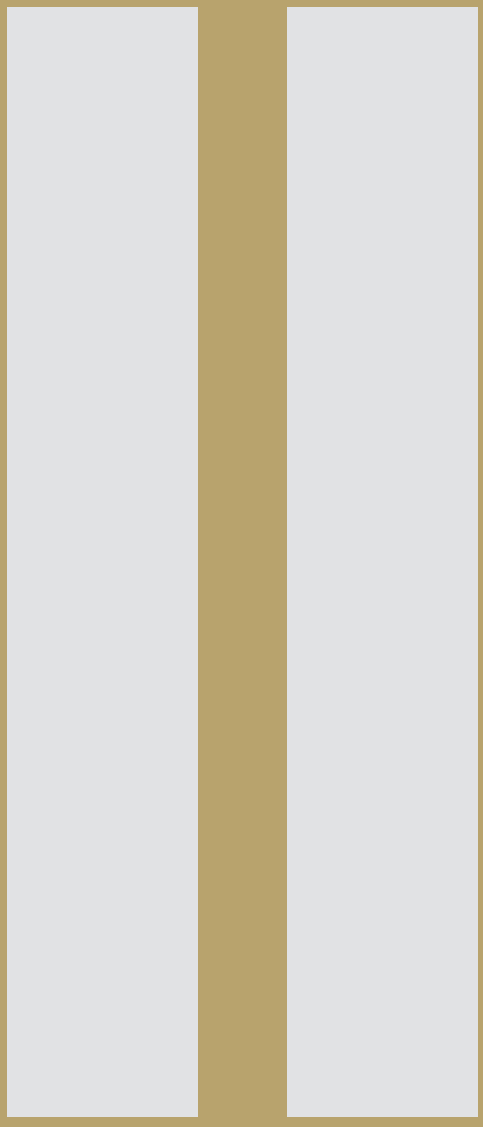

MAPPING THE FIELD

2

SURGICAL MANAGEMENT OF MADELUNG DEFORMITY: A SYSTEMATIC REVIEW

A. Peymani[1,2], A.R. Johnson[2], A.S. Dowlatshahi[2],
J.G.G. Dobbe[1], S.J. Lin[2], J. Upton[2],
G.J. Streekstra[1], S.D. Strackee[1]

[1] Department of Plastic, Reconstructive and Hand Surgery,
Amsterdam UMC, University of Amsterdam, Amsterdam, The Netherlands.
[2] Division of Plastic and Reconstructive Surgery,
Beth Israel Deaconess Medical Center, Harvard Medical School, Boston, MA, USA

Hand (N Y). 2019 Nov;14(6):725-734.

ABSTRACT

Madelung deformity is a congenital wrist condition characterized by a volar subluxation of the wrist caused by premature growth arrest of the distal radius. Progressive symptoms can necessitate surgical intervention, yet optimal treatment strategy remains unknown. The aim of this study is to determine treatment options, surgical indications, and operative outcomes for Madelung deformity. This study adhered to the Meta-Analyses of Observational Studies in Epidemiology (MOOSE) guidelines. A comprehensive systematic review was performed to identify all studies describing surgical interventions for Madelung deformity. All studies were evaluated by the level of evidence and a self-developed quality assessment tool. Twenty-five studies met inclusion criteria; all case series with type IV level of evidence. Studies assessed pain, range of motion, aesthetic deformity, and grip strength. The primary indication for surgery was the presence of wrist pain. Various surgical procedures exist and could be categorized as radial lengthening, ulnar shortening, or a combination of both. All studies report postoperative pain reduction, and most studies report an improved range of motion. A variety of surgical procedures reportedly has satisfactory outcomes. However, outcomes are reported in an inconsistent manner, prohibiting pooling of studies and comparisons of surgical procedures and their outcomes. We propose several methodological changes for implementation in future studies, increasing the quality of evidence to compensate for small patient numbers.

INTRODUCTION

In 1878, Otto W. Madelung reported on a rare disease of the wrist, now known as Madelung deformity.[1] Although the first case was presented years before, Madelung was the first to provide an overview even before the discovery of radiographs.[2] In his clinical observations, he describes a palmar subluxation of the hand, a prominent distal ulna, and volar angulation of the distal radial epiphysis.[1] Currently, we know that the deformity is caused by an abnormal growth arrest of the distal radial epiphysis leading to volar and ulnar tilting of the radial articular surface, and palmar bowing of the distal radius.[3,4] Studies have also identified an abnormally thickened volar ligament, the so-called 'Vickers ligament', that tethers the lunate to the radius and is hypothesized to hinder growth by compressing the epiphyseal plate.[5] Because of its progressive nature, the deformity can lead to wrist pain, restricted range of motion (ROM), and loss of grip strength, heavily interfering with daily activities.[6-8] In addition, patients can complain about the visible deformity caused by prominence of the distal ulna.[8] Madelung deformity often occurs bilaterally,[9] is most often diagnosed in adolescent females,[10] and has been associated with genetic disorders such as Léri-Weill dyschondrosteosis (LWD) and Turner syndrome.[11,12]

Representing less than 2% of pediatric hand deformities,[13] our current understanding of this condition is limited. Despite the small number of affected patients, studies have tried to shed light on various clinical aspects of the deformity, prompting the rise of multiple classification systems[10,14] and various radiographic criteria to be used in the diagnostic process.[4,15] However, the consistency with which these classification systems are applied remains unclear. This is also reflected in patient care, as multiple surgical procedures have been proposed to correct the deformity, without a current consensus.[16-18] Therefore, nearly 200 years after its original description, a significant knowledge gap remains, with respect to the surgical management of Madelung deformity,[16] compromising patients' access to optimal care.

The purpose of this systematic review is to evaluate the current body of literature on Madelung deformity, to identify available surgical treatment options, criteria utilized for surgical decision making, as well as clinical outcomes. The following questions will be addressed:

1. Which criteria are assessed in the preoperative workup?
2. What surgical procedures are available to correct the deformity?
3. What is the primary indication for surgical treatment?
4. What are the outcomes in regard to pain and ROM?

MATERIALS AND METHODS

Search strategy

The study protocol adhered to the Meta-Analyses of Observational Studies in Epidemiology (MOOSE) guidelines (Supplemental File 1).[19] A comprehensive electronic search strategy was developed and reviewed by a senior Harvard Medical School research librarian. On September 12, 2017, an online search was performed using Medline, Embase, and the Cochrane Collaboration Library to identify all original citations that addressed surgical approaches for Madelung deformity.

The search was conducted using both Medical Subject Heading (MeSH) and free-text using the following search terms: 'Madelung Deformity', 'Leri-Weill Syndrome', and 'Dyschondrosteosis'.

In addition, a manual reference check of all articles meeting inclusion criteria was performed to capture additional references not yielded in the initial search. The search was limited to articles published in English, Chinese, Dutch, French, and German from inception to September 2017. Articles published in languages other than English were translated by native speakers in the research team whenever applicable.

Eligibility criteria

Studies eligible for inclusion described a corrective operative procedure for Madelung deformity and included postoperative outcomes. Studies ineligible for inclusion were case reports, case series including fewer than three patients, studies detailing a surgical technique only, and studies including patients with prior corrective procedures of the same wrist. In addition, literature reviews and studies that did not report patient follow-up and outcomes were excluded. If a study described a patient cohort that was used in a previous study, the study with shorter follow-up time was excluded to capture the most current long-term outcomes. Abstracts and unpublished studies were not eligible for inclusion.

Study selection

After completion of an initial electronic database search, all citations were identified and imported into EndNote X7.7.1 (Thomas Reuters, New York, NY). After removal of duplicates, all studies were subject to title and abstract screening by two independent reviewers (A.P., A.R.J.). Subsequently, these two reviewers obtained and screened full-text articles using the eligibility criteria outlined above to obtain the final list of articles. Disagreement was resolved by consensus from a third evaluator (S.D.S.). When full-text articles were not available, efforts were made to obtain these through correspondence with study authors.

Data collection

The final list of articles was independently evaluated by two authors (A.P., A.R.J.) and the following variables were extracted: type of study, number of patients, number of operated wrists, gender, age at surgery, etiology, criteria used in clinical examination, radiographic criteria used in the diagnostic process, surgical procedure, indication for surgical intervention, intraoperative identification of Vickers ligament, and patient follow-up time. Whenever available, data for the following clinical outcome variables were extracted: pain, ROM, grip strength, and presence of aesthetic deformity. For patients who underwent bilateral wrist surgery, age at the time of the first operation was selected for the 'age at surgery' variable, as this would best represent the age at which patients undergo surgical intervention. The majority of surgical procedures were categorized as: (1) radial lengthening (e.g., wedge osteotomy, Ilizarov technique); (2) ulnar shortening (e.g., resection, excision, osteotomy); or (3) a combination of (1) and (2).

Study quality and bias assessment

Each study was evaluated by the level of evidence as proposed by the Centre for Evidence-Based Medicine (Oxford, UK). This classification scheme assigns a level of evidence ranging from I (highest) to V (lowest).

We were unable to find a published and validated scale to assess case series for use in subsequent statistical analyses. Therefore, a novel quality assessment tool was developed in accordance with MOOSE guidelines to accurately reflect important factors in the surgical decision-making process (Supplemental Table 1). The scoring system used the following parameters: (1) sample size; (2) disease etiology; (3) preoperative clinical exam; (4) radiographic criteria; (5) postoperative outcomes; (6) follow-up time; and (7) patient-reported outcome measures. One point was awarded if the sample size was greater than ten patients, follow-up time was greater than one year, and etiology was defined for all patients. For pre- and postoperative assessment, a range of 0 to 2 points were awarded based on reporting of two parameters: pain and ROM. No points were awarded if any of these parameters were not described. One point was awarded if pain and ROM were described subjectively, and 2 points were awarded if both parameters were quantified. Radiographic criteria were assessed using a 0- to 2-point scale: no points if criteria were missing, 1 point for self-defined criteria, and 2 points for standardized criteria (e.g., Dannenberg or McCarroll). Finally, if authors assessed patient-reported outcome measures using a validated tool, 1 point was awarded.

Two authors (A.P., A.R.J.) independently scored each study (Supplemental Table 2). The intraclass correlation coefficient (ICC) was determined using a reliability analysis (IBM SPSS Statistics 25), indicating excellent interrater agreement (ICC = 0.802). Due to the wide variety of surgical procedures and the nature of included studies (exclusively case series), it was not possible to perform bias assessments, heterogeneity assessments, or meta-analyses.

RESULTS

Search results

A total of 1026 citations were identified for potential inclusion after initial electronic database search, with 713 citations remaining after removal of duplicates (Figure 1). Of these, 54 were available for full-text review after title and abstract screening. Twenty-five studies met eligibility criteria and were included in the study. The 29 studies that did not meet eligibility criteria were excluded for reasons including: case report or case series with fewer than three patients (n=10), studies not describing corrective surgery (n=7), literature review (n=4), lack of postoperative outcomes (n=3), prior corrective surgery performed on the same wrist (n=3), and descriptive study of surgical technique (n=1). In addition, one study was excluded[40] as the same patient cohort was used by another author that provided longer follow-up time.[38]

Study characteristics

The 25 included studies are listed in Table 1. All studies were case series with type IV level of evidence. Our self-developed quality assessment tool provided a median quality score of 5 (range,

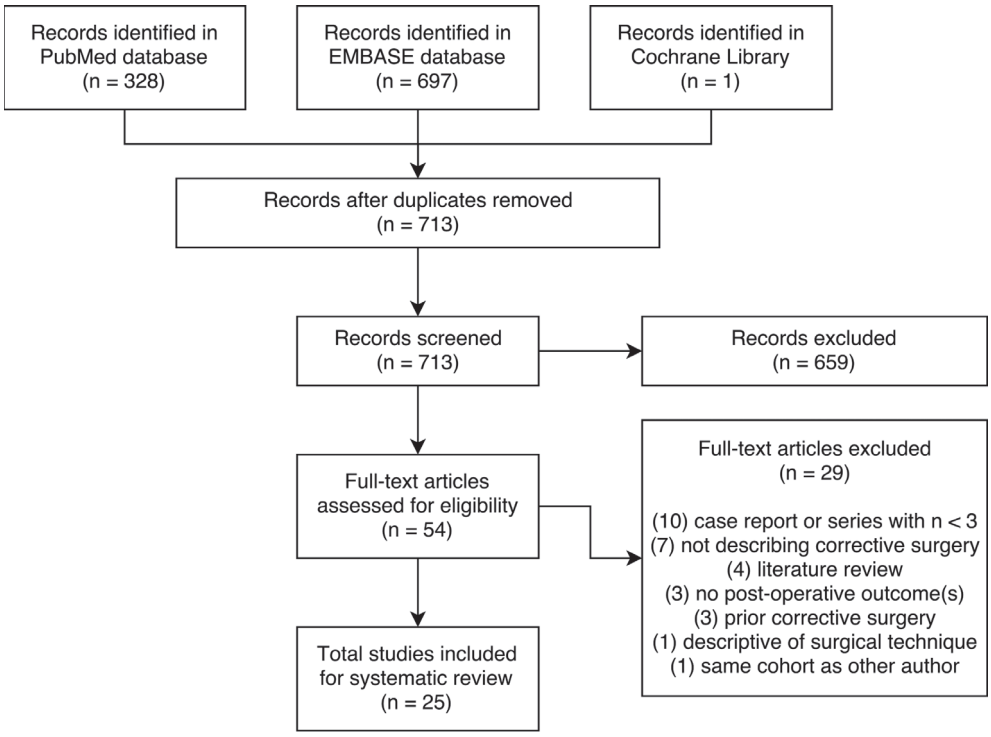

Figure 1. Flow diagram.

2-8). The mean sample size was 9 (range, 3-19). Mean follow-up time was 6.3 years and was available for 20 studies.

Patient characteristics

We identified 215 patients with 288 operated wrists. The majority of patients (90%) were female with a mean age at surgery of 18.5 years (range, 5-57 years). Disease etiology was reported for 166 patients (77%). Most patients were classified as idiopathic Madelung deformity (100 patients; 60%), 55 patients (33%) had a diagnosis of LWD, and 11 patients (7%) had a posttraumatic deformity.

Preoperative evaluation

In the clinical examination process, all studies assessed pain, ROM, and presence of aesthetic deformity. In addition, eight studies assessed grip strength.[6,23,28-30,36,38,39] As part of the diagnostic process, fourteen studies used their own radiographic criteria, five studies used the McCarroll criteria,[4] and three studies used the Dannenberg criteria.[15] The remaining three studies did not specify criteria used.

Table 1. Study characteristics.

	Patients (wrists)	Age, y (range)	Etiology	Radiographic criteria	Follow-up, m (range)	Quality[a]
Burrows, 1937[20]	3 (3)	14 (10-17)	idiopathic (2) post-traumatic (1)	Other	16 (8-34)	4/10
Ranawat et al., 1975[21]	8 (13)	17 (12-26)	idiopathic (8)	Other	96 (12-192)	5/10
Nielsen, 1977[10]	13 (15)	22 (14-57)	LWD (5)	NS	102 (6-240)	4/10
Vickers and Nielsen, 1992[5]	17 (24)	N/A	LWD (17)	Other	NS (15-180)	5/10
Watson et al., 1993[22]	10 (15)	17 (NS)	LWD (9) post-traumatic (1)	NS	48 (3-132)	4/10
Angelini et al., 1996[23]	15 (25)	18 (16-23)	idiopathic (15)	Dannenberg	67 (24-120)	7/10
Murphy et al., 1996[24]	11 (12)	16 (9-31)	LWD (7) post-traumatic (2)	Dannenberg	48 (13-97)	7/10
De Billy et al., 1997[25]	3 (5)	13 (13-13)	idiopathic (3)	Other	NS	4/10
Dos Reis et al., 1998[6]	18 (25)	23 (16-35)	idiopathic (18)	Other	53 (22-76)	6/10
Salon et al., 2000[26]	7 (11)	15 (11-19)	LWD (2)	Other	116 (18-264)	5/10
Schmidt-Rohlfing et al., 2001[9]	5 (6)	21 (NS)	NS	Dannenberg	NS	5/10
Ahmed Mir et al., 2003[27]	7 (7)	13 (12-15)	idiopathic (7)	Other	NS	4/10
Bruno et al., 2003[28]	9 (9)	34 (29-45)	LWD (2)	Other	42 (6-112)	8/10
Houshian et al., 2004[8]	7 (8)	19 (9-44)	LWD (4) post-traumatic (3)	Other	30 (18-66)	7/10
Dagregorio and Saint-Cast, 2005[29]	3 (5)	22 (15-33)	NS	NS	NS	2/10
Aharoni et al., 2006[30]	3 (4)	29 (27-32)	NS	Other	24 (NS)	6/10
de Paula et al., 2006[31]	4 (6)	16 (12-22)	NS	Other	24 (3-53)	4/10
Glard et al., 2007[32]	3 (4)	29 (27-32)	NS	Other	24 (NS)	6/10
Potenza et al., 2007[33]	5 (8)	13 (11-13)	idiopathic (5)	Other	408 (NS)	5/10
Laffosse et al., 2008[34]	11 (14)	13 (9-16)	LWD (2)	McCarroll	61 (48-105)	7/10
Kampa et al., 2010[35]	4 (5)	34 (26-45)	LWD (3)	McCarroll	55 (14-113)	7/10
El-Gafary and El-adly, 2013[36]	7 (7)	10 (5-17)	NS	Other	24 (NS)	4/10
Mallard et al., 2013[37]	5 (10)	27 (NS)	NS	McCarroll	95 (7-227)	6/10
Steinman et al., 2013[38]	18 (26)	13 (9-17)	LWD (4) post-traumatic (4)	McCarroll	132 (84-168)	8/10
Saffar and Badina, 2015[39]	19 (21)	27 (8-51)	NS	McCarroll	51 (7-228)	8/10

NS: Not Specified; LWD: Leri-Weill Dyschondrosteosis.

[a]Score calculated using self-designed quality assessment tool.

Surgical procedures and outcomes

The primary surgical procedures and outcomes for each study are provided in Table 2. The most commonly performed procedure was a combination of radial lengthening and ulnar shortening.

Table 2. Surgical procedures and outcomes.

	Surgical procedures	Primary indication	Pain reduced	ROM improved	Complications
Burrows, 1937[20]	RL/US	deformity	NS	50%	NS
Ranawat et al., 1975[21]	RL/US, US[a]	pain	100%	100%	1 revision surgery
Nielsen, 1977[10]	RL/US, US	pain	69 %	8%	3 revision surgeries
Vickers and Nielsen, 1992[5]	LP	pain	100%	100%	1 iatrogenic injury
Watson et al., 1993[22]	RL, RL/US	pain	100%	NS	8 revision surgeries
Angelini et al., 1996[23]	SK	pain	87%	87%	1 CRPS
Murphy et al., 1996[24]	RL	NS	100%	100%	2 revision surgeries 1 hardware removal
De Billy et al., 1997[25]	RL[b]	pain	100%	100%	1 transient neurological injury
Dos Reis et al., 1998[6]	RL/US	deformity	80%	100%	1 wound infection 1 CRPS requiring revision surgery
Salon et al., 2000[26]	RL/US	pain	100%	100%	1 revision surgery
Schmidt-Rohlfing et al., 2001[9]	RL, US	pain	100%	20%	None
Ahmed Mir et al., 2003[27]	RL[b]	pain	100%	100%	None
Bruno et al., 2003[28]	US	pain	100%	100%	1 revision surgery
Houshian et al., 2004[8]	RL[b]	pain	100%	100%	2 infection 2 revision surgery
Dagregorio and Saint-Cast, 2005[29]	RL	pain	100%	100%	None
Aharoni et al., 2006[30]	US	NS	100%	NS	NS
de Paula et al., 2006[31]	RL	NS	100%	100%	None
Glard et al., 2007[32]	US	NS	100%	100%	NS
Potenza et al., 2007[33]	RL/US	NS	100%	100%	None
Laffosse et al., 2008[34]	RL/US	pain	82%	100%	2 neurological deficits (transient)
Kampa et al., 2010[35]	RL/US[a]	pain	100%	100%	1 hardware removal
El-Gafary and El-adly, 2013[36]	RL[b]	deformity	100%	100%	NS
Mallard et al., 2013[37]	RL	NS	100%	100%	7 hardware removal 1 persistent neurological deficit
Steinman et al., 2013[38]	RL	NS	83%	83%	6 revision surgeries
Saffar and Badina, 2015[39]	RL, RL/US	NS	75%	100%	16 hardware removal 1 revision surgery 1 CRPS

RL: Radial Lengthening; US: Ulnar Shortening; LP: Langenskiöld Procedure; SK: Sauvé-Kapandji procedure; NS: Not Specified; CRPS: Complex Regional Pain Syndrome.

[a]Ulnar shortening through Darrach procedure.

[b]Radial lengthening through Ilizarov technique.

Other procedures in order of decreasing frequency included radial lengthening, ulnar shortening, the Sauvé-Kapandji procedure, and the Langenskiöld procedure. Seventeen studies described the primary indication for surgical intervention, with the occurrence of pain being the decisive factor in fourteen studies. Three studies intraoperatively identified and resected Vickers ligament.[5,24,38]

All studies reported postoperative pain reduction in the majority of patients and 20 studies reported an improved ROM. Patient-reported outcomes were assessed in four studies,[28,35,37,38] of which three used the Disabilities of the Arm, Shoulder and Hand score. One study used a visual analog scale (VAS) to assess pre- and postoperative pain.[8]

The majority of studies reported complications. Revision procedures were reported in ten studies (40%), with varying indications, including complex regional pain syndrome, recurrence of deformity, and need for additional reconstructive procedures.

DISCUSSION

In this review, we evaluated the available literature describing surgical interventions in patients with Madelung deformity, with respect to disease etiology, clinical examination parameters, radiographic criteria, choice and type of intervention, and surgical outcomes. Pain, ROM, aesthetic deformity, and occasionally grip strength were assessed in clinical examination, with pain being the most common indication for surgery. A variety of surgical procedures exist to treat Madelung deformity, with reportedly satisfactory outcomes in terms of pain and ROM. However, the heterogeneity of surgical techniques described, diversity of radiographic criteria used, and inconsistencies in reporting the etiology of the deformity and outcomes did not allow for quantitative comparisons. These factors, combined with the lack of patient-reported outcome measures, compromised our ability to make recommendations regarding optimal treatment.

Strengths and limitations

A major strength of our study is that it is the first systematic review assessing surgical management of Madelung deformity. Our study is largely limited by the nature of included studies: All 25 studies were low-powered case series of low-quality evidence (IV). Also, the possibility of publication bias could weaken the overwhelmingly positive reported outcomes in terms of pain and ROM.

Etiology

Madelung deformity is often classified into four groups based on etiology: (1) posttraumatic; (2) bone dysplasia; (3) chromosome abnormalities; and (4) idiopathic occurrence.[14] Existing literature supports the association between Madelung deformity and skeletal dysplasias or genetic syndromes,[11,12] with mutations or deletions in the short stature homeobox (SHOX) gene identified as key factors.[41] Some studies even suggest that most Madelung deformity patients have an underlying genetic condition.[42,43] In contrast, the majority of patients in our review were classified as idiopathic, yet none of the included studies mentioned genetic testing as part of their clinical management. This could imply that patients described as 'idiopathic' in origin were potentially misclassified due to lack of genetic workup. Furthermore, mutations of the SHOX gene have also been associated

with idiopathic presentations of the deformity.[44] These factors support that the absence of genetic testing could skew our understanding of the true etiology of Madelung deformity.

In addition, there was no clear rationale for selection of the surgical approach based on etiology. Different etiologies can present with unique anatomic deformities which can influence treatment choice. Prior research has shown that LWD patients were more likely to have a deformity involving the entire radius.[43] This is clinically relevant, as this could result in more severe functional and aesthetic manifestations, in turn requiring more complex surgical interventions.

Radiographic criteria and imaging

There were multiple radiographic criteria used across studies. Radiographic criteria based on common findings in Madelung deformity have been described to aid in the diagnostic workup.[4,5,15] However, most studies in our review used their own radiographic criteria. This heterogeneity underscores existing inconsistencies in the radiographic assessment of Madelung deformity. This could be explained by the limitations inherent to two-dimensional assessment and its inability to capture the three-dimensional (3D) nature of Madelung deformity. We anticipate that the application of 3D imaging will revolutionize our understanding of Madelung deformity by providing a roadmap for the development of new morphological parameters for more objective diagnosis and classification. This new spatial assessment could also facilitate the use of innovative techniques such as 3D preoperative planning for osteotomies,[45] with the goal to more accurately restore normal anatomic and functional relationships.

Surgical intervention

A variety of procedures exist to treat Madelung deformity. In our review, it appeared that surgeons almost exclusively chose any of the following approaches for surgical correction: lengthening of the radius, shortening of the ulna, or a combination of both. Vickers and Nielsen were the first to use the Langenskiöld procedure in seventeen patients (24 wrists) with Madelung deformity.[5] The procedure consists of resecting the affected part of the radial physis and interposing fat to prevent recurrence of a bony bridge,[46] enabling radius growth in a more normal fashion. The Sauvé-Kapandji procedure was used primarily in one study.[23]

The main indication for surgical intervention in this review was pain. This is interesting, provided the significance placed on radiographic parameters and degree of deformity as important considerations for operative intervention. Instead, these parameters could be considered as essential components of successful surgical planning.

In this review, most studies reported objective outcome measures such as pain and ROM. However, we were unable to make comparisons across studies because of the diversity of surgical interventions and poor specification of ROM and pain for individual participants. This eliminated the ability to link surgical procedures to postoperative outcomes, in turn compromising our ability to evaluate efficacy of surgical techniques.

Complications occurred in the majority of studies, and the need for a revision procedure was the most common postoperative complication. A prior review of fifteen studies[17] did not

provide information regarding the general incidence of postoperative complications. In our review, there was no identifiable surgical intervention associated with a higher complication rate. This finding may be misleading, as studies often did not specify complications according to the surgical procedure.

Studies have confirmed the presence of Vickers ligament in multiple Madelung deformity patients undergoing magnetic resonance imaging.[47,48] One study even suggested that all congenital cases of Madelung deformity are characterized by the presence of this ligament.[49] This abnormal ligament has been thought to contribute to developmental arrest of the distal radius through compression, and early identification and removal may have significant prophylactic potential.[5] However, underlying etiology and identification of this ligament were not consistently reported. With only three of our included studies describing Vickers ligament, this precluded any discussion about its influence on the anatomical changes seen in Madelung deformity.

Recommendations for future research and practice

We were unable to conduct a meta-analysis due to the low quality of studies as reflected by the scores from our self-developed assessment tool. Therefore, we propose several changes in the methodology of future studies, which we deem necessary considering the rarity of Madelung deformity. During clinical evaluation, a thorough history and physical exam are imperative and include family history of the disorder, existing medical conditions, and prior trauma. An interdisciplinary approach, including coordination with a genetic counselor, should be considered as part of the routine workup. Genetic testing could be particularly helpful in patients with an obscure etiology or lack of preceding wrist trauma to identify potential chromosomal aberrancies.

The pre- and postoperative physical examination should include uniform, quantified measurements of all clinically relevant variables. Pain is quantified using a VAS, a validated instrument commonly used for measuring pain intensity. ROM measurements of the affected and contralateral wrist should include flexion, extension, pronation, supination, radial, and ulnar deviation. Patient satisfaction with the aesthetic appearance could be quantified using patient-reported outcome measures such as the Michigan Hand Outcomes Questionnaire[50] or the Patient-Rated Wrist Evaluation questionnaire.[51] A routine grip strength measurement should be considered, as it may indicate postoperative improvement.[23] In addition, a standardized imaging protocol needs to be developed and uniformly adapted, possibly using a 3D assessment of the deformity. Surgeons should aim to identify and report on the presence of Vickers ligament intraoperatively, as prevalence and existing etiologic association are still unknown and require investigation.

Multiple algorithms have been proposed for the surgical management of Madelung deformity, selecting appropriate treatment based on a variety of factors such as patient age, pain location, skeletal maturity, and the presence of secondary arthritis.[16,52] Yet these algorithms are based on low-quality evidence. Future studies should implement data collection protocols to increase study homogeneity and evidence quality. A suggested template can be found in Figure 2.

CONCLUSION

Despite nearly 200 years of experience with Madelung deformity, there remains a paucity of evidence-based algorithms regarding the surgical decision-making process. Outcomes are reported in an inconsistent manner, prohibiting pooling of studies and comparisons of surgical procedures and their outcomes. We propose multiple changes to serve as the basis for new clinical guidelines that will increase the quality of evidence in future studies, compensating for small sample sizes.

MADELUNG DEFORMITY PROTOCOL FOR FUTURE STUDIES

History	Bilateral Manifestation	▫ No ▫ Yes	
	Familial Occurence	▫ No ▫ Yes:	
	Existing Genetic Disorders	▫ No ▫ Yes:	
	Etiology	▫ Idiopathic ▫ Syndromal	
		▫ Post-traumatic ▫ Chromosomal	
Pre-operative Evaluation	Signs of Syndromal or Chromosomal Etiology	▫ No ▫ Yes → Genetic Consult	
	Pain	▫ No ▫ Yes → Visual Analog Scale → Location: _____	
	Range Of Motion	Flexion: _____	Extension: _____
		Pronation: _____	Supination: _____
		Radial deviation: _____	Ulnar deviation: _____
	Grip Strength	Weight/Force: _____	
	PROM	Score: _____	
Pre-operative	Radiologic Criteria	_____	
	Measurements	Ulnar Tilt: _____	Lunar Fossa Angle: _____
		Lunate Subsidence: _____	
	Epiphyseal Plate	▫ Open ▫ Fused	
Peri-operative	Surgical Intervention	_____	
	Identification of Vickers Ligament	▫ No ▫ Yes	
	Resection of Vickers Ligament	▫ No ▫ Yes	
Post-operative Evaluation	Pain	▫ No ▫ Yes → Visual Analog Scale → Location: _____	
	Range Of Motion	Flexion: _____	Extension: _____
		Pronation: _____	Supination: _____
		Radial deviation: _____	Ulnar deviation: _____
	Grip Strength	Weight/Force: _____	
	PROM	Score: _____	
Post-operative	Radiologic Criteria	_____	
	Measurements	Ulnar Tilt: _____	Lunar Fossa Angle: _____
		Lunate Subsidence: _____	
Complications	Complications	_____	
	Revision Surgery	_____	

Figure 2. Madelung deformity protocol for use in future studies.

REFERENCES

5. Madelung O. Die spontane Subluxation der Hand nach vorne. ***Verh Dtsch Ges Chir.*** 1878;7:259-276.
6. Arora AS, Chung KC. Otto W. Madelung and the recognition of Madelung's deformity. ***J Hand Surg Am.*** 2006;31(2):177-182.
7. Anton JI, Reitz GB, Spiegel MB. Madelung's Deformity. ***Ann Surg.*** 1938;108(3):411-439.
8. McCarroll HR, Jr., James MA, Newmeyer WL, 3rd, Molitor F, Manske PR. Madelung's deformity: quantitative assessment of x-ray deformity. ***J Hand Surg Am.*** 2005;30(6):1211-1220.
9. Vickers D, Nielsen G. Madelung deformity: surgical prophylaxis (physiolysis) during the late growth period by resection of the dyschondrosteosis lesion. ***J Hand Surg Br.*** 1992;17(4):401-407.
10. dos Reis FB, Katchburian MV, Faloppa F, Albertoni WM, Laredo Filho J, Jr. Osteotomy of the radius and ulna for the Madelung deformity. ***J Bone Joint Surg Br.*** 1998;80(5):817-824.
11. Fagg PS. Wrist pain in the Madelung's deformity of dyschondrosteosis. ***J Hand Surg Br.*** 1988;13(1):11-15.
12. Houshian S, Schroder HA, Weeth R. Correction of Madelung's deformity by the Ilizarov technique. ***J Bone Joint Surg Br.*** 2004;86(4):536-540.
13. Schmidt-Rohlfing B, Schwobel B, Pauschert R, Niethard FU. Madelung deformity: clinical features, therapy and results. ***J Pediatr Orthop B.*** 2001;10(4):344-348.
14. Nielsen JB. Madelung's deformity. A follow-up study of 26 cases and a review of the literature. ***Acta Orthop Scand.*** 1977;48(4):379-384.
15. Belin V, Cusin V, Viot G, Girlich D, Toutain A, Moncla A, et al. SHOX mutations in dyschondrosteosis (Leri-Weill syndrome). ***Nat Genet.*** 1998;19(1):67-69.
16. Clement-Jones M, Schiller S, Rao E, Blaschke RJ, Zuniga A, Zeller R, et al. The short stature homeobox gene SHOX is involved in skeletal abnormalities in Turner syndrome. ***Hum Mol Genet.*** 2000;9(5):695-702.
17. Flatt AE. ***The care of congenital hand anomalies.*** Quality Medical Publishing; 1994.
18. Henry A, Thorburn MJ. Madelung's deformity. A clinical and cytogenetic study. ***J Bone Joint Surg Br.*** 1967;49(1):66-73.
19. Dannenberg M, Anton J, Spiegel M. Madelung's deformity: consideration of its roentgenological diagnostic criteria. ***Am J Roentgenol.*** 1939;42:671-676.
20. Dubey A, Fajardo M, Green S, Lee SK. Madelung's deformity: a review. ***J Hand Surg Eur Vol.*** 2009;35(3):174-181.
21. Ghatan AC, Hanel DP. Madelung deformity. ***J Am Acad Orthop Surg.*** 2013;21(6):372-382.
22. Kozin SH, Zlotolow DA. Madelung Deformity. ***J Hand Surg Am.*** 2015;40(10):2090-2098.
23. Stroup DF, Berlin JA, Morton SC, Olkin I, Williamson GD, Rennie D, et al. Meta-analysis of observational studies in epidemiology: a proposal for reporting. Meta-analysis Of Observational Studies in Epidemiology (MOOSE) group. ***JAMA.*** 2000;283(15):2008-2012.
24. Burrows HJ. An Operation for the Correction of Madelung's Deformity and Similar Conditions: (Section of Orthopaedics). ***Proc R Soc Med.*** 1937;30(5):565-572.
25. Ranawat CS, DeFiore J, Straub LR. Madelung's deformity. An end-result study of surgical treatment. ***J Bone Joint Surg Am.*** 1975;57(6):772-775.
26. Watson HK, Pitts EC, Herber S. Madelung's deformity. A surgical technique. ***J Hand Surg Br.*** 1993;18(5):601-605.

27. Angelini LC, Leite VM, Faloppa F. Surgical treatment of Madelung disease by the Sauve-Kapandji technique. ***Ann Chir Main Memb Super.*** 1996;15(4):257-264.

28. Murphy MS, Linscheid RL, Dobyns JH, Peterson HA. Radial opening wedge osteotomy in Madelung's deformity. ***J Hand Surg Am.*** 1996;21(6):1035-1044.

29. de Billy B, Gastaud F, Repetto M, Chataigner H, Clavert JM, Aubert D. Treatment of Madelung's deformity by lengthening and reaxation of the distal extremity of the radius by Ilizarov's technique. ***Eur J Pediatr Surg.*** 1997;7(5):296-298.

30. Salon A, Serra M, Pouliquen JC. Long-term follow-up of surgical correction of Madelung's deformity with conservation of the distal radioulnar joint in teenagers. ***J Hand Surg Br.*** 2000;25(1):22-25.

31. Ahmed Mir N, Ahmed Kawoosa A, Mir GR. Ilizarov's technique for treatment of madelung's deformity by lengthening and re-axation of the distal extremity of the radius. ***JK Science.*** 2003;5(3):118-121.

32. Bruno RJ, Blank JE, Ruby LK, Cassidy C, Cohen G, Bergfield TG. Treatment of Madelung's deformity in adults by ulna reduction osteotomy. ***J Hand Surg Am.*** 2003;28(3):421-426.

33. Dagregorio G, Saint-Cast Y. [Reorientation of the distal radial articular surface in Madelung's deformity by a reversed cuneiform osteotomy]. ***Chir Main.*** 2005;24(2):109-112.

34. Aharoni C, Glard Y, Launay F, Gay A, Legre R. Madelung deformity: isolated ulnar wedge osteotomy. [French]. ***Chirurgie de la Main.*** 2006;25(6):309-314.

35. de Paula EJ, Cho AB, Junior RM, Zumiotti AV. Madelung's deformity: treatment with radial osteotomy and insertion of a trapezoidal wedge. ***J Hand Surg Am.*** 2006;31(7):1206-1213.

36. Glard Y, Gay A, Launay F, Guinard D, Legre R. Isolated wedge osteotomy of the ulna for mild Madelung's deformity. ***J Hand Surg Am.*** 2007;32(7):1037-1042.

37. Potenza V, Farsetti P, Caterini R, Tudisco C, Nicoletti S, Ippolito E. Isolated Madelung's deformity: long-term follow-up study of five patients treated surgically. ***J Pediatr Orthop B.*** 2007;16(5):331-335.

38. Laffosse JM, Abid A, Accadbled F, Knor G, Sales de Gauzy J, Cahuzac JP. Surgical correction of Madelung's deformity by combined corrective radioulnar osteotomy: 14 cases with four-year minimum follow-up. ***Int Orthop.*** 2008;33(6):1655-1661.

39. Kampa R, Al-Beer A, Axelrod T. Madelung's deformity: radial opening wedge osteotomy and modified Darrach procedure using the ulnar head as trapezoidal bone graft. ***J Hand Surg Eur Vol.*** 2010;35(9):708-714.

40. El-Gafary K, El-adly W. Forearm lengthening using Ilizarov external fixator. ***European Orthopaedics and Traumatology.*** 2013;4(4):217-224.

41. Mallard F, Jeudy J, Rabarin F, Raimbeau G, Fouque PA, Cesari B, et al. Reverse wedge osteotomy of the distal radius in Madelung's deformity. ***Orthop Traumatol Surg Res.*** 2013;99(4 Suppl):S279-283.

42. Steinman S, Oishi S, Mills J, Bush P, Wheeler L, Ezaki M. Volar ligament release and distal radial dome osteotomy for the correction of Madelung deformity: long-term follow-up. ***J Bone Joint Surg Am.*** 2013;95(13):1198-1204.

43. Saffar P, Badina A. Treatment of Madelung's deformity. ***Chirurgie de la Main.*** 2015;34(6):279-285.

44. Harley BJ, Brown C, Cummings K, Carter PR, Ezaki M. Volar ligament release and distal radius dome osteotomy for correction of Madelung's deformity. ***J Hand Surg Am.*** 2006;31(9):1499-1506.

45. Rappold GA, Fukami M, Niesler B, Schiller S, Zumkeller W, Bettendorf M, et al. Deletions of the homeobox gene SHOX (short stature homeobox) are an important cause of growth failure in children with short stature. ***J Clin Endocrinol Metab.*** 2002;87(3):1402-1406.

46. Herdman RC, Langer LO, Good RA. Dyschondrosteosis. The most common cause of Madelung's deformity. ***J Pediatr.*** 1966;68(3):432-441.

47. Zebala LP, Manske PR, Goldfarb CA. Madelung's deformity: a spectrum of presentation. ***J Hand Surg Am.*** 2007;32(9):1393-1401.

48. Grigelioniene G, Eklof O, Ivarsson SA, Westphal O, Neumeyer L, Kedra D, et al. Mutations in short stature homeobox containing gene (SHOX) in dyschondrosteosis but not in hypochondroplasia. ***Human Genetics.*** 2000;107(2):145-149.

49. Dobbe JGG, Strackee SD, Streekstra GJ. Minimizing the Translation Error in the Application of an Oblique Single-Cut Rotation Osteotomy: Where to Cut? ***IEEE Trans Biomed Eng.*** 2018;65(4):821-827.

50. Langenskiold A. An operation for partial closure of an epiphysial plate in children, and its experimental basis. ***J Bone Joint Surg Br.*** 1975;57(3):325-330.

51. Cook PA, Yu JS, Wiand W, Lubbers L, Coleman CR, Cook AJ, 2nd, et al. Madelung deformity in skeletally immature patients: morphologic assessment using radiography, CT, and MRI. ***J Comput Assist Tomogr.*** 1996;20(4):505-511.

52. Stehling C, Langer M, Nassenstein I, Bachmann R, Heindel W, Vieth V. High resolution 3.0 Tesla MR imaging findings in patients with bilateral Madelung's deformity. ***Surg Radiol Anat.*** 2009;31(7):551-557.

53. Ali S, Kaplan S, Kaufman T, Fenerty S, Kozin S, Zlotolow DA. Madelung deformity and Madelung-type deformities: a review of the clinical and radiological characteristics. ***Pediatr Radiol.*** 2015;45(12):1856-1863.

54. Chung KC, Hamill JB, Walters MR, Hayward RA. The Michigan Hand Outcomes Questionnaire (MHQ): assessment of responsiveness to clinical change. ***Ann Plast Surg.*** 1999;42(6):619-622.

55. MacDermid JC, Turgeon T, Richards RS, Beadle M, Roth JH. Patient rating of wrist pain and disability: a reliable and valid measurement tool. ***J Orthop Trauma.*** 1998;12(8):577-586.

56. Hawkes DH, Nixon MF. Evidence-based treatment of Madelung's deformity. In: ***Paediatric Orthopaedics.*** Springer; 2017:317-321.

SUPPLEMENTAL DATA

Supplemental File 1. MOOSE checklist.

Background	
Problem definition	✔
Hypothesis statement	✔
Description of study outcome(s)	✔
Type of exposure or intervention used	✔
Study population	✔
Search strategy	
Qualifications of searchers	✔
Search strategy, including time period included in synthesis and keywords	✔
Effort to include all available studies, including contact with authors	✔
Databases and registries searched	✔
Search software used, name and version, including special features used	✔
Use of hand searching	✔
List of citations located and those excluded, including justification	✔
Method of addressing articles published in languages other than English	✔
Method of handling abstracts and unpublished articles	✔
Description of any contact with authors	✔
Methods	
Description of relevance or appropriateness of studies assembled	✔
Rationale for the selection and coding of data	✔
Documentation of how data were classified and coded	✔
Assessment of confounding	✘
Assessment of study quality	✔
Assessment of heterogeneity	✘
Description of statistical methods in sufficient detail to be replicated	✘
Provision of appropriate tables and graphics	✔
Results	
Graphic summarizing individual study estimates and overall estimate	✘
Table giving descriptive information for each study included	✔
Results of sensitivity testing	✘
Indication of statistical uncertainty of findings	✔
Discussion	
Quantitative assessment of bias	✔
Justification for exclusion	✔
Assessment of quality of included studies	✔
Conclusions	
Consideration of alternative explanations for observed results	✔
Generalization of the conclusions	✔
Guidelines for future research	✔
Disclosure of funding source	✔

Supplemental Table 1. Quality assessment tool.

	Description	Score
Sample size	Patients <10	0
	Patients ≥10	1
Etiology	Undefined	0
	Defined	1
Preoperative exam	Pain or ROM undefined or missing	0
	Pain and ROM described subjectively	1
	Pain and ROM quantified	2
Radiographic criteria	Not described	0
	Described; but no pre-defined criteria used	1
	Described; pre-defined criteria used	2
Postoperative outcomes	Pain or ROM undefined or missing	0
	Pain and ROM described subjectively	1
	Pain and ROM quantified	2
Follow-up time	<1 years	0
	≥1 years	1
PROM	Not included	0
	Included	1

PROM: Patient-Reported Outcome Measures.

Supplemental Table 2. Quality assessment scoring.

	Sample size	Etiology	Pre-op exam	Radiographic criteria	Follow-up	Post-op outcome	PROM	Total
Burrows, 1937[20]	0	1	1	1	1	0	0	4
Ranawat et al., 1975[21]	0	1	1	1	1	1	0	5
Nielsen, 1977[10]	1	1	0	0	1	1	0	4
Vickers and Nielsen, 1992[5]	1	1	0	1	1	1	0	5
Watson et al., 1993[22]	1	1	0	0	1	1	0	4
Angelini et al., 1996[23]	1	1	1	2	1	1	0	7
Murphy et al., 1996[24]	1	1	1	2	1	1	0	7
De Billy et al., 1997[25]	0	1	1	1	0	1	0	4
Dos Reis et al., 1998[6]	1	1	1	1	1	1	0	6
Salon et al., 2000[26]	0	1	1	1	1	1	0	5
Schmidt- Rohlfing et al., 2001[9]	0	1	1	2	0	1	0	5
Ahmed Mir et al., 2003[27]	0	1	1	1	0	1	0	4
Bruno et al., 2003[28]	0	1	2	1	1	2	1	8
Houshian et al., 2004[8]	0	1	2	1	1	2	0	7
Dagregorio and Saint-Cast, 2005[29]	0	0	1	0	0	1	0	2
Aharoni et al., 2006[30]	0	0	2	1	1	2	0	6
de Paula et al., 2006[31]	0	0	1	1	1	1	0	4
Glard et al., 2007[32]	0	0	2	1	1	2	0	6
Potenza et al., 2007[33]	0	1	1	1	1	1	0	5
Laffosse et al., 2008[34]	1	1	1	2	1	1	0	7
Kampa et al., 2010[35]	0	1	1	2	1	1	1	7
El-Gafary and El-adly, 2013[36]	0	0	1	1	1	1	0	4
Mallard et al., 2013[37]	0	0	1	2	1	1	1	6
Steinman et al., 2013[38]	1	1	1	2	1	1	1	8
Saffar and Badina, 2015[39]	1	0	2	2	1	2	0	8

PROM: Patient-Reported Outcome Measures.

3

#MADELUNGDEFORMITY: INSIGHTS INTO A RARE CONGENITAL HAND DIFFERENCE UTILIZING SOCIAL MEDIA

A. Peymani [1,2], M.M. Lokhorst [1],
A.D. Chen [2], C.M.A.M. van der Horst [1],
B.T. Lee [2], S.J. Lin [2], S.D. Strackee [1]

[1] Department of Plastic, Reconstructive and Hand Surgery,
Amsterdam UMC, University of Amsterdam, Amsterdam, The Netherlands.
[2] Division of Plastic and Reconstructive Surgery, Beth Israel Deaconess Medical Center,
Harvard Medical School, Boston, MA, USA.

Submitted.

ABSTRACT

Madelung deformity is a rare congenital hand difference with little known in regard to the patient perspective. In this cross-sectional survey study, we harnessed the global reach of social media to understand the clinical spectrum of Madelung deformity and its impact on physical, mental, and social health. A survey was developed based on a previously published protocol and multiple Patient-Reported Outcomes Measurement Information System (PROMIS) short forms. The survey was distributed on several Madelung deformity communities on Facebook and Instagram. T-scores were calculated, interpreted, and compared between patients who underwent surgery and those who did not. Correlations between scores were calculated using the Spearman's rank correlation coefficient. Mean PROMIS scores for adults were as follows: pain intensity 4.9±2.8, pain interference 57.6±10.0, upper extremity 35.2±8.1, depression 53.8±11.1, anxiety 55.4±11.4, and ability to participate in social roles and activities 42.5±7.7. Mean scores for children were: pain intensity 5.0±2.8, pain interference 55.7±11.3, upper extremity function 24.6±10.4, depressive symptoms 57.7±11.3, anxiety 57.3±11.9, and peer relationships 42.2±10.3. Madelung deformity has significant effects on patients' physical, mental, and social well-being, even after surgical treatment. Using social media, we were able to compensate for Madelung deformity's rarity by engaging an international audience, demonstrating the feasibility to conduct research through it, and providing a global perspective of the disease entity.

INTRODUCTION

In April 1878, after a lecture in Berlin by a German surgeon, the condition 'Madelung deformity' was introduced to the surgical community.[1,2] This congenital hand difference is caused by a premature growth arrest of the distal radius, leading to a shortened radius with a volar and ulnar angulation, relative overgrowth of the ulna, and pyramidization of the proximal carpal row.[3-7] The deformity is often caused by mutations in the short stature homeobox (SHOX) gene, which is associated with both Leri-Weill dyschondrosteosis and Turner Syndrome.[8,9] Madelung deformity is extremely rare, and its incidence and prevalence are relatively unknown, with hand surgeons seeing very few, if any, cases during their surgical career.[10] This is evident by the sparse literature, with the largest recently published case series study including nineteen patients,[11] raising several unanswered questions regarding etiology, diagnostics, classifications, treatment options, and surgical outcomes.[12-17] Furthermore, small-powered studies often inadequately describe functional status,[18] and only a handful of studies have even considered the patient perspective.[19-22]

This is remarkable, given that it is well established that congenital hand differences have a profound and lifelong impact on the physical, mental, and social aspects of patients' lives.[23] To increase our understanding of these deformities, it is therefore paramount to perform studies using validated patient-reported outcome measures (PROMs) in a large sample size of patients.[24] While the investigation of PROMs through combining data from multiple centers has provided us insights into other congenital hand differences,[25] this has not translated to an increased understanding of Madelung deformity due to the low numbers of patients captured.[26] Despite starting several prospective studies over the past years at our institute and other tertiary/quaternary centers worldwide, low patient numbers have limited any firm conclusions.[27] To date, one potentially useful tool to study these rare patient populations that may otherwise be extremely difficult to reach is social media.[28]

This study's primary aim is to understand the clinical spectrum of Madelung deformity and its impact on physical, mental, and social health by harnessing the global reach of social media. Using the universal Patient-Reported Outcomes Measure Information System (PROMIS),[29] advised for use in rare diseases,[30-32] we collaborated with several social media communities to conduct a cross-sectional survey. PROMIS allows for an assessment of multiple physical, mental, and social health domains and has been proven to be efficient and reliable for different upper extremity conditions.[33-36] To the best of our knowledge this is the first and largest to date study of patient-reported outcome measures for Madelung deformity.

MATERIALS AND METHODS

Study population and data collection

Ethical approval for this cross-sectional survey study was waived by our hospital Medical Ethics Committee. Data was collected through an online survey created with Google Forms. The survey was distributed through a post (Figure 1) on existing online Madelung deformity communities on Facebook and an Instagram community established by the authors ('@madelungdeformity'). The survey was kept online for a total of nine days from the initial launch date (February 11,

2020). Figure 2 shows an overview of the geographic locations of all persons that visited the link (n=207). The exact location of participants that fully completed the survey was not available due to privacy reasons. The survey consisted of questions on demographic characteristics and PROMIS short forms.[29]

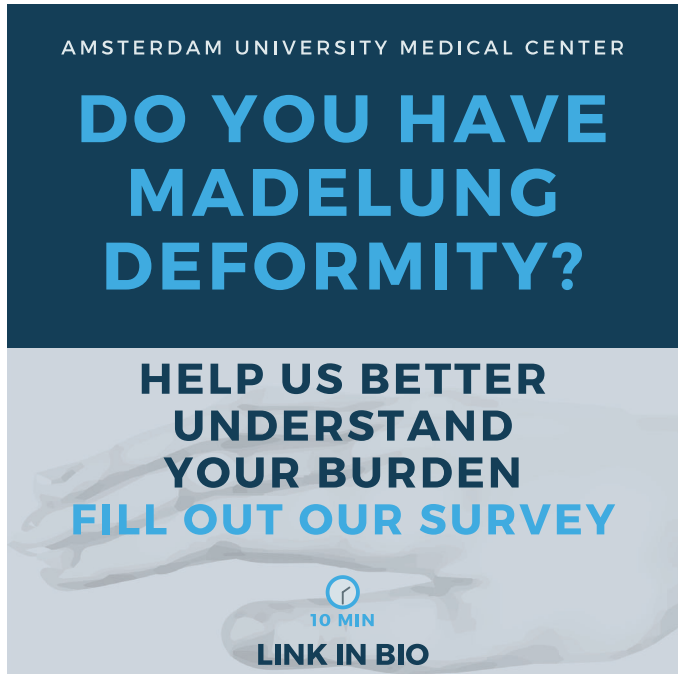

Figure 1. Example post on social media platform Instagram.

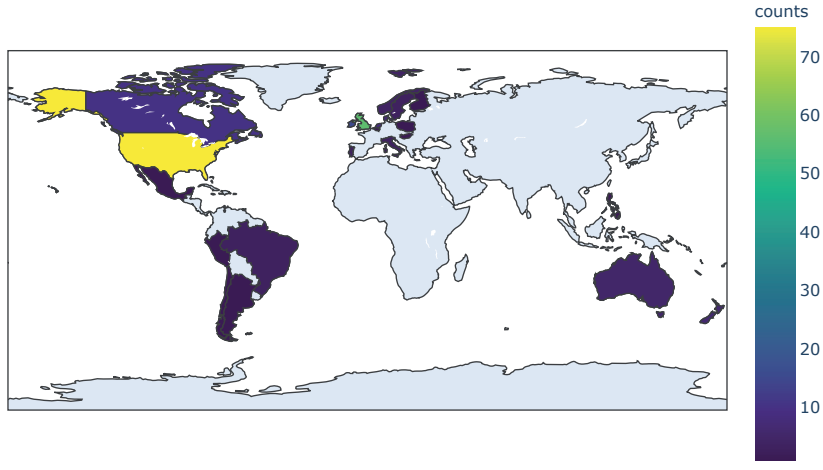

Figure 2. Heatmap showing initial engagement from social media.

Survey: demographic characteristics

Questions regarding demographic characteristics were based on a previously published protocol that proposed various changes in the methodology of future Madelung deformity studies.[18] The following variables were collected: age, assigned gender at birth, height, weight, affected arm(s), previously diagnosed genetic conditions, previously diagnosed medical conditions, medication use (including painkillers), family history of Madelung deformity, and any (corrective) surgeries of the hand, wrist, or arm. Based on the selected age range (18+ or 8-17 years), participants were either presented with adult or pediatric versions of the PROMIS forms. The complete question list is available in Supplementary File 1.

Survey: PROMIS short forms

The PROMIS short forms consisted of fixed sets of questions for six health domains,[29] covering physical, mental and social health. For adults the following forms and versions were used: (1) Pain Intensity 1a v1.0, (2) Pain Interference 8a v1.0, (3) Upper Extremity 7a v2.0, (4) Depression 8a v1.0, (5) Anxiety 8a v1.0, and (6) Ability to Participate in Social Roles and Activities 8a v2.0. For children we used the short forms: (1) Pediatric Pain Intensity 1a v1.0, (2) Pediatric Pain Interference 8a v2.0, (3) Pediatric Upper Extremity 8a v2.0, (4) Pediatric Depressive Symptoms 8a v2.0, (5) Pediatric Anxiety 8a v2.0, and (6) Pediatric Peer Relationships 8a v2.0. In regard to pain, 'Pain Intensity' assesses how much a person hurts, while 'Pain Interference' considers self-reported consequences of pain on relevant aspects of one's life.

Post-processing and data analysis

After exporting raw survey data from Google Forms, each entry was manually inspected to remove errors (e.g., previous surgeries not involving the upper extremity), perform metric unit conversions (e.g., pounds to kilograms for weight), and to determine analgesic use by reviewing all listed medications. PROMIS short forms were scored using a T-score metric, in which 50 is the mean and 10 is the standard deviation of a relevant reference population.[37] T-scores were calculated based on scoring tables of each domain's published manuals, using self-developed software in Python (Python v3.7.4). Higher scores represent a higher level of the measured domain,[29] and their interpretation in different domains[38] is shown in Figure 3.

Means were compared between patients who underwent surgery and those who did not. For normally distributed scores, an independent samples t-test (variances equal) or Welch's t-test (variances not equal) was performed. Equality of variances was assessed using Levene's test. For non-normally distributed scores, the Mann-Whitney U test was performed. All analyses were performed separately for adult and pediatric patients. Correlations between the different PROMIS short form scores were calculated using the Spearman's rank correlation coefficient (ρ), with correlation strength interpreted as either low (<0.3), moderate (0.3-0.5), or high (>0.5).[39]

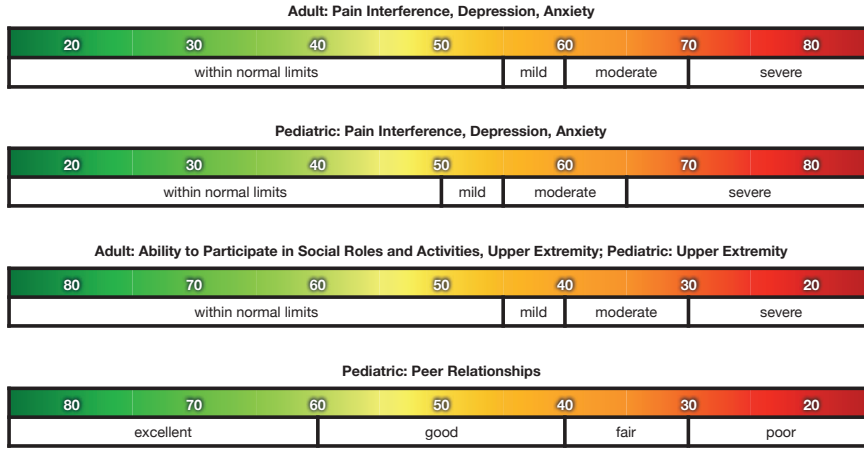

Figure 3. Interpreting PROMIS T-scores for adult and pediatric domains.

RESULTS

Patient characteristics

An overview of the patient characteristics is shown in Table 1. Of the 207 persons who opened the survey, 133 (64%) completed the survey. Participants' mean age was 34.8±12.5, with 116 adults and seventeen children. Nearly all participants (99%) were assigned female gender at birth. A total of 55 participants (41%) reported that they had undergone previous surgical correction of the wrist with a mean age of 20.5±9.5 at their first surgery and a mean of 2.4±2.7 surgeries in total per participant. The majority of participants (92%) reported the deformity to occur bilaterally.

PROMIS outcomes

Descriptive data of the PROMIS short forms are presented for adults and children in Table 2 and Table 3 respectively. Mean PROMIS scores for adults were as follows: pain intensity 4.9±2.8, pain interference 57.6±10.0, upper extremity 35.2±8.1, depression 53.8±11.1, anxiety 55.4±11.4, and ability to participate in social roles and activities 42.5±7.7. No significant differences were found between patients who underwent surgery and those who did not. Mean scores for children were: pain intensity 5.0±2.8, pain interference 55.7±11.3, upper extremity function 24.6±10.4, depressive symptoms 57.7±11.3, anxiety 57.3±11.9, and peer relationships 42.2±10.3. A significantly lower level of pain interference was seen in pediatric patients who underwent surgery (51.0±12.0 versus 62.3±5.2; P=0.045).

Correlations between PROMIS short forms

Correlations between the PROMIS short form scores are shown in Table 4 for adults and Table 5 for children. Notably, upper extremity function showed an inversely high correlation with pain intensity (ρ = -0.67), pain interference (ρ = -0.70), and depression (ρ = -0.54) in adults, and with pain intensity (ρ = -0.64) and pain interference (ρ = -0.66) in children.

Table 1. Patient characteristics.

	Madelung deformity (n=133)	Adult (n=116)	Children (n=17)
Age, y	34.8±12.5	37.6±10.8	15.6±2.8
Age at diagnosis, y	19.4±11.3	20.5±11.6	11.7±2.4
Female	132 (99%)	115 (99%)	17 (100%)
Height, cm	156.9±9.7	157.0±9.6	156.2±10.4
Weight, kg	71.1±21.1	73.7±21.1	52.8±8.8
Body mass index	28.8±8.3	29.9±8.3	21.6±2.6
Right hand dominance	118 (89%)	102 (88%)	16 (94%)
Bilateral deformity	123 (92%)	107 (92%)	16 (94%)
Familiar history	62 (47%)	58 (50%)	4 (24%)
Confirmed genetic mutation	37 (28%)	32 (28%)	5 (29%)
Analgesics use	65 (49%)	57 (49%)	8 (47%)
Underwent surgery	55 (41%)	45 (39%)	10 (59%)
Age at first surgery, y	20.5±9.5	21.8±9.9	14.6±4.3
Mean number of surgeries	2.4±2.7	2.4±2.9	2.1±1.4

Table 2. Mean PROMIS scores in adults with Madelung deformity.

	Madelung deformity (n=116)	Unoperated patients (n=71)	Operated patients (n=45)	P
Pain Intensity	4.9±2.8	4.7±2.8	5.0±2.9	0.567
Pain Interference	57.6±10.0	57.2±10.5	58.3±9.1	0.650
Upper Extremity	35.2±8.1	36.2±8.2	33.5±7.6	0.081
Depression	53.8±11.1	53.5±10.5	54.3±12.1	0.692
Anxiety	55.4±11.4	54.9±11.3	56.1±11.4	0.733
Social[a]	42.5±7.7	43.0±7.6	41.8±7.8	0.455

[a]Ability to Participate in Social Roles and Activities.

Table 3. Mean PROMIS scores in children with Madelung deformity.

	Madelung deformity (n=17)	Unoperated patients (n=7)	Operated patients (n=10)	P
Pain Intensity	5.0±2.8	6.3±2.2	4.1±2.8	0.129
Pain Interference	55.7±11.3	62.3±5.2	51.0±12.0	**0.045**
Upper Extremity Function	24.6±10.4	21.7±8.2	26.7±11.3	0.363
Depressive Symptoms	57.7±11.3	57.9±11.6	57.5±11.2	0.943
Anxiety	57.3±11.9	59.3±14.0	56.0±10.0	0.607
Peer Relationships	42.2±10.3	42.1±5.7	42.3±12.5	0.969

Table 4. Spearman's Rank Correlation for PROMIS scores in adults with Madelung deformity.

	Pain Intensity	Pain Interference	Upper Extremity Function	Depression	Anxiety	Social*
Pain Intensity	—	0.80	-0.67	0.37	0.32	-0.74
Pain Interference	0.80	—	-0.70	0.46	0.46	-0.81
Upper Extremity Function	-0.67	-0.70	—	-0.54	-0.48	0.80
Depression	0.37	0.46	-0.54	—	0.76	-0.50
Anxiety	0.32	0.46	-0.48	0.76	—	-0.46
Social*	-0.74	-0.81	0.80	-0.50	-0.46	—

[a]Ability to Participate in Social Roles and Activities.

Table 5. Spearman's Rank Correlation for PROMIS scores in children with Madelung deformity.

	Pain Intensity	Pain Interference	Upper Extremity Function	Depressive Symptoms	Anxiety	Peer Relationships
Pain Intensity	—	0.79	-0.64	0.52	0.30	-0.45
Pain Interference	0.79	—	-0.66	0.24	0.27	-0.17
Upper Extremity Function	-0.64	-0.66	—	-0.04	0.07	0.01
Depressive Symptoms	0.52	0.24	-0.04	—	0.67	-0.54
Anxiety	0.30	0.27	0.07	0.67	—	-0.41
Peer Relationships	-0.45	-0.17	0.01	-0.54	-0.41	—

DISCUSSION

This cross-sectional survey highlights Madelung deformity's impact from the patient perspective, showing significant effects of the disease on one's physical, mental, and social health. Even after surgical treatment, the health burden of this congenital hand difference remains. Despite Madelung deformity's rarity, we were able to engage a relatively broad international audience through the use of social media, allowing us to assess patient outcomes and determine demographic characteristics.

Demographic characteristics

The overwhelmingly female patient composition and bilateral occurrence of Madelung deformity have been extensively described;[16,40,41] however, no population-based data or epidemiological studies are available. Therefore, our knowledge in regard to demographic characteristics has been derived from small-powered studies.[11,22,42,43] Mean reported adult patient height in our study was 157 cm (5'2"), which is at the 27th percentile for females in the United States. Previous studies reported average heights of 159 cm or below standard heights at the 19th percentile,[5,44] not surprising given that a substantial proportion of Madelung deformity patients have confirmed SHOX gene mutations, which is strongly associated with short stature and dyschondrosteosis.[8,9] Of our

participants, 28% reported having this genetic mutation, and 47% reported on Madelung deformity occurring in family members. Interestingly, it has been hypothesized that a substantial amount of patients have underlying diagnoses of dyschondrosteosis.[12,45] The collection of genetic material in future prospective studies, as recommended in a previously published protocol[18], will hopefully provide a definite answer.

Pain

While the often-reported pain is the primary indication for surgical treatment, its quantification in a pre- or postoperative setting has not been consistent. Some studies measured pain using an NRS or VAS, reporting preoperative scores of 9/10 and 50/100, and postoperative scores of 0/10 and 22.5/100, respectively.[46,47] One study using a 'Pain Score' (0 = requiring narcotic mediation, 30 = no pain) reported scores of 14.5 before, and 25.0 after surgery.[48] Another study only reported preoperative measurements of 3.3/4 (0 = no pain, 4 = continuous pain).[11] This widely heterogeneous registration of pain is suboptimal, and studies should quantify pain in an analogous manner utilizing a VAS or NRS, both before and after surgery, without merging the variable in a 'wrist score'.[19] In this study, we not only recorded pain intensity, but also highlighted the consequences of pain on a person's life,[49] showing mild interference in adults, moderate interference in children who did not undergo surgery, and mild interference in children who underwent surgery; notably, 49% of participants reported the use of analgesics. The presence of pain in surgical patients postoperatively seems in stark contrast to the literature. On the one hand, there is potential for bias in this cross-sectional survey study as symptomatic persons might be more vocal about their symptoms and engage in social media communities. On the other hand, it may be that a short follow-up period or loss of follow-up results in underreporting of this outcome in literature, as most studies have not quantified pain or have only reported preoperative measurements.[11,18] Nevertheless, in future studies we would be most interested in the difference between preoperative and postoperative pain instead of single cross-sectional measurements.

Upper extremity function

The Oberg-Manske-Tonkin (OMT) classification, a proven and adopted classification framework for congenital hand and upper limb anomalies,[24,50] most recently re-classified Madelung deformity as an entire upper limb malformation of the radioulnar (anteroposterior) axis (OMT type IA2.vii).[51] A previous study applying PROMIS to congenital hand anomalies, reports median upper extremity scores of 37 (<11 years) and 45 (11-17 years) in children with entire limb malformations (OMT type IA), and worse upper extremity function in children with bilateral compared to unilateral deformities.[25] In contrast, another study reported scores within the normal range in 41 children (5-17 years) with a similar OMT type.[52] Our results show moderately impaired functioning in adults (35.2±8.1) and severely impaired functioning in children (24.6±10.4). A noteworthy point is the slightly lower postoperative score in adults and a slightly higher score in children, albeit not significant. The results of our study, which mainly involves data entries from adults with Madelung deformity (a subset of type IA malformations), can unfortunately not be compared to these aforementioned studies.

However, the bilateral occurrence (92%), the lack of consensus regarding optimal treatment, and the relatively late age of onset, diagnosis, and corrective surgery might all play a role in decreased upper extremity function.[15,53]

Mental and social health

Our findings suggest that Madelung deformity has a significant impact on one's mental and social health. We found that both adults and children experience higher levels of depression and anxiety in comparison to population norms. For adult patients, we found slightly increased depression levels still within normal limits and a mild level of anxiety. For children, depression and anxiety levels were both moderate. Scores varied widely, and both groups included patients with severe levels of depression and anxiety. Regarding social health, adults reported a mildly decreased ability to participate in social roles and activities compared to the general population. Children reported good peer relationships; however, scores again ranged widely, with 53% reporting fair to poor peer relationships. To our knowledge, no other studies on mental or social health in patients with Madelung deformity exist. Previous studies of other congenital upper extremity differences have reported varying results in regard to mental and social health outcomes, ranging from no effect to significant impairments.[23,25] It could be argued that Madelung deformity is associated with higher levels of pain compared to other congenital upper limb differences, in turn resulting in poorer mental and social health.

Associations between physical, mental, and social health

For both adults and children, decreased physical health appears to be associated with decreased mental and social health levels. Pain and impaired physical functioning have bidirectional associations with depression,[54] anxiety,[55] and social participation.[56,57] It is plausible that pain and impaired function leads to a vicious circle with decreased levels of physical, mental, and social health, emphasizing the need for treatments improving pain and functioning. Moreover, it also highlights the need for psychological screening and support in both initial work-up and post-surgical follow-up.

Future applications and social media

The patient perspective is crucial in the treatment of rare congenital anomalies. For most rare diseases, it is unfeasible to develop disease-specific measures or conduct methodologically sound validation studies due to insufficient patient numbers.[30-32] As demonstrated by Timberlake et al., social media appears to be a potentially useful tool to study these specific populations,[28] however, an implementation to investigate patient outcomes has not been described. We were able to engage a considerable international audience, compensating the low patient numbers as seen in single-center and even multicenter study designs,[26] by harnessing social media to assess patient outcomes in a rare population. We believe that selecting an appropriate survey or questionnaire is paramount; PROMIS offers a suitable solution, given that its measurement properties have been thoroughly examined, and it is intended for use in every patient population, including the variety

of congenital hand differences.[29] The possibility of distributing PROMIS with short forms or computer-adaptive tests allows for the measurement of multiple health domains with relatively few questions,[58] enabling a full assessment of a patient's health status without being too much of a burden, whilst taking into consideration the importance of material readability.[59] Moving forward, the relatively low presence of surgeons and academic institutions on social media platforms has been demonstrated, and there is substantial room for improvement both for research and education.[60] As clinicians need to gain a full understanding of the burden their patients carry, the combination of our and previous study designs utilizing social media surveys[61,62] could serve as a blueprint for assessing the health status of other rare conditions.

Limitations

The main limitation was that our survey data was obtained from social media communities on Facebook and Instagram, making the methodology prone to self-reporting bias.[63] Additionally, while we limited the survey to participants with 'diagnosed' Madelung deformity after a medical assessment, the possibility remained that an undiagnosed or wrongly diagnosed (e.g., post-traumatic 'Madelung-like' deformity) person would participate. That being said, we considered the probability of obtaining incorrect data to be relatively limited, as each entry was checked manually, and questions were added for screening purposes. Lastly, we did not distribute our survey on the social media platform Twitter. However, since it has the fewest patient users and minimal engagement we believe the effect on inclusions to be negligible.[64] Despite these limitations, to the best of our knowledge, this is the largest study on Madelung deformity outcomes and the first to assess the patient outcomes in regard to physical, mental, and social health. We used PROMIS as a self-assessment tool, which has been extensively validated in large populations and proven to be more feasible than other known instruments for patients with congenital hand differences.[65-68]

Conclusion

Madelung deformity has significant effects on patients' physical, mental, and social well-being. Even after surgical treatment, the health burden of this congenital hand difference is observed. Using social media, we were able to compensate for Madelung deformity's rarity by engaging an international audience, demonstrating the feasibility to conduct research through it, and providing a global perspective of the disease entity.

REFERENCES

1. Madelung O. Die spontane Subluxation der Hand nach vorne. ***Verh Dtsch Ges Chir.*** 1878;7:259-276.
2. Arora AS, Chung KC. Otto W. Madelung and the recognition of Madelung's deformity. ***J Hand Surg Am.*** 2006;31(2):177-182.
3. Anton JI, Reitz GB, Spiegel MB. Madelung's Deformity. ***Ann Surg.*** 1938;108(3):411-439.
4. Dannenberg M, Anton J, Spiegel M. Madelung's deformity: consideration of its roentgenological diagnostic criteria. ***Am J Roentgenol.*** 1939;42:671-676.
5. Schmidt-Rohlfing B, Schwobel B, Pauschert R, Niethard FU. Madelung deformity: clinical features, therapy and results. ***J Pediatr Orthop B.*** 2001;10(4):344-348.
6. Harley BJ, Carter PR, Ezaki M. Volar surgical correction of Madelung's deformity. ***Tech Hand Up Extrem Surg.*** 2002;6(1):30-35.
7. Stehling C, Langer M, Nassenstein I, Bachmann R, Heindel W, Vieth V. High resolution 3.0 Tesla MR imaging findings in patients with bilateral Madelung's deformity. ***Surg Radiol Anat.*** 2009;31(7):551-557.
8. Clement-Jones M, Schiller S, Rao E, et al. The short stature homeobox gene SHOX is involved in skeletal abnormalities in Turner syndrome. ***Hum Mol Genet.*** 2000;9(5):695-702.
9. Belin V, Cusin V, Viot G, et al. SHOX mutations in dyschondrosteosis (Leri-Weill syndrome). ***Nature genetics.*** 1998;19(1):67-69.
10. Flatt AE. ***The care of congenital hand anomalies.*** Quality Medical Publishing; 1994.
11. Saffar P, Badina A. Treatment of Madelung's deformity. ***Chirurgie de la Main.*** 2015;34(6):279-285.
12. Herdman RC, Langer LO, Good RA. Dyschondrosteosis. The most common cause of Madelung's deformity. ***The Journal of pediatrics.*** 1966;68(3):432-441.
13. Henry A, Thorburn MJ. Madelung's deformity. A clinical and cytogenetic study. ***The Journal of bone and joint surgery British volume.*** 1967;49(1):66-73.
14. Grigelioniene G, Eklof O, Ivarsson SA, et al. Mutations in short stature homeobox containing gene (SHOX) in dyschondrosteosis but not in hypochondroplasia. ***Human Genetics.*** 2000;107(2):145-149.
15. Dubey A, Fajardo M, Green S, Lee SK. Madelung's deformity: a review. ***The Journal of hand surgery, European volume.*** 2009;35(3):174-181.
16. Ghatan AC, Hanel DP. Madelung deformity. ***J Am Acad Orthop Surg.*** 2013;21(6):372-382.
17. Kozin SH, Zlotolow DA. Madelung Deformity. ***J Hand Surg Am.*** 2015;40(10):2090-2098.
18. Peymani A, Johnson AR, Dowlatshahi AS, et al. Surgical Management of Madelung Deformity: A Systematic Review. ***Hand (N Y).*** 2019;14(6):725-734.
19. Bruno RJ, Blank JE, Ruby LK, Cassidy C, Cohen G, Bergfield TG. Treatment of Madelung's deformity in adults by ulna reduction osteotomy. ***J Hand Surg Am.*** 2003;28(3):421-426.
20. Kampa R, Al-Beer A, Axelrod T. Madelung's deformity: radial opening wedge osteotomy and modified Darrach procedure using the ulnar head as trapezoidal bone graft. ***The Journal of hand surgery, European volume.*** 2010;35(9):708-714.
21. Mallard F, Jeudy J, Rabarin F, et al. Reverse wedge osteotomy of the distal radius in Madelung's deformity. ***Orthop Traumatol Surg Res.*** 2013;99(4 Suppl):S279-283.

22. Steinman S, Oishi S, Mills J, Bush P, Wheeler L, Ezaki M. Volar ligament release and distal radial dome osteotomy for the correction of Madelung deformity: long-term follow-up. ***J Bone Joint Surg Am.*** 2013;95(13):1198-1204.

23. Franzblau LE, Chung KC, Carlozzi N, Chin AY, Nellans KW, Waljee JF. Coping with congenital hand differences. ***Plast Reconstr Surg.*** 2015;135(4):1067-1075.

24. Bae DS, Canizares MF, Miller PE, et al. Intraobserver and Interobserver Reliability of the Oberg-Manske-Tonkin (OMT) Classification: Establishing a Registry on Congenital Upper Limb Differences. ***J Pediatr Orthop.*** 2018;38(1):69-74.

25. Bae DS, Canizares MF, Miller PE, Waters PM, Goldfarb CA. Functional Impact of Congenital Hand Differences: Early Results From the Congenital Upper Limb Differences (CoULD) Registry. ***J Hand Surg Am.*** 2018;43(4):321-330.

26. Goldfarb CA, Wall LB, Bohn DC, Moen P, Van Heest AE. Epidemiology of congenital upper limb anomalies in a midwest United States population: an assessment using the Oberg, Manske, and Tonkin classification. ***J Hand Surg Am.*** 2015;40(1):127-132 e121-122.

27. Peymani A, Dobbe JGG, Streekstra GJ, McCarroll HR, Strackee SD. Quantitative three-dimensional assessment of Madelung deformity. ***The Journal of hand surgery, European volume.*** 2019;44(10):1041-1048.

28. Timberlake AT, Wu RT, Cabrejo R, Gabrick K, Persing JA. Harnessing Social Media to Advance Research in Plastic Surgery. ***Plast Reconstr Surg.*** 2018;142(4):1094-1100.

29. Cella D, Riley W, Stone A, et al. The Patient-Reported Outcomes Measurement Information System (PROMIS) developed and tested its first wave of adult self-reported health outcome item banks: 2005-2008. ***J Clin Epidemiol.*** 2010;63(11):1179-1194.

30. Sabino G, Mills A, Jonker A, Lau L, Ayme S. Patient-centered outcome measures in the field of rare diseases. ***Task Force on Patient-Centered Outcome Measures, IRDiRC.*** 2016:30.

31. Benjamin K, Vernon MK, Patrick DL, Perfetto E, Nestler-Parr S, Burke L. Patient-Reported Outcome and Observer-Reported Outcome Assessment in Rare Disease Clinical Trials: An ISPOR COA Emerging Good Practices Task Force Report. ***Value Health.*** 2017;20(7):838-855.

32. Slade A, Isa F, Kyte D, et al. Patient reported outcome measures in rare diseases: a narrative review. ***Orphanet J Rare Dis.*** 2018;13(1):61.

33. Doring AC, Nota SP, Hageman MG, Ring DC. Measurement of upper extremity disability using the Patient-Reported Outcomes Measurement Information System. ***J Hand Surg Am.*** 2014;39(6):1160-1165.

34. Hung M, Stuart AR, Higgins TF, Saltzman CL, Kubiak EN. Computerized Adaptive Testing Using the PROMIS Physical Function Item Bank Reduces Test Burden With Less Ceiling Effects Compared With the Short Musculoskeletal Function Assessment in Orthopaedic Trauma Patients. ***J Orthop Trauma.*** 2014;28(8):439-443.

35. Tyser AR, Beckmann J, Franklin JD, et al. Evaluation of the PROMIS physical function computer adaptive test in the upper extremity. ***J Hand Surg Am.*** 2014;39(10):2047-2051 e2044.

36. Phillips JLH, Freedman MK, Simon JI, Beredjiklian PK. The PROMIS Upper Extremity Computer Adaptive Test Correlates With Previously Validated Metrics in Patients With Carpal Tunnel Syndrome. ***Hand (N Y).*** 2019:1558944719851182.

37. Liu H, Cella D, Gershon R, et al. Representativeness of the Patient-Reported Outcomes Measurement Information System Internet panel. ***J Clin Epidemiol.*** 2010;63(11):1169-1178.

38. Rothrock NE, Hays RD, Spritzer K, Yount SE, Riley W, Cella D. Relative to the general US population, chronic diseases are associated with poorer health-related quality of life as measured by the Patient-Reported Outcomes Measurement Information System (PROMIS). ***J Clin Epidemiol.*** 2010;63(11):1195-1204.

39. De Vet HC, Terwee CB, Mokkink LB, Knol DL. ***Measurement in medicine: a practical guide.*** Cambridge University Press; 2011.

40. Golding JS, Blackburne JS. Madelung's disease of the wrist and dyschondrosteosis. ***The Journal of bone and joint surgery British volume.*** 1976;58(3):350-352.

41. Dobyns J. Madelung's deformity. ***Operative Hand Surgery.*** 1993;11:515-520.

42. Angelini LC, Leite VM, Faloppa F. Surgical treatment of Madelung disease by the Sauve-Kapandji technique. ***Ann Chir Main Memb Super.*** 1996;15(4):257-264.

43. dos Reis FB, Katchburian MV, Faloppa F, Albertoni WM, Laredo Filho J, Jr. Osteotomy of the radius and ulna for the Madelung deformity. ***The Journal of bone and joint surgery British volume.*** 1998;80(5):817-824.

44. Zebala LP, Manske PR, Goldfarb CA. Madelung's deformity: a spectrum of presentation. ***J Hand Surg Am.*** 2007;32(9):1393-1401.

45. Langer LO, Jr. Dyschondrosteosis, a Hereditable Bone Dysplasia with Characteristic Roentgenographic Features. ***Am J Roentgenol Radium Ther Nucl Med.*** 1965;95:178-188.

46. Houshian S, Schroder HA, Weeth R. Correction of Madelung's deformity by the Ilizarov technique. ***The Journal of bone and joint surgery British volume.*** 2004;86(4):536-540.

47. Aharoni C, Glard Y, Launay F, Gay A, Legre R. Madelung deformity: isolated ulnar wedge osteotomy. [French]. ***Chirurgie de la Main.*** 2006;25(6):309-314.

48. Glard Y, Gay A, Launay F, Guinard D, Legre R. Isolated wedge osteotomy of the ulna for mild Madelung's deformity. ***J Hand Surg Am.*** 2007;32(7):1037-1042.

49. Amtmann D, Cook KF, Jensen MP, et al. Development of a PROMIS item bank to measure pain interference. ***Pain.*** 2010;150(1):173-182.

50. Tonkin MA, Tolerton SK, Quick TJ, et al. Classification of congenital anomalies of the hand and upper limb: development and assessment of a new system. ***J Hand Surg Am.*** 2013;38(9):1845-1853.

51. Goldfarb CA, Ezaki M, Wall LB, Lam WL, Oberg KC. The Oberg-Manske-Tonkin (OMT) Classification of Congenital Upper Extremities: Update for 2020. ***J Hand Surg Am.*** 2020.

52. Manske MCB, Abarca N, James MA. Comparison of Patient-Reported Outcomes Measurement Information System (PROMIS) Scores for Children with Congenital Hand and Upper-Limb Malformations: Level 1 Evidence. ***J Hand Surg Am.*** 2018;43(9):S22-S23.

53. Nielsen JB. Madelung's deformity. A follow-up study of 26 cases and a review of the literature. ***Acta orthopaedica Scandinavica.*** 1977;48(4):379-384.

54. Bair MJ, Robinson RL, Katon W, Kroenke K. Depression and pain comorbidity: a literature review. ***Arch Intern Med.*** 2003;163(20):2433-2445.

55. Kroenke K, Outcalt S, Krebs E, et al. Association between anxiety, health-related quality of life and functional impairment in primary care patients with chronic pain. ***Gen Hosp Psychiatry.*** 2013;35(4):359-365.

56. Gureje O, Von Korff M, Kola L, et al. The relation between multiple pains and mental disorders: results from the World Mental Health Surveys. ***Pain.*** 2008;135(1-2):82-91.

57. de Heer EW, Gerrits MM, Beekman AT, et al. The association of depression and anxiety with pain: a study from NESDA. ***PLoS One.*** 2014;9(10):e106907.

58. Cella D, Gershon R, Lai JS, Choi S. The future of outcomes measurement: item banking, tailored short-forms, and computerized adaptive assessment. ***Qual Life Res.*** 2007;16 Suppl 1:133-141.

59. Chen AD, Ruan QZ, Bucknor A, et al. Social Media: Is the Message Reaching the Plastic Surgery Audience? ***Plast Reconstr Surg.*** 2019;144(3):773-781.

60. Maldonado AA, Lemelman BT, Le Hanneur M, et al. Analysis of #PlasticSurgery in Europe: An Opportunity for Education and Leadership. ***Plast Reconstr Surg.*** 2019.

61. Chatterjee S, Humby T, Davies W. Behavioural and Psychiatric Phenotypes in Men and Boys with X-Linked Ichthyosis: Evidence from a Worldwide Online Survey. ***PLoS One.*** 2016;11(10):e0164417.

62. Davies W. Insights into rare diseases from social media surveys. ***Orphanet J Rare Dis.*** 2016;11(1):151.

63. Althubaiti A. Information bias in health research: definition, pitfalls, and adjustment methods. ***J Multidiscip Healthc.*** 2016;9:211-217.

64. Sorice SC, Li AY, Gilstrap J, Canales FL, Furnas HJ. Social Media and the Plastic Surgery Patient. ***Plast Reconstr Surg.*** 2017;140(5):1047-1056.

65. Hudak PL, Amadio PC, Bombardier C. Development of an upper extremity outcome measure: the DASH (disabilities of the arm, shoulder and hand) [corrected]. The Upper Extremity Collaborative Group (UECG). ***Am J Ind Med.*** 1996;29(6):602-608.

66. Chung KC, Hamill JB, Walters MR, Hayward RA. The Michigan Hand Outcomes Questionnaire (MHQ): assessment of responsiveness to clinical change. ***Ann Plast Surg.*** 1999;42(6):619-622.

67. Lerman JA, Sullivan E, Barnes DA, Haynes RJ. The Pediatric Outcomes Data Collection Instrument (PODCI) and functional assessment of patients with unilateral upper extremity deficiencies. ***J Pediatr Orthop.*** 2005;25(3):405-407.

68. Waljee JF, Carlozzi N, Franzblau LE, Zhong L, Chung KC. Applying the Patient-Reported Outcomes Measurement Information System to Assess Upper Extremity Function among Children with Congenital Hand Differences. ***Plast Reconstr Surg.*** 2015;136(2):200e-207e.

SUPPLEMENTAL DATA

Madelung Deformity Survey

1	**What is your age?**	
2	**What gender were you assigned at birth?**	□ Female □ Male □ Prefer not to say
3	**What is your height?**	
4	**What is your weight? (please add 'pounds' or 'kg')**	
5	**At what age (approximately) were you diagnosed with Madelung deformity?**	
6	**Which hand is your dominant hand?**	□ Left □ Right □ Both (ambidextrous)
7	**Which arm(s) is/are affected?**	□ Both (left and right) □ Left only □ Right only
8	**If you have any genetic conditions, please list below:**	
9	**If you have any other medical conditions, please list below:**	
10	**If you use any medication (including painkillers), please list below:**	
11	**If Madelung deformity occurs in your family, please list below:** *Example: mother, aunt on mother's side, etc.*	
12	**Have you ever had surgery for Madelung deformity?**	□ Yes □ No
13	**List all the surgeries you underwent for Madelung deformity. Include your age at surgery, which hand, and the name of the procedure (if you remember):** *Example: 19, left, osteotomy | 24, right, ligament release*	

Question 13 only appears if the answer to Question 12 was 'Yes'.

Supplementary File 1. Madelung Deformity Survey.

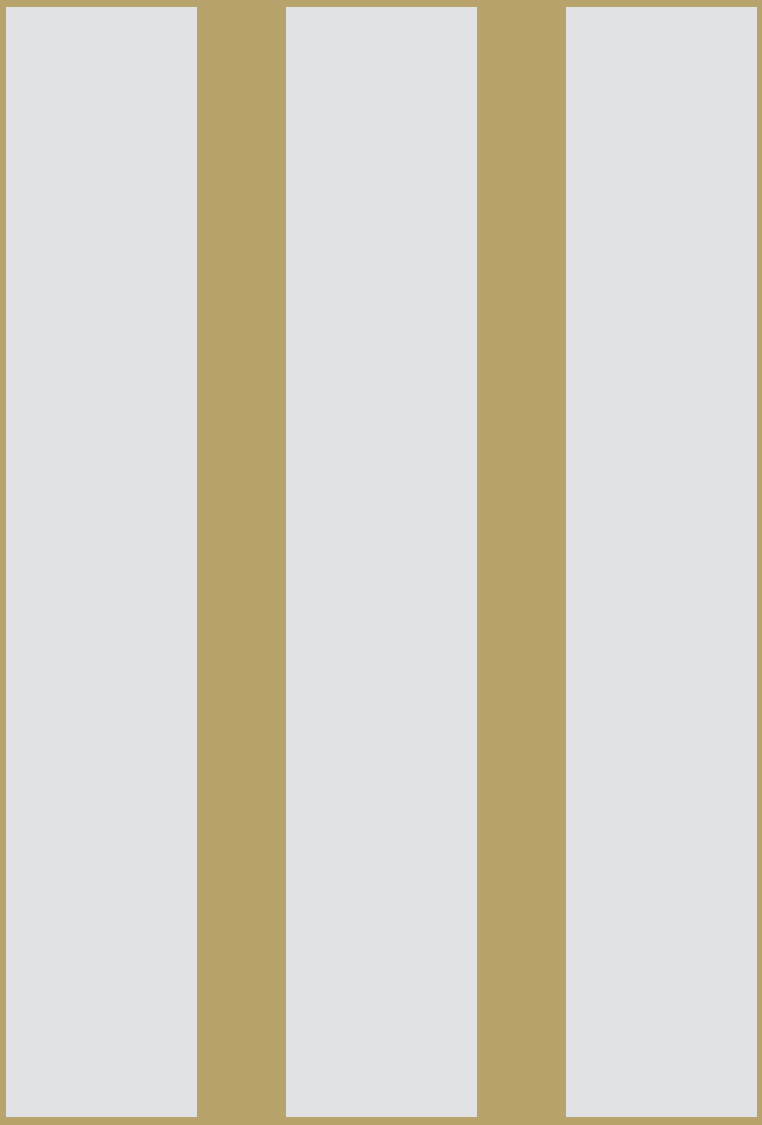

EVOLVING OUR APPROACH

4

COMPUTATIONAL ANALYSES OF THE WRIST: 3D, 4D, AND SHAPE

A. Peymani[1]

[1] Department of Plastic, Reconstructive and Hand Surgery, Amsterdam UMC, University of Amsterdam, Amsterdam, The Netherlands.

Based on: Peymani A, Foumani M, Dobbe JGG, Strackee SD, Streekstra GJ. Four-dimensional rotational radiographic scanning of the wrist in patients after proximal row carpectomy. J Hand Surg Eur Vol. 2017 Oct;42(8):846-851.

WRIST MOTION CAPTURE: FROM 3D TO 4D

Medical evaluations of the hand and wrist are often performed through two-dimensional (2D) representations of three-dimensional (3D) anatomy, resulting in limited diagnostic accuracy.[1,2] Obtaining computed tomography (CT) imaging allows for an assessment of relevant wrist anatomy in 3D. To further increase our understanding of wrist functioning, however, it is highly beneficial to evaluate the wrist in 3D during motion. Capturing wrist movement patterns has been made possible through so-called four-dimensional (4D) x-ray imaging.[3] First, the methodology involves using a static CT scan to obtain virtual three-dimensional (3D) models of the radius, ulna, and carpal bones through segmentation by the use of a previously described algorithm.[4] Next, using a regular 3D rotational X-ray system (BV Pulsera, Philips Healthcare, The Netherlands), the static CT scans are combined with dynamic scans made during three motions: flexion-extension motion, radio-ulnar deviation, and dart-throwing motion. Finally, virtual bone models are aligned with dynamic scans by registration, thereby quantifying motion patterns of wrist bones in vivo.[5,6] A motorized hand-shaker device[4] is used to move the wrist with an imposed range of motion (ROM) set for each patient individually to avoid any pain or discomfort. During each of the three motions, the X-ray source is rotated around the wrist to acquire 20 volume reconstructions, each reconstruction corresponding to a unique wrist position. Assessment of the resulting 4D rotational x-ray imaging data in a previous study has demonstrated a precision of 0.02±0.005 mm for translation and 0.12±0.07 degrees for rotation.[4]

OPENING DOORS: SURFACE AREA AND JOINT SPACE THICKNESS

Capturing movement patterns not only allows for visualization of osseous and ligamentous wrist pathology but also opens doors for quantification of wrist joint kinematics, crucially responsible for human hand functionality. Currently, individual articular cartilage layers cannot be visualized due to CT imaging limitations; however, the subchondral bone just below the cartilage layer is clearly definable. Total cartilage thickness in a joint space can therefore be approximated by determining the distance between opposing subchondral bones.

For each wrist position during motion, joint space thickness can be calculated using a previously developed methodology.[6] To this end, for each point on a bone, the nearest point to the opposite bone is determined using a k-Nearest Neighbors algorithm. To filter points contributing to the articular surface, two constraints are applied. First, the distance between a point on a bone and a point on an opposite bone should be less than 4 mm. The second constraint is a maximum angle difference of 15 degrees between the normal vector of a point (vector perpendicular to the bone surface) and the normal vector of an opposite point. Thresholds of 4 mm and 15 degrees are chosen pragmatically.[6] Joining all these points during motion provides the articular surface area defined as the area on the radius with which the carpal bones articulates (Figure 2).

The minimum distance to the opposite bone during motion is determined for each point, representing a situation where articular cartilage layers are minimal. The mean of these distances for all points in the articular surface area provides the joint space thickness. The joint space

thickness and articular surface areas can be recalculated for the combination of flexion-extension motion, radio-ulnar deviation, and dart-throwing motion (60 wrist positions in all).

Figure 1.

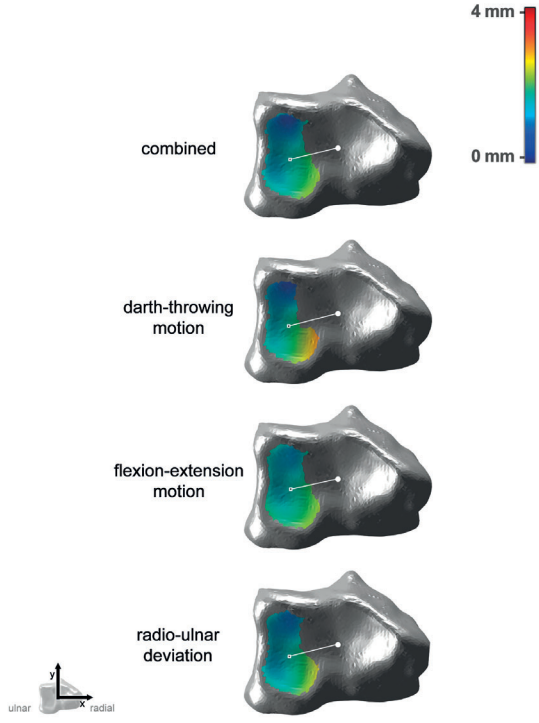

Figure 2. Articular surface areas of the radius with the lunate. The color map indicates the shortest distance to the neighboring bone during the entire motion.

A SIMPLE ANALYSIS OF SHAPE

To enable shape analyses of virtual 3D models of the bones, one can describe a bone as an ellipsoid with the gravitational axes[7] of lengths (ranked in order, from largest to smallest) A, B, and C (Figure 3). Quantifying an anatomical shape (i.e., converting it into numbers) allows us to make comparisons. This quantification can help compare the anatomy between healthy volunteers and patients and track changes over time due to altered biomechanics.

APPLICATIONS IN MADELUNG DEFORMITY

The techniques mentioned in the former paragraphs (3D, 4D, and shape analysis) were first applied in a previously published study, included in the addendum of this thesis for your reference.[8] Building on these foundations, we further developed each of these techniques, making them applicable for studying anatomical changes in wrists of Madelung deformity patients. The 4D imaging technique was evolved to use dynamic CT imaging, using a Philips Brilliance 64 CT Scanner (Philips, Cleveland, OH), in addition to the static CT scan obtained for segmentation. Also, instead of using a motorized hand-shaker device to move the wrist with an imposed ROM,[4] we custom-developed a new hand positioning device, allowing patients to perform full wrist motion with either flexion-extension or radio-ulnar deviation. The new hand positioning device allows for natural wrist motion instead of a machine-induced movement pattern with a limited ROM. In our Madelung deformity patients, this improved combination of hardware was used to capture wrist motion, visualize and quantify kinematics, and calculate surface area and joint space thickness of the wrist joints.

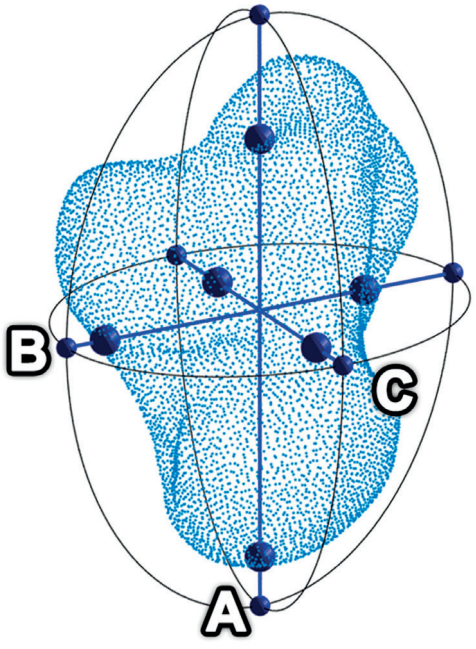

Figure 3. The capitate bone is represented as an ellipsoid with axes A, B, and C.

Our aforementioned methodology of studying shape through quantification is relatively simple and easily reproducible in future imaging studies. It was first used to quantify capitate bone shape to investigate left-right symmetry and analyze the wrist's adaptive capacity after altering its anatomical configuration.[8] As the anatomical changes in Madelung deformity are quite prominent, it would be interesting to use the same technique to quantify these changes, advancing our understanding to potentially improve diagnostic criteria and surgical management. As the complex anatomy in Madelung deformity requires a more delicate and thorough analysis of shape, we collaborated with the Graphics and Vision Research Group at the University of Basel, developers of the leading 3D statistical shape modeling library 'Scalismo'.[9] In addition to providing an extensive online course on shape modeling through the FutureLearn learning platform (www.futurelearn.com), the developers offer a week-long summer program to expand on the theoretical basis of shape modeling. We further developed and implemented these techniques for the distal radius in Madelung deformity, using the resulting quantifications to visualize the anatomical spectrum and advance our diagnostic toolkit.

REFERENCES

1. Balci A, Basara I, Cekdemir EY, Tetik F, Aktas G, Acarer A, et al. Wrist fractures: sensitivity of radiography, prevalence, and patterns in MDCT. ***Emerg Radiol.*** 2015;22(3):251-256.
2. Jorgsholm P, Thomsen NO, Besjakov J, Abrahamsson SO, Bjorkman A. The benefit of magnetic resonance imaging for patients with posttraumatic radial wrist tenderness. ***J Hand Surg Am.*** 2013;38(1):29-33.
3. Carelsen B, Bakker NH, Strackee SD, Boon SN, Maas M, Sabczynski J, et al. 4D rotational x-ray imaging of wrist joint dynamic motion. ***Med Phys.*** 2005;32(9):2771-2776.
4. Carelsen B, Jonges R, Strackee SD, Maas M, van Kemenade P, Grimbergen CA, et al. Detection of in vivo dynamic 3-D motion patterns in the wrist joint. ***IEEE Trans Biomed Eng.*** 2009;56(4):1236-1244.
5. Foumani M, Strackee SD, Jonges R, Blankevoort L, Zwinderman AH, Carelsen B, et al. In-vivo three-dimensional carpal bone kinematics during flexion-extension and radio-ulnar deviation of the wrist: Dynamic motion versus step-wise static wrist positions. ***J Biomech.*** 2009;42(16):2664-2671.
6. Foumani M, Strackee SD, van de Giessen M, Jonges R, Blankevoort L, Streekstra GJ. In-vivo dynamic and static three-dimensional joint space distance maps for assessment of cartilage thickness in the radiocarpal joint. ***Clin Biomech (Bristol, Avon).*** 2013;28(2):151-156.
7. Goldstein H, Poole C, Safko J. Classical mechanics. 3rd. In: Addison Wesley; 2002.
8. Peymani A, Foumani M, Dobbe JGG, Strackee SD, Streekstra GJ. Four-dimensional rotational radiographic scanning of the wrist in patients after proximal row carpectomy. ***J Hand Surg Eur Vol.*** 2017;42(8):846-851.
9. Lüthi M, Gerig T, Jud C, Vetter T. Gaussian process morphable models. ***IEEE transactions on pattern analysis and machine intelligence.*** 2017;40(8):1860-1873.

5

QUANTITATIVE THREE-DIMENSIONAL ASSESSMENT OF MADELUNG DEFORMITY

A. Peymani[1,2], J.G.G. Dobbe[2], G.J. Streekstra[2,3],
H.R. McCarroll[4], S.D. Strackee[1]

[1] Department of Plastic, Reconstructive and Hand Surgery, Amsterdam UMC, University of Amsterdam, Amsterdam, The Netherlands.
[2] Department of Biomedical Engineering and Physics, Amsterdam UMC, University of Amsterdam, Amsterdam, The Netherlands.
[3] Department of Radiology and Nuclear Medicine, Amsterdam UMC, University of Amsterdam, Amsterdam, The Netherlands.
[4] Department of Orthopaedic Surgery, California Pacific Medical Center, San Francisco, CA, USA.

J Hand Surg Eur Vol. 2019 Dec;44(10):1041-1048.

ABSTRACT

In the diagnostic work-up of Madelung deformity, conventional radiographic imaging is often used, assessing the three-dimensional deformity in a two-dimensional manner. A three-dimensional approach could expand our understanding of Madelung deformity's complex wrist anatomy while removing inter- and intra-rater differences. We measured previous two-dimensional-based and newly developed three-dimensional-based parameters in eighteen patients with Madelung deformity (28 wrists) and 35 healthy participants (56 wrists). Madelung deformity wrists have increased levels of ulnar tilt, lunate subsidence, lunate fossa angle, and palmar carpal displacement. The lunate fossa is more concave and irregular, and angles between scaphoid, lunate, and triquetral bones are decreased. These findings validate the underlying principles of current two-dimensional criteria and reveal previously unknown anatomical abnormalities by utilizing novel three-dimensional parameters to quantify the radiocarpal joint.

INTRODUCTION

Guillaume Dupuytren presented the first case of a rare wrist deformity[1]. Otto Wilhelm Madelung was the first, however, to publish an in-depth analysis of the condition that later came to bear his name[2]. Madelung deformity is an uncommon congenital deformity characterized by volar subluxation of the hand, dislocation of the ulna, and ulnar and volar angulation of the distal radial epiphysis.

Various two-dimensional (2D) radiographic criteria have been proposed for the diagnostic work-up, with the McCarroll criteria currently being the most used.[3] These criteria are based on manual X-ray measurements, thereby introducing inter- and intra-rater differences and reducing the complex three-dimensional (3D) anatomy to a 2D view. This 2D assessment has shown to be of limited diagnostic value[4,5] and has prevented the quantification of several clinical features, including abnormalities of the lunate fossa and the proximal carpal row[6]. Nearly all previous studies have evaluated the deformity in 2D form, with the majority adhering to the McCarroll criteria.[7-11]

This study investigates the 3D anatomy of Madelung deformity in eighteen patients. The reusability of previous 2D criteria is investigated, and new 3D parameters are developed. This automatic and objective approach could expand our understanding of Madelung deformity's complex anatomy while removing inter- and intra-rater differences.

MATERIALS AND METHODS

Study population

Patients with a diagnosis of Madelung deformity were identified by searching the electronic medical record database of our hospital, using the International Classification of Diseases, Ninth Revision, Clinical Modification (ICD-9-CM) code: 755.54. Patients that visited our medical center between 2002 and 2018 for outpatient or inpatient care in our department were identified. Patients were included if they had undergone CT scanning of at least one wrist prior to any surgical interventions. The accuracy of the ICD-9-CM codes was confirmed by reviewing medical notes of each patient; wrongly coded patients were excluded. In total, eighteen patients were included, for which CT scans of 28 wrists were available. In addition, previously acquired CT scans of 56 wrists from 35 healthy participants (21 bilateral, fourteen unilateral) were included to quantitatively investigate anatomical differences. None of the healthy participants had a medical history of disorders or a history of surgical interventions on the wrists.

Image segmentation and processing

CT scans were segmented using a custom-made software package,[12] to acquire virtual 3D models of the following wrist bones: radius, ulna, scaphoid, lunate, triquetrum, and capitate (Figure 1). These virtual models were exported and further processed using self-developed software programmed in MATLAB R2018b (MathWorks Inc., Natick, MA, USA). This software performs the following functions automatically: wrist alignment, detection of radial and ulnar landmarks, and calculation of multiple 3D-based measurements.

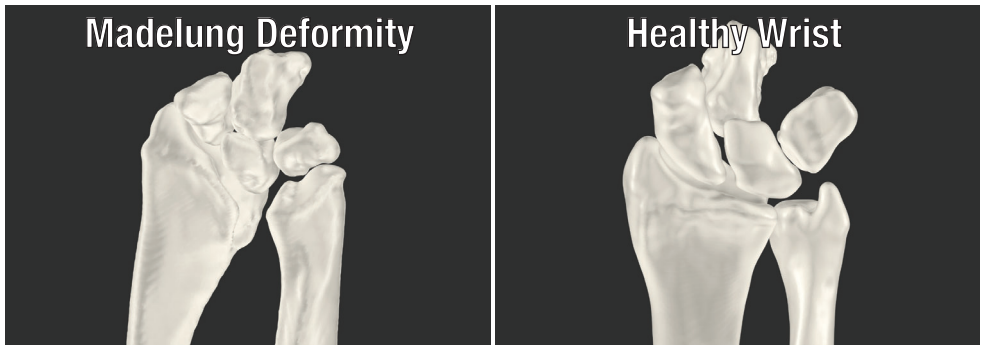

Figure 1. Three-dimensional reconstruction of the wrist after segmentation of CT scan.

Computation of 3D measurements

The McCarroll criteria comprise four measurements: ulnar tilt, lunate subsidence, lunate fossa angle, and palmar carpal displacement.[3] Based on the underlying concepts defined in the initial study, these measurements were translated for usage in a 3D model. Next, several new parameters were developed based on previously described anatomical abnormalities, including dysplasia of the lunate fossa and the pyramidal configuration of the bones in the proximal carpal row.[6,13-15] Scaphoid and lunate fossae were quantified through three parameters: articular surface area, concavity, and irregularity. To quantify the configuration of the proximal carpal row, we calculated the angle between scaphoid, lunate, and triquetral bones. All calculations were done for Madelung deformity wrists (n = 28) and healthy wrists (n = 56). All measurement results were rounded to one decimal place.

Ulnar tilt measures the ulnar angulation of the distal radial articular surface on a postero-anterior (PA) wrist view. Ulnar tilt was calculated as 3D by defining a vector connecting the centers of the scaphoid and lunate fossae, and subsequently recording the complement of the angle (defined as 90 minus the angle) in degrees between this vector and the longitudinal axis of the ulna (Figure 2a). The analysis of scaphoid and lunate fossae is further described below. The longitudinal axis of the ulna was calculated by performing a principal component analysis on its virtual model and recording the direction of maximal variance. Lunate subsidence measures the proximal displacement of the lunate bone (PA view). Lunate subsidence was calculated in our 3D model by measuring the height difference between the ulnar styloid process and the base of the lunate bone (Figure 2b). The Lunate fossa angle measures the ulnar angulation of the lunate fossa (PA view). First, a 3D plane was computed to fit the lunate fossa using a least-squares fitting procedure. The lunate fossa angle was calculated by recording the complement of the angle in degrees, between the planes' normal vector and the longitudinal axis of the ulna (Figure 2c). Palmar carpal displacement measures the palmar-directed displacement of the carpus (represented by the lunate and capitate) relative to the longitudinal axis of the ulna (lateral view). To simulate a lateral wrist view, a 3D plane was computed through the longitudinal axis of the ulna and the radial styloid process. Next, we calculated two vectors: one perpendicular vector from the plane to the most

palmar point on the capitate, and one perpendicular vector from the plane to the most palmar point on the lunate. The length in millimeters of the longest vector was defined as the palmar carpal displacement (Figure 2d).

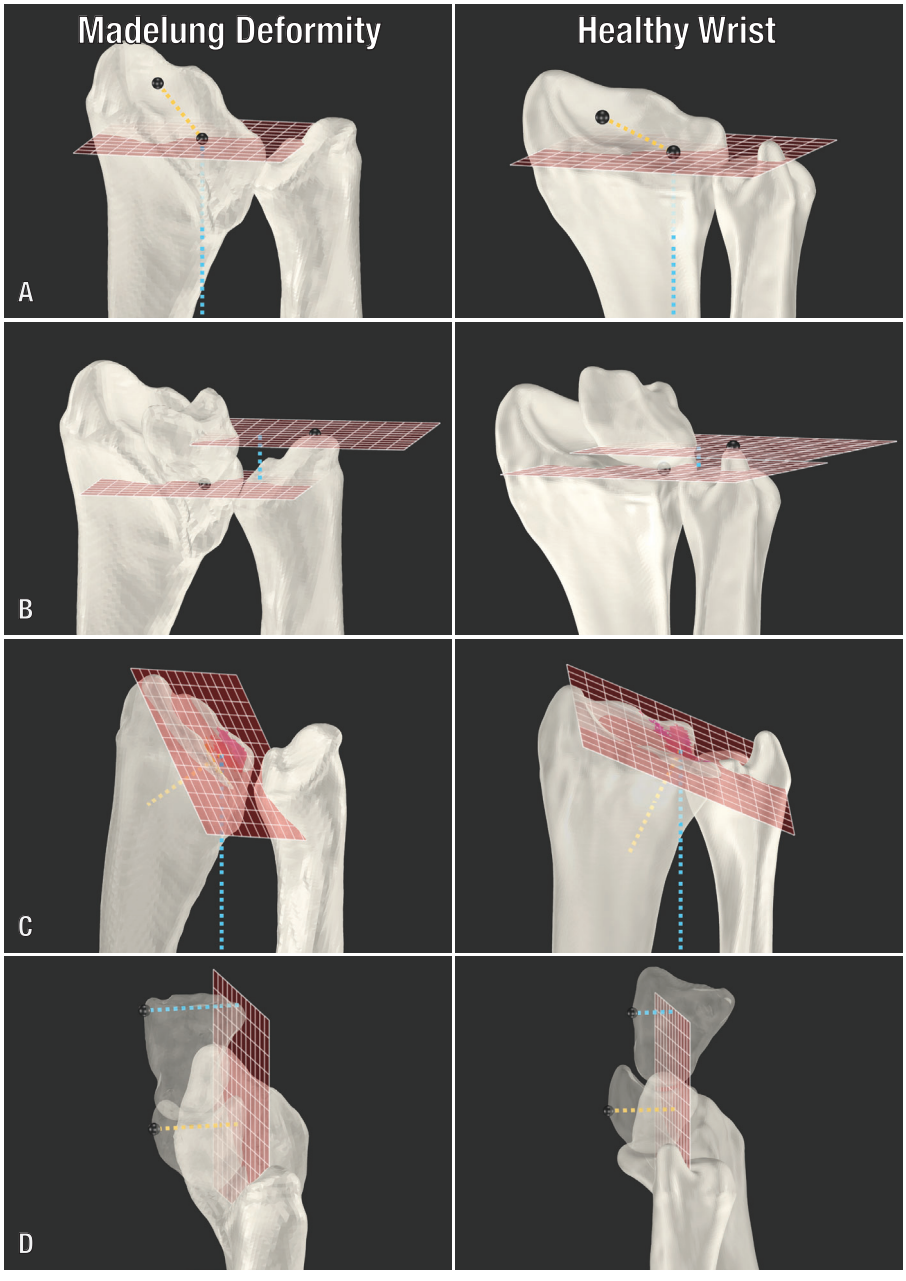

Figure 2. Visualization of 3D wrist calculations based on the McCarroll criteria: (a) ulnar tilt; (b) lunate subsidence; (c) lunate fossa angle; (d) palmar carpal displacement.

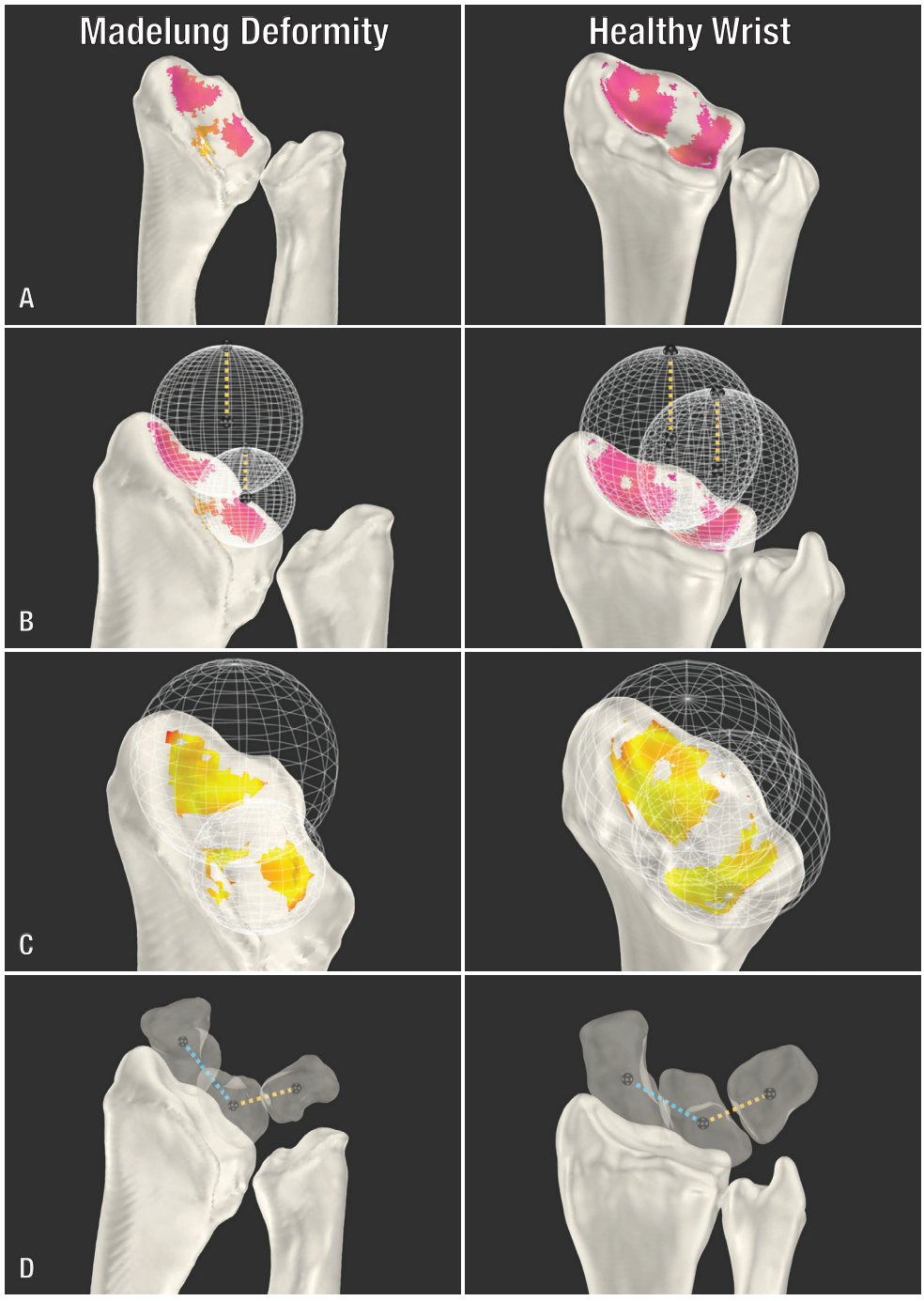

Figure 3. Visualization of novel 3D wrist calculations: (a) articular surface areas of the scaphoid and lunate fossae; (b) concavity of the scaphoid and lunate fossae; (c) irregularity of the scaphoid and lunate fossae; (d) scapholunotriquetral angle.

The articular surface areas of the scaphoid and lunate fossae were calculated in square millimeters (Figure 3a), using a method previously developed by the authors.[16,17] The fossa concavity was calculated by fitting a sphere to its surface area, using a least-squares fitting procedure (Figure 3b). The inverse (1/R) of the sphere's radius in centimeters (R) defined the concavity of the fossa; higher value indicating a more concave (i.e., inwardly curved) shape of the fossa. Fossa irregularity was defined as the deviation of points on the articular surface area relative to the computed sphere; higher value indicating a more irregular (i.e., bumpy) surface area of the fossa (Figure 3c). Scapholunotriquetral (SLT) angle was calculated by recording the angle in degrees between 2 vectors: one vector from the centroid of the lunate bone to the centroid of the scaphoid bone, and one vector from the centroid of the lunate bone to the centroid of the triquetral bone (Figure 3d).

Statistical analysis

The following 3D-based variables were used in statistical analyses: ulnar tilt, lunate subsidence, lunate fossa angle, palmar carpal displacement, articular surface area of the scaphoid/lunate fossae, concavity of the scaphoid/lunate fossae, irregularity of the scaphoid/lunate fossae, and SLT angle. To investigate differences between Madelung deformity wrists and healthy wrists, we compared the means of both groups. If a variable was normally distributed in both groups, an independent samples t-test (variances equal) or Welch's t-test (variances not equal) was performed. Equality of variances was assessed using Levene's test. If a variable was not normally distributed, the Mann–Whitney U test was performed. To control for possible confounding effects of age, binary logistic regression models were developed for each of our statistical analyses.

RESULTS

Madelung deformity patients (n = 18) had a mean age of 21±10 years, and all were women. Of these patients, fifteen had a bilateral deformity (four confirmed genetic causes), and three had a unilateral deformity. Healthy participants (n = 35) had a mean age of 24±6 years, and 24 were women.

There were significant differences in all 3D-based parameters based on McCarroll criteria, between wrists of Madelung deformity patients and wrists of healthy participants (Table 1). After adjusting for age and excluding male participants from the healthy wrists, wrists of patients showed significantly increased levels of ulnar tilt, lunate subsidence, lunate fossa angle, and palmar carpal displacement.

For the newly developed 3D-based wrist parameters (Table 2), significant age- and gender-adjusted differences were found between Madelung deformity wrists and healthy wrists. In patients' wrists, the articular surface areas of the scaphoid and lunate fossae were smaller, the lunate fossa was more concavely shaped, and the articular surface area of the lunate fossa was more irregular. Compared with healthy wrists, the proximal carpal row of Madelung deformity wrists showed a significantly increased SLT angle. No significant differences were found for concavity or irregularity of the scaphoid fossa.

Table 1. Three-dimensional-based wrist parameters based on McCarroll's criteria.

	Madelung deformity (n=28)	Healthy wrists (n=56)	P	P[a]
Ulnar tilt, degrees	37±7.3	23±3.4	**<0.001**	**0.001**
Lunate subsidence, mm	8.7±4.0	1.8±2.2	**<0.001**	**<0.001**
Lunate fossa angle, degrees	52±13	25±4.0	**<0.001**	**0.005**
Palmar carpal displacement, mm	16±7.7	13±1.7	**0.001**	**0.014**

[a]Adjusted for age and gender.

Table 2. Novel three-dimensional-based wrist parameters.

	Madelung deformity (n=28)	Healthy wrists (n=56)	P	P[a]
Scaphoid fossa surface area, mm^2	77±32	130±30	**<0.001**	**<0.001**
Lunate fossa surface area, mm^2	70±25	103±26	**<0.001**	**0.009**
Scaphoid fossa concavity, cm^{-1}	0.8±0.1	0.7±0.1	**0.003**	0.074
Lunate fossa concavity, cm^{-1}	0.9±0.2	0.8±0.1	**<0.001**	**0.005**
Scaphoid fossa irregularity, mm	0.2±0.1	0.2±0.1	0.178	0.789
Lunate fossa irregularity, mm	0.3±0.1	0.2±0.1	**<0.001**	**<0.001**
SLT angle, degrees	115±7	122±5	**<0.001**	**0.002**

[a]Adjusted for age and gender.

DISCUSSION

Our present study quantitatively assessed Madelung deformity in 3D form and confirms that Madelung wrists have increased levels of ulnar tilt, lunate subsidence, lunate fossa angle, and palmar carpal displacement. The lunate fossa is more concave and irregular, and angles between scaphoid, lunate, and triquetral bones are decreased. A strength of this approach is that measurements are calculated automatically, using self-developed algorithms that could find easy implementations in third-party software. Additionally, automatic analyses remove inter- and intra-rater differences, likely increasing data quality. The only manual step is the segmentation process, which is expected to have a negligible impact. The small number of patients is a limitation, although we included considerably more wrists (n=28) than patients (n=18) due to the high bilateral occurrence. Lastly, only a subset of our patients underwent corrective surgery and their outcomes were not reported in a homogenous manner; this precluded any discussion about the association between 3D parameters and outcomes.

The McCarroll criteria are used to identify Madelung deformity and to monitor changes.[18] However, measurements show differences both within and between raters.[3] Also, despite previously established thresholds, considerable overlap with healthy wrists exists.[18,19] Hegazy et al. recently developed a modified 2D technique using the capitate as a bony landmark instead of the ulna, observing an improved inter-and intra-rater agreement for some, but not all measurements.[20]

While our automatic approach solves this issue, the overlap with healthy wrists was also evident in our study, giving rise to the question of whether three-dimension holds any diagnostic advantages over two-dimension. Even if automatic 3D measurements could decrease overlap due to their objective nature, both methods should be further investigated in regards to diagnostic efficacy. Nonetheless, our findings validate the underlying principles of previous McCarroll criteria, with significant differences being visible in 3D assessments.

In the normal wrist, the distal radial articular surface is concave in both sagittal and coronal planes, containing the triangular-shaped scaphoid fossa and the quadrangular-shaped lunate fossa. Whereas patients' lunate fossa angles have been widely reported,[5,18,21] the fossa shape has not been investigated. The abnormal lunate fossa shape in Madelung deformity is not surprising, as the deformity's pathogenesis involves a premature growth plate arrest at the volar/ulnar aspects of the distal radius,[22] while leaving the anatomy at the radial aspect relatively intact.

The proximal carpal bones have been reported to be pyramiding,[6,14] angular-shaped,[15] or V-shaped[23] rather than smoothly convex.[24] Kosowicz quantified a so-called 'carpal angle' on 2D radiographs of healthy participants (132±7.2°) and gonadal dysgenesis patients (118±6.6°).[15] Instead, we quantified the proximal carpal row in Madelung deformity using a 3D approach. Interestingly, Madelung deformity has been strongly associated with Turner syndrome, one of the causes of gonadal dysgenesis,[25] and we found comparable decreases.

Currently, most surgeons treat the deformity with osteotomies of the radius and/or ulna, the rationale being that restoring skeletal angles improves wrist biomechanics and function.[26] Although postoperative outcomes seem satisfactory, some patients require revision surgery due to complications.[27] To advance our understanding of the anatomy and clinical outcomes of Madelung deformity, it is important to expand our scope beyond the traditional toolkit. In this study, we developed new parameters to quantify the radiocarpal joint. It is not unthinkable that a 'too abnormal' fossa concavity would indicate anatomical mismatching of the radiocarpal joint. Likewise, fossa irregularities could prognosticate joint degeneration. The aforementioned examples might inspire the surgeon to consider alternative treatment options in certain patients. Since there are still no evidence-based guidelines for corrective surgery in Madelung deformity,[27] improving existing and introducing new ways of wrist quantification might prove valuable in future prognostic models. However, further prospective studies are necessary to identify any association between these parameters and postoperative outcomes.

All our measurements were calculated using static CT scans. It would be beneficial to perform these calculations using dynamic four-dimensional imaging.[17] In addition to increasing the accuracy of fossae measurements by covering wrist bone positions during a patients' entire range of motion, it would reveal potential differences in carpal motion.[12] The scope of this study was limited to the skeletal deformities, yet it may also be useful to investigate soft-tissue anomalies, including Vickers ligament[11,28] and the radiotriquetral ligament,[29,30] as the interplay between skeletal and ligamentous abnormalities is still unclear.

In summary, a 3D approach to Madelung deformity validates the underlying principles of current 2D criteria and reveals previously unknown anatomical abnormalities by utilizing novel 3D parameters to quantify the radiocarpal joint.

REFERENCES

1. Dupuytren G. Lecons Orales de Clinique Chirurgicale, faites a l'Hotel Dieu de Paris. ***Med Chir Rev.*** 1834;21(42):289-330.
2. Madelung O. Die spontane Subluxation der Hand nach vorne. ***Verh Dtsch Ges Chir.*** 1878;7:259-276.
3. McCarroll HR, Jr., James MA, Newmeyer WL, 3rd, Molitor F, Manske PR. Madelung's deformity: quantitative assessment of x-ray deformity. ***J Hand Surg Am.*** 2005;30(6):1211-1220.
4. Farr S, Guitton TG, Ring D, Science of Variation G. How Reliable is the Radiographic Diagnosis of Mild Madelung Deformity? ***J Wrist Surg.*** 2018;7(3):227-231.
5. Tuder D, Frome B, Green DP. Radiographic spectrum of severity in Madelung's deformity. ***J Hand Surg Am.*** 2008;33(6):900-904.
6. Stehling C, Langer M, Nassenstein I, Bachmann R, Heindel W, Vieth V. High resolution 3.0 Tesla MR imaging findings in patients with bilateral Madelung's deformity. ***Surg Radiol Anat.*** 2009;31(7):551-557.
7. Kampa R, Al-Beer A, Axelrod T. Madelung's deformity: radial opening wedge osteotomy and modified Darrach procedure using the ulnar head as trapezoidal bone graft. ***J Hand Surg Eur Vol.*** 2010;35(9):708-714.
8. Laffosse JM, Abid A, Accadbled F, Knor G, Sales de Gauzy J, Cahuzac JP. Surgical correction of Madelung's deformity by combined corrective radioulnar osteotomy: 14 cases with four-year minimum follow-up. ***Int Orthop.*** 2009;33(6):1655-1661.
9. Mallard F, Jeudy J, Rabarin F, et al. Reverse wedge osteotomy of the distal radius in Madelung's deformity. ***Orthop Traumatol Surg Res.*** 2013;99(4 Suppl):S279-283.
10. Saffar P, Badina A. Treatment of Madelung's deformity. ***Chir Main.*** 2015;34(6):279-285.
11. Steinman S, Oishi S, Mills J, Bush P, Wheeler L, Ezaki M. Volar ligament release and distal radial dome osteotomy for the correction of Madelung deformity: long-term follow-up. ***J Bone Joint Surg Am.*** 2013;95(13):1198-1204.
12. Dobbe JGG, de Roo MGA, Visschers JC, Strackee SD, Streekstra GJ. Evaluation of a Quantitative Method for Carpal Motion Analysis Using Clinical 3-D and 4-D CT Protocols. ***IEEE Trans Med Imaging.*** 2019;38(4):1048-1057.
13. Cook PA, Yu JS, Wiand W, et al. Madelung deformity in skeletally immature patients: morphologic assessment using radiography, CT, and MRI. ***J Comput Assist Tomogr.*** 1996;20(4):505-511.
14. Harley BJ, Carter PR, Ezaki M. Volar surgical correction of Madelung's deformity. ***Tech Hand Up Extrem Surg.*** 2002;6(1):30-35.
15. Kosowicz J. The carpal sign in gonadal dysgenesis. ***J Clin Endocrinol Metab.*** 1962;22:949-952.
16. Foumani M, Strackee SD, van de Giessen M, Jonges R, Blankevoort L, Streekstra GJ. In-vivo dynamic and static three-dimensional joint space distance maps for assessment of cartilage thickness in the radiocarpal joint. ***Clin Biomech (Bristol, Avon).*** 2013;28(2):151-156.
17. Peymani A, Foumani M, Dobbe JGG, Strackee SD, Streekstra GJ. Four-dimensional rotational radiographic scanning of the wrist in patients after proximal row carpectomy. ***J Hand Surg Eur Vol.*** 2017;42(8):846-851.
18. McCarroll HR, Jr., James MA, Newmeyer WL, 3rd, Manske PR. Madelung's deformity: diagnostic thresholds of radiographic measurements. ***J Hand Surg Am.*** 2010;35(5):807-812.
19. McCarroll HR, James MA, Newmeyer WL, 3rd, Manske PR. Madelung's deformity: quantitative radiographic comparison with normal wrists. ***J Hand Surg Eur Vol.*** 2008;33(5):632-635.

20. Hegazy G, Mansour T, Alshal E, Abdelaziz M, Alnahas M, El-Sebaey I. Madelung's deformity: capitate-related versus ulna-related measurement methods. ***J Hand Surg Eur Vol.*** 2019;44(5):524-531.

21. Zebala LP, Manske PR, Goldfarb CA. Madelung's deformity: a spectrum of presentation. ***J Hand Surg Am.*** 2007;32(9):1393-1401.

22. Ghatan AC, Hanel DP. Madelung deformity. ***J Am Acad Orthop Surg.*** 2013;21(6):372-382.

23. Henry A, Thorburn MJ. Madelung's deformity. A clinical and cytogenetic study. ***J Bone Joint Surg Br.*** 1967;49(1):66-73.

24. Gilula LA. Carpal injuries: analytic approach and case exercises. ***AJR Am J Roentgenol.*** 1979;133(3):503-517.

25. Zhong Q, Layman LC. Genetic considerations in the patient with Turner syndrome--45,X with or without mosaicism. ***Fertil Steril.*** 2012;98(4):775-779.

26. dos Reis FB, Katchburian MV, Faloppa F, Albertoni WM, Laredo Filho J, Jr. Osteotomy of the radius and ulna for the Madelung deformity. ***J Bone Joint Surg Br.*** 1998;80(5):817-824.

27. Peymani A, Johnson AR, Dowlatshahi AS, et al. Surgical Management of Madelung Deformity: A Systematic Review. ***Hand (N Y).*** 2019;14(6):725-734.

28. Vickers D, Nielsen G. Madelung deformity: surgical prophylaxis (physiolysis) during the late growth period by resection of the dyschondrosteosis lesion. ***J Hand Surg Br.*** 1992;17(4):401-407.

29. Ali S, Kaplan S, Kaufman T, Fenerty S, Kozin S, Zlotolow DA. Madelung deformity and Madelung-type deformities: a review of the clinical and radiological characteristics. ***Pediatr Radiol.*** 2015;45(12):1856-1863.

30. Hanson TJ, Murthy NS, Shin AY, Kakar S, Collins MS. MRI appearance of the anomalous volar radiotriquetral ligament in true Madelung deformity. ***Skeletal Radiol.*** 2019;48(6):915-918.

6

CARPAL KINEMATICS IN MADELUNG DEFORMITY

A. Peymani[1,2], M.G.A. de Roo[1,2],
J.G.G. Dobbe[2], G.J. Streekstra[2,3],
H.R. McCarroll[4], S.D. Strackee[1]

[1] Department of Plastic, Reconstructive and Hand Surgery, Amsterdam UMC, University of Amsterdam, Amsterdam, The Netherlands.
[2] Department of Biomedical Engineering and Physics, Amsterdam UMC, University of Amsterdam, Amsterdam, The Netherlands.
[3] Department of Radiology and Nuclear Medicine, Amsterdam UMC, University of Amsterdam, Amsterdam, The Netherlands.
[4] Department of Orthopaedic Surgery, California Pacific Medical Center, San Francisco, CA, USA.

J Hand Surg Am. Accepted.

ABSTRACT

Various skeletal and soft tissue abnormalities have been identified in Madelung deformity and have been hypothesized to play a causal role in its progressive symptomatology; however, our pathological understanding of these changes remains limited. In this study, we biomechanically assessed the Madelung deformity wrist, using four-dimensional computed tomography imaging. Nine Madelung deformity wrists (five patients; age, 24±5 years) and eighteen healthy wrists (nine volunteers; age, 28±3 years) underwent four-dimensional imaging during flexion-extension motion and radioulnar deviation. Carpal kinematics and radiocarpal joint parameters were quantified and compared. In Madelung deformity wrists, significantly decreased rotation was seen in the lunate (-4.6 degrees) and the triquetrum (-4.8 degrees) during flexion-extension motion. During radioulnar deviation, significant decreases were visible in lunate bone translation (-0.7 mm), triquetrum bone translation (-0.6 mm), and triquetrum bone rotation (-1.9 degrees). Patients had significantly decreased articulating surface areas of the scaphoid (1.4±0.2 cm^2 versus 1.6±0.2 cm^2) and lunate (1.2±0.4 cm^2 versus 1.5±0.3 cm^2) fossa, and significantly increased radioscaphoid (1.3±0.1 mm versus 1.2±0.1 mm) and radiolunate (1.6±0.2 mm versus 1.3±0.3 mm) joint space thicknesses. There is a decreased mobility of the lunate and triquetrum bones in Madelung deformity. Four-dimensional imaging could be used in future studies that investigate the effect of surgical ligament release on carpal kinematics and subsequent wrist mobility.

INTRODUCTION

Madelung deformity is a rare congenital deformity[1] that commonly manifests bilaterally[2] and emerges clinically in early adolescence.[3] Symptoms include wrist pain and a reduced range of motion (ROM),[4,5] both important factors in deciding whether a patient could benefit from undergoing surgical treatment.[2] Owing to its rarity, with incidence and prevalence still unknown, our understanding of Madelung deformity is incomplete.[6] There is no consensus among clinicians and researchers in regards to various clinical aspects such as true etiology,[7-9] assessment of bony features,[10,11] and optimal treatment strategies.[12-14]

Previous studies have established a spectrum of skeletal abnormalities, particularly in the distal radius, which have been quantified for use in diagnosis.[15,16] Furthermore, imaging studies have revealed various soft tissue abnormalities, including the volar radiolunate ligament known as 'Vickers ligament' and the anomalous volar radiotriquetral ligament.[17-21] These anatomical changes are thought to play a causal role in the progressive symptomatology of the condition, with the purpose of surgery being to restore the anatomical configuration and normalize the anatomy in order to improve wrist biomechanics.[22] Whereas previous biomechanical studies have substantially expanded our knowledge of wrist anatomy,[23-25] pathology,[26-28] and surgery,[29,30] no in vitro or in vivo biomechanical studies have been performed for Madelung deformity.

The objective of this study was to investigate the wrist biomechanics of Madelung deformity patients, using four-dimensional (4D) computed tomography (CT) imaging during flexion-extension motion and radio-ulnar deviation, and comparing those biomechanical features with wrists of healthy volunteers.

MATERIALS AND METHODS

Setting and study population

For this study, we retrospectively included patients with Madelung deformity, for which 4D CT scans of one or both wrists were available. All Madelung deformity patients visiting our outpatient care clinic undergo 4D CT imaging to visualize carpal bone kinematics based on a previously developed protocol, independent of the severity of the deformity.[31] In the diagnostic work-up, the McCarroll criteria[11] were used, quantifying the deformity with four measurements: ulnar tilt, lunate subsidence, lunate fossa angle, and palmar carpal displacement. Ali et al.[21] have previously hypothesized the deformity to be true Madelung deformity in the presence of a Vickers ligament or if a patient is bilaterally affected with an underlying diagnosis of Leri-Weill dyschondrosteosis,[32] although there is no consensus on this definition. Patient charts were reviewed to determine any underlying genetic disorders and surgical notes were reviewed to assess the presence of Vickers ligament. For patients who did not undergo surgical treatment, we reviewed preoperative x-ray and CT imaging instead to identify the ligamentous origin.[21] We excluded patients with a posttraumatic Madelung deformity and wrists that had previously undergone surgical correction. A total of five patients were eligible for inclusion; all with bilateral Madelung deformity. After excluding one wrist (previous corrective osteotomy of the radius), this resulted in a total of nine included wrists. In addition, previously acquired 4D CT scans of nine healthy female volunteers (eighteen

wrists) were included in the kinematic analysis for comparison. None of the healthy volunteers had a medical history of skeletal disorders or a surgical history of wrist interventions. Volunteers with hypermobility, assessed using the Beighton score,[33] were excluded. This study was approved by our medical center institutional review board.

Image acquisition

The 4D CT scans were acquired using a Philips Brilliance 64 CT scanner (Philips, Cleveland, OH). First, a static CT scan was performed of the wrist in a neutral position (120kV, 75mAs). Next, the participant gripped the handle of a custom-made positioning device (Figure 1), limiting wrist movement to either flexion-extension or radio-ulnar deviation. Participants performed each motion over twelve seconds while dynamic 4D CT scans were acquired (120 kV, 30 mAs; collimation, 64x0.625mm; axial field of view, 4 cm; rotation time, 0.4 s), resulting in a total of 30 reconstructions per motion. The static high quality CT scan was used for segmentation; the dynamic low quality CT scans were used for position detection. Participants received a total dose of 0.3 mSv.

Image segmentation and position detection

The static CT scan of the wrist in neutral position was segmented using a custom-made software package[31] to obtain virtual three-dimensional (3D) models of the radius, ulna, scaphoid, lunate, triquetrum, and capitate bones. The scaphoid, lunate, and triquetrum were used to assess radiocarpal motion; the capitate was used to assess overall wrist motion. The virtual bone models were aligned with the dynamic 4D CT scans (30 per motion) to quantify the position of each carpal bone during movement using two parameters: translation (x, y, and z-coordinates of the virtual bone models' centroid), and rotation (φ, θ, and ψ-angles relative to the neutral position). Total translation was calculated using the formula $\sqrt{x^2 + y^2 + z^2}$, and total rotation was calculated using the formula $\sqrt{\varphi^2 + \theta^2 + \psi^2}$.

Image processing and computation

The virtual 3D models and corresponding kinematics parameters were exported and further processed using self-developed software programmed in MATLAB R2018b (MathWorks Inc., Natick, MA). This software performed the following functions automatically: wrist alignment, detection of radial and ulnar landmarks (e.g., radial styloid process, ulnar styloid process), visualization of the wrist during motion (Figure 2), and the computations described later.

To quantify the position of the wrist during motion in flexion-extension or radioulnar deviation angles, we first determined the longitudinal axis of the capitate bone in neutral position. Next, we calculated the angle in degrees between this neutral axis and the dynamic longitudinal axis of the capitate bone during each of the 30 positions per motion. To visualize a full motion in a graph, flexion and radial deviation angles were represented as negative values; extension and ulnar deviation angles were represented as positive values.

Articular surface area and joint space thickness (Figure 3) were calculated using a previously described method.[34,35] Briefly, for each of the 30 positions during a motion, we calculate for each

Figure 1. Wrist positioning device to keep the carpus in the field of view during 4D imaging. The patient can either move the wrist about the flexion-extension axis or the radio-ulnar deviation axis.

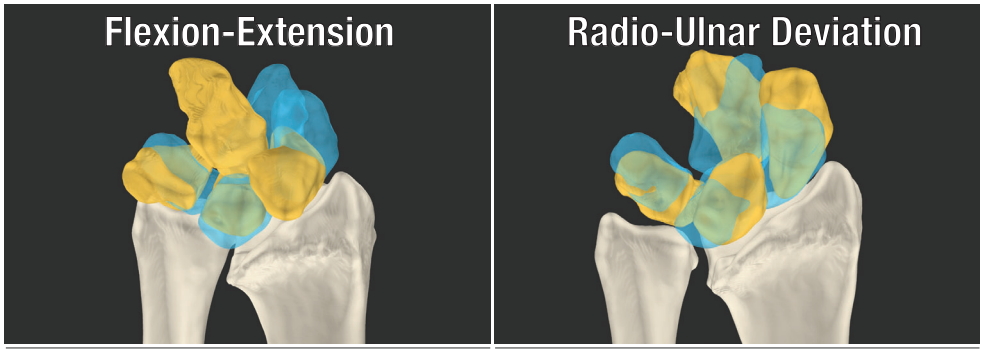

Figure 2. Visualizing movement of virtually segmented wrist models. Colors indicate different positions during motion (blue: first position; orange: last position).

point on the radius the nearest point to the scaphoid or lunate. Next, these points are filtered using two pragmatically chosen constraints: (1) a maximum distance of 4 mm between opposing points; (2) a maximum angle difference of 15 degrees between the normal lines of opposing points. The articular surface area per motion is acquired by merging the points of 30 positions; a combined version is calculated by merging the points of all 60 positions from two motions (flexion-extension and radio-ulnar deviation). For each position within the motion trajectory, the minimum distance

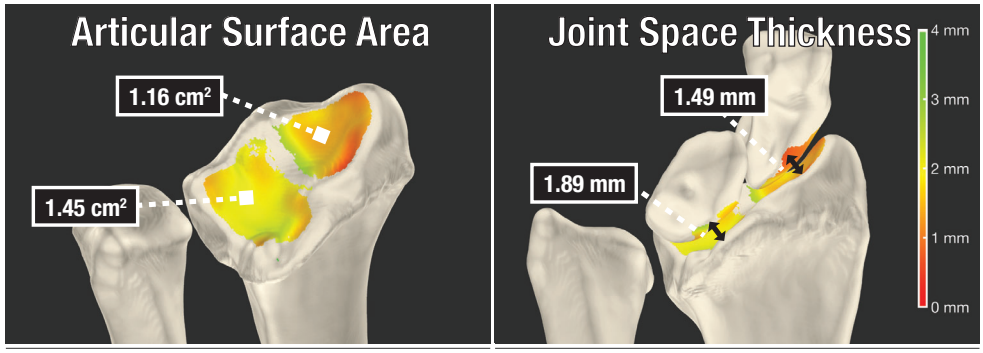

Figure 3. Articular surface area and joint space thickness.

to the opposing point is taken for each point in the articular surface area. The mean of these minimum distances provides the joint space thickness, defined as the articular cartilage thickness between the radius and the scaphoid (radioscaphoid joint space thickness) or between the radius and the lunate (radiolunate joint space thickness).

Carpal bone kinematics, articular surface area, and joint space thickness are visualized in Supplemental Video 1 (Figure 4, Figure 5).

Data processing and statistical analysis

Python v3.7.2 (Python Software Foundation. Python Language Reference, version 3.7.2) was used to process MATLAB data files and to perform statistical analyses and graphical data visualization using the SciPy, StatsModels, and Seaborn packages.

For ROM, articular surface area, and joint space thickness, we compared the means of the calculated parameters between Madelung deformity wrists and healthy wrists. Data normality was determined using the Shapiro-Wilk test. If a variable was normally distributed in both groups, an independent samples t-test (variances equal) or Welch's t-test (variances not equal) was performed. Equality of variances was assessed using Levene's test. If a variable was not normally distributed, the Mann-Whitney U test was performed.

To compare carpal bone kinematics while adjusting for ROM (flexion-extension and radioulnar deviation angles), we developed mixed-effects models for each combination of three proximal carpal bones (scaphoid, lunate, and triquetrum), two distinct motions (flexion-extension and radioulnar deviation), and two outcomes of interest (total translation and total rotation); this resulted in a total of twelve models. As fixed effects, we entered angle (ROM) and wrist type (healthy or Madelung). In addition, to account for possible size differences between Madelung patients and healthy volunteers, we added wrist size as a fixed effect, defined as the absolute distance between the centroids of capitate and the lunate. Lastly, to optimally fit each model, we added angle^2 and angle^3 as fixed effects, depending on the outcome curve being quadratic- or cubic-shaped, respectively. Intercepts for different wrists were added as random effects. The P values were obtained by likelihood ratio tests of the full model including wrist type and the model without wrist

type. To determine which specific parameters were responsible for an altered total translation or rotation, we performed separate subanalyses for translation over x, y, and z coordinates

RESULTS

Patients with Madelung deformity (n = 5) had a mean age of 23.7±4.9 years; healthy volunteers (n=9) had a mean age of 28.0±2.6 years. All participants were women. Study characteristics are described in Table 1. Wrists of Madelung deformity patients had a significantly lower maximum angle of flexion (degrees, 47.9±16.5 versus 72.8±7.2°; P<0.05) and radial deviation (degrees, 12.5± 8.5 versus 23.3±5.5; P<0.05) compared with wrists of healthy volunteers (Table 2). No significant differences were found for maximum extension and maximum ulnar deviation.

During flexion-extension motion (Table 3) a significantly decreased rotation was seen in both the lunate bone (difference in degrees, -4.6; 95% CI -7.1 to -2.2; P<0.05) and the triquetrum bone (difference in degrees, -4.8; 95% CI -6.7 to -3.0; P<0.05) for Madelung deformity wrists. Carpal kinematics during radio-ulnar deviation (Table 4) showed significant decreases in lunate bone translation (difference in mm, -0.7; 95% CI -1.0 to -0.4; P<0.05), triquetrum bone translation (difference in mm, -0.6; 95% CI -0.9 to -0.3; P=0.05), and triquetrum bone rotation (difference in

Table 1. Characteristics of the study group.

	Madelung deformity patients (n=5)	Healthy volunteers (n=9)
Wrists	9	18
Age, y	23.7±4.9	28.0±2.6
Female	5	9
Bilateral deformity	5	N/A
Confirmed genetic cause	3	N/A
Radiographic measurements		
Ulnar tilt, degrees	41.1±19.3	N/A
Lunate subsidence, mm	9.2±4.2	N/A
Lunate fossa angle, degrees	56.5±17.4	N/A
Palmar carpal displacement, mm	15.5±7.0	N/A

N/A: Not Applicable.

Table 2. Maximum range of motion with respect to the capitate bone.

	Madelung deformity wrists (n=9)	Healthy wrists (n=18)	P
Flexion, degrees	47.9±16.5	72.8±7.2	**P<0.05**
Extension, degrees	43.8±12.4	44.4±5.3	0.894
Radial deviation, degrees	12.5±8.5	23.2±5.5	**P<0.05**
Ulnar deviation, degrees	19.2±7.0	19.8±10.4	0.882

Table 3. Carpal kinematics during flexion-extension motion.

	Mean difference	Standard error	95% CI	P
Scaphoid translation, mm	-0.3	0.1	-0.5 to 0.0	0.064
Scaphoid rotation, degrees	-1.4	1.0	-3.3 to 0.6	0.182
Lunate translation, mm	-0.2	0.1	-0.4 to 0.0	0.119
Lunate rotation, degrees	-4.6	1.3	-7.1 to -2.2	**P<0.05**
Triquetrum translation, mm	-0.2	0.2	-0.6 to 0.1	0.248
Triquetrum rotation, degrees	-4.8	0.9	-6.7 to -3.0	**P<0.05**

Table 4. Carpal kinematics during radio-ulnar deviation.

	Mean difference	Standard error	95% CI	P
Scaphoid translation, mm	-0.3	0.2	-0.7 to 0.1	0.136
Scaphoid rotation, degrees	2.5	1.6	-0.7 to 5.6	0.131
Lunate translation, mm	-0.7	0.2	-1.0 to -0.4	**P<0.05**
Lunate rotation, degrees	-1.4	1.2	-3.9 to 1.0	0.256
Triquetrum translation, mm	-0.6	0.2	-0.9 to -0.3	**P<0.05**
Triquetrum rotation, degrees	-1.9	0.9	-3.7 to -0.1	**P<0.05**

degrees, -1.9; 95% CI -3.7 to -0.1; P=0.05). There were no significant differences found for scaphoid bone translation and rotation during flexion-extension motion or radio-ulnar deviation.

Table 5 describes the articular surface area and joint space thickness of the distal radius during motion. Patients with Madelung deformity had significantly decreased articulating surface areas of the scaphoid (cm^2, 1.4±0.2 versus 1.6±0.2; P<0.05) and lunate fossa (cm^2, 1.2±0.4 versus 1.5±0.3; P<0.05), and significantly increased radioscaphoid (mm, 1.3±0.1 versus 1.2±0.1; P<0.05) and radiolunate joint space thickness (mm, 1.6±0.2 versus 1.3±0.3; P<0.05).

DISCUSSION

In this study, we imaged patients' wrist bones during flexion-extension motion and radioulnar deviation through a previously developed 4D CT protocol. In comparison with wrists of healthy volunteers, wrists of Madelung deformity patients have decreased mobility of the lunate and triquetrum bones. The articular surface areas of the scaphoid and lunate fossa are decreased, and radiocarpal cartilage thickness does not significantly differ from healthy wrists.

A major strength of this in vivo study is that all measurements are performed automatically through self-developed software algorithms[34] leading to an objective assessment in a dynamic setup. Another strength is that the mixed-model analysis of 4D CT data allows for the quantification of individual carpal bone mobility, while considering the differences in wrist ROM between patients and volunteers. Because wrist ROM is intrinsically linked to carpal bone mobility, correcting for this parameter in our analyses shows that the reported differences in mobility occur despite, and

Table 5. Articular surface area and joint space thickness.

	Madelung deformity wrists (n=9)	Healthy wrists (n=18)	P
Articular surface area, cm²			
Scaphoid fossa			
Combined[a]	1.4±0.2	1.6±0.2	**P<0.05**
Flexion-extension motion	1.3±0.2	1.5±0.2	**P<0.05**
Radio-ulnar deviation	1.3±0.1	1.5±0.1	**P<0.05**
Lunate fossa			
Combined[a]	1.2±0.4	1.5±0.3	**P<0.05**
Flexion-extension motion	1.1±0.4	1.4±0.3	0.097
Radio-ulnar deviation	1.2±0.4	1.5±0.3	**P<0.05**
Joint space thickness, mm			
Radioscaphoid joint			
Combined[a]	1.3±0.1	1.2±0.1	**P<0.05**
Flexion-extension motion	1.4±0.1	1.2±0.1	**P<0.05**
Radio-ulnar deviation	1.4±0.1	1.4±0.1	0.643
Radiolunate joint			
Combined[a]	1.6±0.2	1.3±0.3	**P<0.05**
Flexion-extension motion	1.7±0.2	1.4±0.2	**P<0.05**
Radio-ulnar deviation	1.7±0.3	1.4±0.3	**P<0.05**

[a]Combined for both motions.

not because of, differences in ROM. A limitation of this study is the small number of wrists (n = 9) and corresponding limited statistical power because most of the patients in our database could not be included owing to previously undergoing surgical procedures to correct the deformity. Another limitation was that 2 patients received growth hormone therapy, shown to be effective in the treatment of short stature associated with SHOX gene deficiency,[36] possibly influencing wrist kinematics owing to altered skeletal growth. Lastly, the investigative scope of this study was limited to flexion-extension motion and radioulnar deviation (radiocarpal articulation), yet multiple studies have shown decreased mobility to be particularly prominent in forearm pronation and supination (radioulnar articulation).[37-40] The configuration of our 4D CT protocol did not allow for capturing kinematics during forearm rotation because of motion artifacts.

Our findings in regards to the decreased radial deviation seen in patients seem to be in concordance with previous findings.[40-42] Furthermore, we found patients to have lower maximum angles of flexion with no significant differences for extension. Previous studies that performed preoperative goniometer measurements in a clinical setting found decreases to be primarily in wrist extension rather than flexion,[37] with extension ranging from 32 to 49 degrees.[39-41,43] This discrepancy is likely a result of our automatic 3D measurements, in which our 0-point is defined by the orientation of the capitate with the wrist in a neutral position. One of the clinically visible features of Madelung deformity is the palmar displacement of the carpus.[8,44] This is also visible in the configuration of the virtual bones in 3D space, in which the capitate is palmarly rotated

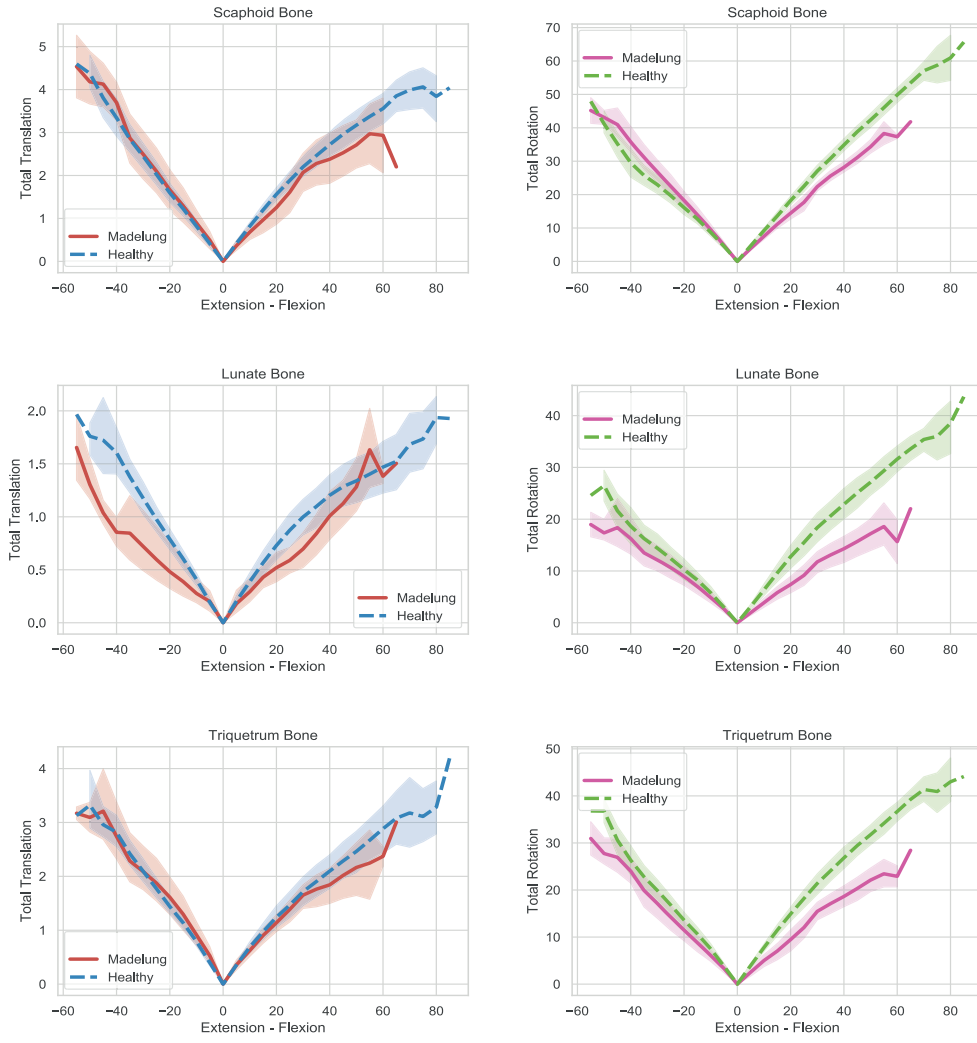

Figure 4. Carpal bone kinematics during flexion-extension motion.

in a neutral wrist position. Therefore, this shift of the zero-point toward flexion translates into relatively higher degrees of extension and, thus, relatively lower degrees of flexion in our 3D measurements.

Clinically measured decreases of ROM have been extensively quantified,[37-41,43] but it is still unknown whether these are caused by pain, intrinsic mechanical properties, or other reasons. In our study, the lunate and triquetrum show decreased mobility during flexion-extension motion and radioulnar deviation, yet scaphoid bone mobility remains normal. We hypothesize that scaphoid and lunate kinematics should be closely intertwined owing to the ligamentous connections of the scapholunate joint.[45] However, it has been demonstrated in vivo that these interosseous ligaments allow for the occurrence of considerable multiplanar motion between the 2 bones,[46]

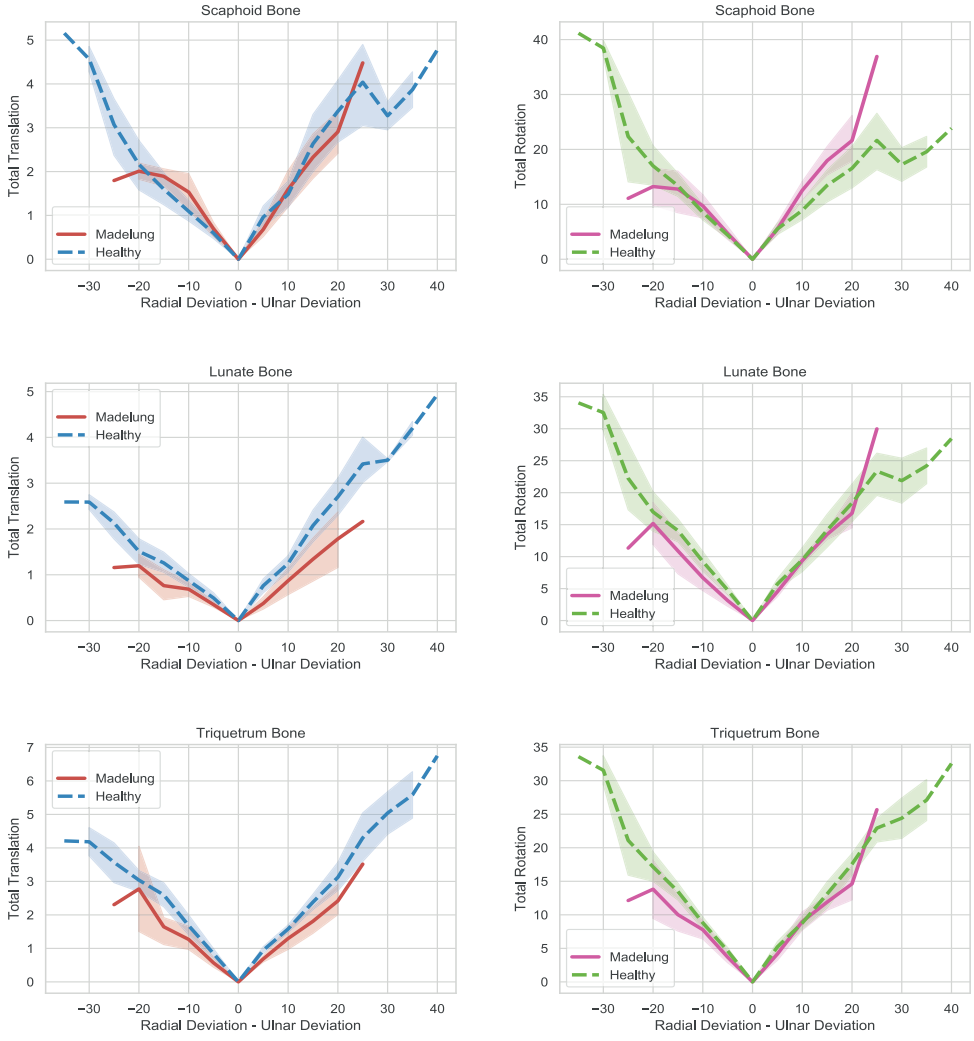

Figure 5. Carpal bone kinematics during radio-ulnar deviation.

resulting in comparable, yet distinct, motion patterns. Interestingly, the lunate and the triquetrum are the only carpal bones for which anomalous ligaments have been identified.[17,19-21,47] In addition to the established skeletal abnormalities, Vickers et al.[19] were the first to report on a thick volar ligament that firmly restrains the lunate to the radius. Cook et al.[17] identified the radiotriquetral ligament, extending from the radius to the volar aspect of the triquetrum. Although their occurrence has not been reported consistently,[22] imaging studies have confirmed their presence in true bilateral Madelung deformity, and their absence in acquired Madelung-type or pseudo-Madelung deformity.[20,21,47] Ali et al[21] have previously hypothesized the deformity to be true in the presence of a Vickers ligament or if a patient is bilaterally affected with an underlying diagnosis of Leri-Weill dyschondrosteosis.[32] We confirmed ligamentous anomalies in one patient during

surgery. Three other patients exhibited the characteristic radiolucent flame-shaped notch on imaging, revealed to represent the ligament origin.[14,18,48] However, we did not assess each patient using appropriate imaging techniques such as magnetic resonance imaging, which is better suited to confirm ligamentous anomalies.[17,19,47] Whereas retrospectively searching for this abnormality could hypothetically bias our objectivity, the ligament origin is quite distinguishable from any normal anatomical variations.[21]

Studies have reported increased supination of 17 to 23 degrees after surgical release, but strong evidence is lacking.[19,49] Furthermore, the causative mechanism could very well be the abnormal skeletal configuration instead of the anomalous ligamentous bands. Because the spectrum of skeletal abnormalities has been shown to vary widely, this could limit the generalizability of conclusions regarding carpal kinematics in a subset of patients.[15] Prospective studies could reveal the effects of different skeletal configurations by assessing the associations between kinematics and parameters that quantify the skeletal deformity, such as ulnar tilt and lunate fossa angle.[11]

The impact of Madelung deformity on the radiocarpal joints has not been investigated before. Previous studies reported a decreased radiolunate surface area in Madelung deformity patients by quantifying the percentage of the lunate that is in contact with the articular radial surface on static x-ray imaging,[40] or by calculating joint parameters in 3D space.[16] In addition to quantifying carpal kinematics, 4-dimensional CT imaging allows a dynamic determination of the articular surface areas and cartilage thickness of the radioscaphoid and radiolunate joints.[35] Both joints showed significantly smaller surface areas in patients, especially the lunate fossa. Given the decreased ROM during flexion-extension and radio-ulnar deviation, it is expected that a smaller contact area is being utilized. Also, it has been hypothesized that a subset of patients experiences pain due to osteoarthritis.[8,13,50] An abnormal radiocarpal joint could result in altered forces being applied on the wrist that could lead to degeneration of the joints.[51] Despite the abnormal carpal kinematics seen in this study, radiocarpal cartilage remained intact; our patient group was relatively young (mean age, 23.7±4.9 years) and wrist joint osteoarthritis in the general population has been seen mainly in older individuals.[52,53] However, a more plausible explanation could be that, because the deformity slowly progresses until becoming clinically apparent in early adolescence, the wrist can fully utilize its adaptive capacity,[13] which has been shown to occur even after major anatomical changes.[34] These parameters should be investigated in a larger postsurgical patient group with long-term follow-up.

In conclusion, radiocarpal kinematics in Madelung deformity are abnormal, showing a decreased mobility of the lunate and triquetrum bones. It remains unknown whether this is caused by the anomalous radiolunate and radiotriquetral ligaments or by the distorted skeletal configuration. Prospective studies could use the 4D CT analysis to investigate the biomechanical effects of surgical ligament release..

REFERENCES

1. Madelung O. Die spontane Subluxation der Hand nach vorne. ***Verh Dtsch Ges Chir.*** 1878;7:259-276.
2. Schmidt-Rohlfing B, Schwobel B, Pauschert R, Niethard FU. Madelung deformity: clinical features, therapy and results. ***J Pediatr Orthop B.*** 2001;10(4):344-348.
3. Nielsen JB. Madelung's deformity. A follow-up study of 26 cases and a review of the literature. ***Acta orthopaedica Scandinavica.*** 1977;48(4):379-384.
4. Fagg PS. Wrist pain in the Madelung's deformity of dyschondrosteosis. ***J Hand Surg Br.*** 1988;13(1):11-15.
5. de Billy B, Gastaud F, Repetto M, Chataigner H, Clavert JM, Aubert D. Treatment of Madelung's deformity by lengthening and reaxation of the distal extremity of the radius by Ilizarov's technique. ***Eur J Pediatr Surg.*** 1997;7(5):296-298.
6. Flatt AE. ***The care of congenital hand anomalies.*** Quality Medical Publishing; 1994.
7. Herdman RC, Langer LO, Good RA. Dyschondrosteosis. The most common cause of Madelung's deformity. ***The Journal of pediatrics.*** 1966;68(3):432-441.
8. Henry A, Thorburn MJ. Madelung's deformity. A clinical and cytogenetic study. ***The Journal of bone and joint surgery British volume.*** 1967;49(1):66-73.
9. Grigelioniene G, Eklof O, Ivarsson SA, et al. Mutations in short stature homeobox containing gene (SHOX) in dyschondrosteosis but not in hypochondroplasia. ***Human Genetics.*** 2000;107(2):145-149.
10. Dannenberg M, Anton J, Spiegel M. Madelung's deformity: consideration of its roentgenological diagnostic criteria. ***Am J Roentgenol.*** 1939;42:671-676.
11. McCarroll HR, Jr., James MA, Newmeyer WL, 3rd, Molitor F, Manske PR. Madelung's deformity: quantitative assessment of x-ray deformity. ***The Journal of hand surgery.*** 2005;30(6):1211-1220.
12. Dubey A, Fajardo M, Green S, Lee SK. Madelung's deformity: a review. ***The Journal of hand surgery, European volume.*** 2009;35(3):174-181.
13. Ghatan AC, Hanel DP. Madelung deformity. ***J Am Acad Orthop Surg.*** 2013;21(6):372-382.
14. Kozin SH, Zlotolow DA. Madelung Deformity. ***J Hand Surg Am.*** 2015;40(10):2090-2098.
15. McCarroll HR, James MA, Newmeyer WL, 3rd, Manske PR. Madelung's deformity: quantitative radiographic comparison with normal wrists. ***The Journal of hand surgery, European volume.*** 2008;33(5):632-635.
16. Peymani A, Dobbe JGG, Streekstra GJ, McCarroll HR, Strackee SD. Quantitative three-dimensional assessment of Madelung deformity. ***The Journal of hand surgery, European volume.*** 2019;44(10):1041-1048.
17. Cook PA, Yu JS, Wiand W, et al. Madelung deformity in skeletally immature patients: morphologic assessment using radiography, CT, and MRI. ***Journal of computer assisted tomography.*** 1996;20(4):505-511.
18. Créteur V, Madani A, Bianchi S. Sonographic Findings in Adult Congenital Madelung Deformity: A Case Study. ***Journal of Diagnostic Medical Sonography.*** 2020;36(1):65-71.
19. Vickers D, Nielsen G. Madelung deformity: surgical prophylaxis (physiolysis) during the late growth period by resection of the dyschondrosteosis lesion. ***J Hand Surg Br.*** 1992;17(4):401-407.
20. Stehling C, Langer M, Nassenstein I, Bachmann R, Heindel W, Vieth V. High resolution 3.0 Tesla MR imaging findings in patients with bilateral Madelung's deformity. ***Surg Radiol Anat.*** 2009;31(7):551-557.

21. Ali S, Kaplan S, Kaufman T, Fenerty S, Kozin S, Zlotolow DA. Madelung deformity and Madelung-type deformities: a review of the clinical and radiological characteristics. ***Pediatric radiology.*** 2015;45(12):1856-1863.

22. Peymani A, Johnson AR, Dowlatshahi AS, et al. Surgical Management of Madelung Deformity: A Systematic Review. ***Hand (N Y).*** 2019;14(6):725-734.

23. Berger RA. The anatomy and basic biomechanics of the wrist joint. ***J Hand Ther.*** 1996;9(2):84-93.

24. Crisco JJ, McGovern RD, Wolfe SW. Noninvasive technique for measuring in vivo three-dimensional carpal bone kinematics. ***J Orthop Res.*** 1999;17(1):96-100.

25. Moojen TM, Snel JG, Ritt MJ, Venema HW, Kauer JM, Bos KE. In vivo analysis of carpal kinematics and comparative review of the literature. ***The Journal of hand surgery.*** 2003;28(1):81-87.

26. Short WH, Palmer AK, Werner FW, Murphy DJ. A biomechanical study of distal radial fractures. ***The Journal of hand surgery.*** 1987;12(4):529-534.

27. Moore DC, Hogan KA, Crisco JJ, 3rd, Akelman E, Dasilva MF, Weiss AP. Three-dimensional in vivo kinematics of the distal radioulnar joint in malunited distal radius fractures. ***The Journal of hand surgery.*** 2002;27(2):233-242.

28. Crisco JJ, Moore DC, Marai GE, et al. Effects of distal radius malunion on distal radioulnar joint mechanics--an in vivo study. ***J Orthop Res.*** 2007;25(4):547-555.

29. Blankenhorn BD, Pfaeffle HJ, Tang P, Robertson D, Imbriglia J, Goitz RJ. Carpal kinematics after proximal row carpectomy. ***The Journal of hand surgery.*** 2007;32(1):37-46.

30. Foumani M, Strackee SD, Stekelenburg CM, Blankevoort L, Streekstra GJ. Dynamic in vivo evaluation of radiocarpal contact after a 4-corner arthrodesis. ***The Journal of hand surgery.*** 2015;40(4):759-766.

31. Dobbe JGG, de Roo MGA, Visschers JC, Strackee SD, Streekstra GJ. Evaluation of a Quantitative Method for Carpal Motion Analysis Using Clinical 3-D and 4-D CT Protocols. ***IEEE Trans Med Imaging.*** 2019;38(4):1048-1057.

32. Belin V, Cusin V, Viot G, et al. SHOX mutations in dyschondrosteosis (Leri-Weill syndrome). ***Nature genetics.*** 1998;19(1):67-69.

33. Smits-Engelsman B, Klerks M, Kirby A. Beighton score: a valid measure for generalized hypermobility in children. ***The Journal of pediatrics.*** 2011;158(1):119-123, 123 e111-114.

34. Peymani A, Foumani M, Dobbe JGG, Strackee SD, Streekstra GJ. Four-dimensional rotational radiographic scanning of the wrist in patients after proximal row carpectomy. ***The Journal of hand surgery, European volume.*** 2017;42(8):846-851.

35. Foumani M, Strackee SD, van de Giessen M, Jonges R, Blankevoort L, Streekstra GJ. In-vivo dynamic and static three-dimensional joint space distance maps for assessment of cartilage thickness in the radiocarpal joint. ***Clin Biomech (Bristol, Avon).*** 2013;28(2):151-156.

36. Scalco RC, Melo SS, Pugliese-Pires PN, et al. Effectiveness of the combined recombinant human growth hormone and gonadotropin-releasing hormone analog therapy in pubertal patients with short stature due to SHOX deficiency. ***J Clin Endocrinol Metab.*** 2010;95(1):328-332.

37. Ranawat CS, DeFiore J, Straub LR. Madelung's deformity. An end-result study of surgical treatment. ***The Journal of bone and joint surgery American volume.*** 1975;57(6):772-775.

38. Salon A, Serra M, Pouliquen JC. Long-term follow-up of surgical correction of Madelung's deformity with conservation of the distal radioulnar joint in teenagers. ***J Hand Surg Br.*** 2000;25(1):22-25.

39. Zebala LP, Manske PR, Goldfarb CA. Madelung's deformity: a spectrum of presentation. ***J Hand Surg Am.*** 2007;32(9):1393-1401.

40. Murphy MS, Linscheid RL, Dobyns JH, Peterson HA. Radial opening wedge osteotomy in Madelung's deformity. ***The Journal of hand surgery.*** 1996;21(6):1035-1044.

41. dos Reis FB, Katchburian MV, Faloppa F, Albertoni WM, Laredo Filho J, Jr. Osteotomy of the radius and ulna for the Madelung deformity. ***The Journal of bone and joint surgery British volume.*** 1998;80(5):817-824.

42. Eid A, Abdel Salam MA, Elgawhary S. Management of idiopathic Madelung deformity with the Sauve-Kapandji procedure. ***Current orthopaedic practice.*** 2018;29(5):491-496.

43. Bruno RJ, Blank JE, Ruby LK, Cassidy C, Cohen G, Bergfield TG. Treatment of Madelung's deformity in adults by ulna reduction osteotomy. ***J Hand Surg Am.*** 2003;28(3):421-426.

44. McCarroll HR, Jr., James MA, Newmeyer WL, 3rd, Manske PR. Madelung's deformity: diagnostic thresholds of radiographic measurements. ***The Journal of hand surgery.*** 2010;35(5):807-812.

45. Kitay A, Wolfe SW. Scapholunate instability: current concepts in diagnosis and management. ***The Journal of hand surgery.*** 2012;37(10):2175-2196.

46. Wolfe SW, Neu C, Crisco JJ. In vivo scaphoid, lunate, and capitate kinematics in flexion and in extension. ***The Journal of hand surgery.*** 2000;25(5):860-869.

47. Hanson TJ, Murthy NS, Shin AY, Kakar S, Collins MS. MRI appearance of the anomalous volar radiotriquetral ligament in true Madelung deformity. ***Skeletal Radiol.*** 2019;48(6):915-918.

48. Babu S, Turner J, Seewoonarain S, Chougule S. Madelung's Deformity of the Wrist-Current Concepts and Future Directions. ***J Wrist Surg.*** 2019;8(3):176-179.

49. Otte JE, Popp JE, Samora JB. Treatment of Madelung Deformity With Vicker Ligament Release and Radial Physiolyses: A Case Series. ***The Journal of hand surgery.*** 2019;44(2):158 e151-158 e159.

50. Glard Y, Gay A, Launay F, Guinard D, Legre R. Isolated wedge osteotomy of the ulna for mild Madelung's deformity. ***J Hand Surg Am.*** 2007;32(7):1037-1042.

51. Weiss KE, Rodner CM. Osteoarthritis of the wrist. ***The Journal of hand surgery.*** 2007;32(5):725-746.

52. van Saase JL, van Romunde LK, Cats A, Vandenbroucke JP, Valkenburg HA. Epidemiology of osteoarthritis: Zoetermeer survey. Comparison of radiological osteoarthritis in a Dutch population with that in 10 other populations. ***Ann Rheum Dis.*** 1989;48(4):271-280.

53. Dodge HJ, Mikkelsen WM, Duff IF. Age-sex specific prevalence of radiographic abnormalities of the joints of the hands, wrists and cervical spine of adult residents of the Tecumseh, Michigan, Community Health Study area, 1962-1965. ***J Chronic Dis.*** 1970;23(3):151-159.

SUPPLEMENTAL DATA

Supplemental Video 1. Scan the QR code to view the video.

Supplemental Table 1. Carpal kinematics during flexion-extension motion.

	Mean difference	Standard error	95% CI	P
Scaphoid translation, mm	-0.3	0.1	-0.5 to 0.0	0.064
X-axis	0	0.1	-0.2 to 0.1	0.644
Y-axis	0.4	0.2	0.0 to 0.7	**0.045**
Z-axis	0.2	0.2	-0.2 to 0.6	0.302
Scaphoid rotation, degrees	-1.4	1	-3.3 to 0.6	0.182
X-axis	-4.5	1.3	-7.1 to -1.9	1
Y-axis	0.2	0.7	-1.2 to 1.6	0.765
Z-axis	-1.8	0.9	-3.6 to -0.0	0.057
Lunate translation, mm	-0.2	0.1	-0.4 to 0.0	0.119
X-axis	-0.2	0.1	-0.4 to -0.1	**0.006**
Y-axis	0.0	0.1	-0.2 to 0.2	0.921
Z-axis	0.0	0.1	-0.2 to 0.3	0.740
Lunate rotation, degrees	-4.6	1.3	-7.1 to -2.2	**0.001**
X-axis	-2.8	1.2	-5.2 to -0.5	1.000
Y-axis	0.5	0.5	-0.4 to 1.5	0.279
Z-axis	-0.3	0.5	-1.3 to 0.6	0.469
Triquetrum translation, mm	-0.2	0.2	-0.6 to 0.1	0.248
X-axis	-0.2	0.1	-0.4 to -0.1	**0.006**
Y-axis	0.2	0.2	-0.1 to 0.5	0.293
Z-axis	0.1	0.1	-0.1 to 0.4	0.348
Triquetrum rotation, degrees	-4.8	0.9	-6.7 to -3.0	**<0.001**
X-axis	-2.4	1.1	-4.6 to -0.3	**0.035**
Y-axis	0.6	0.6	-0.5 to 1.7	0.271
Z-axis	-0.3	0.6	-1.5 to 0.9	0.607

Supplemental Table 2. Carpal kinematics during radio-ulnar deviation.

	Mean difference	Standard error	95% CI	P
Scaphoid translation, mm	-0.3	0.2	-0.7 to 0.1	0.136
X-axis	0.1	0.1	-0.1 to 0.2	0.468
Y-axis	0.0	0.1	-0.2 to 0.2	0.876
Z-axis	-0.4	0.2	-0.7 to -0.0	0.058
Scaphoid rotation, degrees	2.5	1.6	-0.7 to 5.6	0.131
X-axis	-5.4	1.7	-8.7 to -2.1	**0.003**
Y-axis	3.1	1.1	1.0 to 5.2	**0.006**
Z-axis	-3.2	1.0	-5.2 to -1.3	**0.003**
Lunate translation, mm	-0.7	0.2	-1.0 to -0.4	**<0.001**
X-axis	-0.5	0.1	-0.8 to -0.2	**0.002**
Y-axis	0.0	0.1	-0.1 to 0.1	0.771
Z-axis	-0.2	0.1	-0.4 to 0.0	0.108
Lunate rotation, degrees	-1.4	1.2	-3.9 to 1.0	0.256
X-axis	-2.6	1.2	-5.0 to -0.2	**0.041**
Y-axis	3.3	0.9	1.5 to 5.0	**0.001**
Z-axis	-2.7	0.7	-4.1 to -1.3	1.000
Triquetrum translation, mm	-0.6	0.2	-0.9 to -0.3	**0.001**
X-axis	-0.5	0.2	-0.8 to -0.2	**0.002**
Y-axis	0.6	0.2	0.2 to 0.9	**0.002**
Z-axis	0.2	0.2	-0.2 to 0.6	0.325
Triquetrum rotation, degrees	-1.9	0.9	-3.7 to -0.1	**0.049**
X-axis	-3.3	1.1	-5.4 to -1.1	**0.006**
Y-axis	2.6	0.8	1.0 to 4.2	**0.003**
Z-axis	-1.4	0.5	-2.4 to -0.4	**0.009**

7

THE DISTAL RADIUS IN MADELUNG DEFORMITY: A STATISTICAL SHAPE ANALYSIS

A. Peymani [1,2], J.G.G. Dobbe [2],
S.K. van Rijn [1], H.R. McCarroll [3],
G.J. Streekstra [2,4], S.D. Strackee [1]

[1] Department of Plastic, Reconstructive and Hand Surgery, Amsterdam UMC, University of Amsterdam, Amsterdam, The Netherlands.
[2] Department of Biomedical Engineering and Physics, Amsterdam UMC, University of Amsterdam, Amsterdam, The Netherlands.
[3] Department of Orthopaedic Surgery, California Pacific Medical Center, San Francisco, CA, USA.
[4] Department of Radiology and Nuclear Medicine, Amsterdam UMC, University of Amsterdam, Amsterdam, The Netherlands.

Submitted.

ABSTRACT

Due to the rarity of Madelung deformity, our anatomical knowledge and diagnostic efficacy are limited. We developed three-dimensional statistical shape models to quantify distal radial shape, visualize the shape spectrum, determine classifications, and assess the efficacy of shape information in predictive modeling. Using wrist CT scans of 26 Madelung deformity and 26 healthy wrists, statistical shape models could represent shape variations as 'modes' of variation. Over 80% of variation can be explained using five modes. No subclassification of Madelung deformity could be defined using our model. Combining modes, a binary logistic regression model can accurately (94%) predict radius bones to belong to either Madelung deformity or healthy wrists. These findings show promise for the use of shape quantifications in future diagnostic predictive models. Quantifying three-dimensional shape, even if the absolute number of shapes is small, could be especially useful in rare congenital conditions in which minimal patient numbers have limited clinicians' anatomical exposure.

INTRODUCTION

Madelung deformity is a rare congenital disease of the wrist caused by premature fusion of the epiphyseal plate of the radius bone.[1-3] While several skeletal and soft tissue abnormalities have been identified,[4-7] it has been hypothesized that the source of primary pathology is the radius, with other wrist joint abnormalities of compensatory nature.[2] The deformed radius bone in Madelung deformity presents on a spectrum that affects the entire radius or only the distal part,[8] with a significant degree of variability existing within patients' distal radius bones.[9,10]

Since Madelung deformity's introduction, studies have increased our anatomical knowledge through quantifications on two-dimensional (2D) imaging.[4,6] This has led to a paradigm shift in the diagnostic work-up and surgical management of patients, with the McCarroll criteria being the most commonly used in quantifying the deformity.[11] Automatic three-dimensional (3D) measurements have eliminated inter- and intra-rater measurement differences and expanded our diagnostic toolkit.[12] However, there is a significant overlap between Madelung deformity and healthy wrists in both 2D and 3D assessments,[9,10,12] and this suboptimal distinction has limited the diagnostic efficacy.[13] Could it be that in our collective journey to fathom this condition, we might have restricted ourselves by 'handpicking' the points of interest, manually measuring lengths and angles instead of computationally analyzing all available information contained in a 3D shape?

This study aimed to develop a 3D statistical shape model (SSM), a computer-generated model that encodes all anatomical shape characteristics and variations of the distal radius.[14] This model is used to investigate the following objectives:

1. Which shape characteristics and variations exist within the distal radius of Madelung deformity wrists?
2. Is it possible to develop a classification within Madelung deformity based on shape differences?
3. Can distal radial shape differences be used in a diagnostic predictive model?

This methodology, if proven successful, could be a valuable asset for our anatomical knowledge, surgical planning, and diagnostics of skeletal deformities, especially in rare congenital conditions such as Madelung deformity where limited patient numbers have restricted our anatomical understanding.

MATERIALS AND METHODS

Patient selection

In this retrospective cohort study, we included wrist CT scans of patients diagnosed with Madelung deformity, identified using the International Classification of Diseases, Ninth Revision, Clinical Modification (ICD-9-CM) code: 755.54. Scans were only included if no surgery before the scan date had taken place; post-traumatic cases were excluded. A total of 26 scans were eligible. Next, 26 previously acquired wrist CT scans of healthy volunteers were added, matched by age and gender. An overview of the workflow to generate SSMs from CT scans of the distal radius is shown in Figure 1. Our institutional review board approved this study.

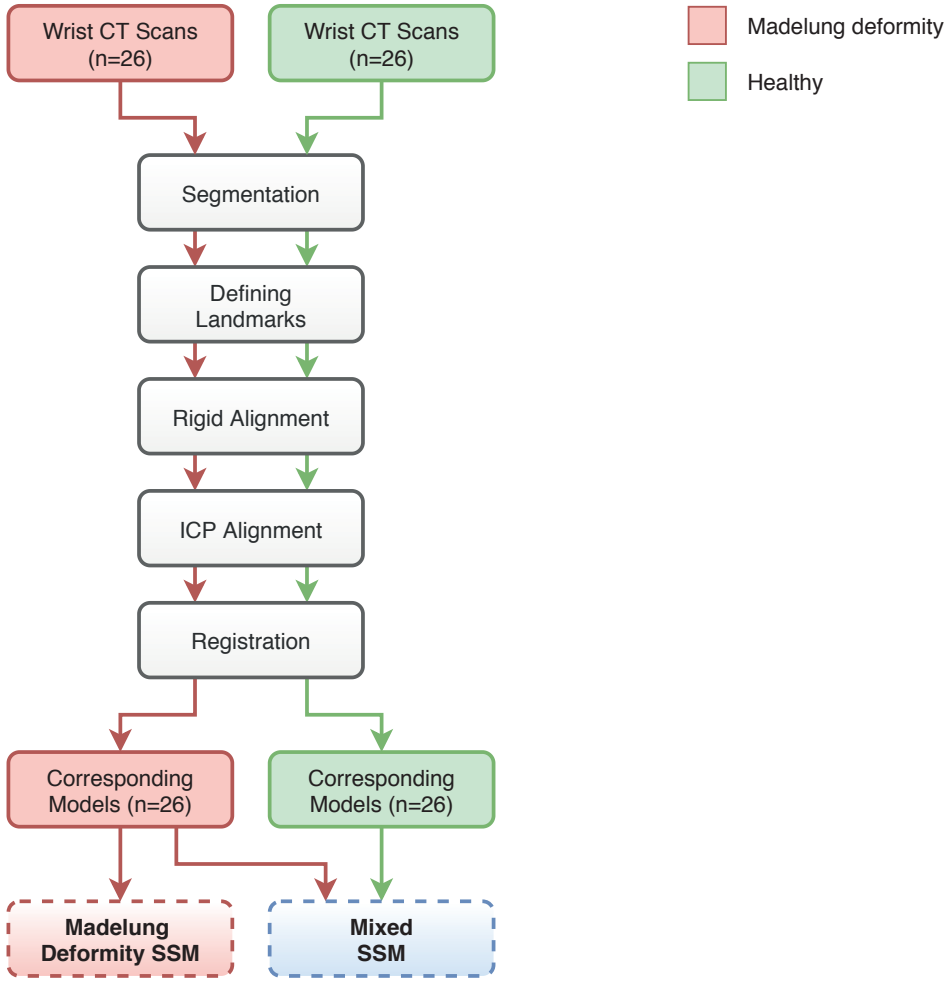

Figure 1. Overview of the workflow from initial CT-scan to statistical shape model.

Image segmentation and normalization

The distal radius in each scan was segmented using a custom-made software package.[15] The resulting virtual 3D shapes were exported as polygon meshes. Polygon meshes were clipped to the most distal 53 mm, ensuring equally sized distal radius 'height' throughout the dataset. All 'left-hand' shapes were mirrored to obtain a homogenous set of 'right-hand' shapes of the distal radius.

Alignment and registration

SSMs were built using the open-source software package Scalismo (University of Basel), an extensive library for statistical shape modeling and model-based image analysis.[16] First, four landmarks were identified: (1) radial styloid process; (2) Lister's tubercle; (3) dorsal edge of the lunate fossa; and (4) palmar edge of the lunate fossa. Using these landmark coordinates, the best rigid transformation

could be determined, minimizing mean squared error over the landmark points to achieve an initial alignment of 3D shapes. This was an imprecise alignment as landmarks were placed manually, and the dorsal and palmar edge of the deformed lunate fossa were not easily identifiable in Madelung deformity.[17] Next, an automatic rigid alignment was performed using an iterative closest points (ICP) algorithm, minimizing the distances between point clouds of shapes.[18] Both alignment steps were performed to minimize translational and rotational variations between shapes. No scaling was implemented because we were interested in any possible size differences for both shape variation analyses and diagnostic predictive potential. Finally, all individual points of the aligned shapes were brought into correspondence using a parametric and non-rigid registration algorithm;[19] thereafter, two defined points on two corresponding models would denote the same semantic point (e.g., the radial styloid process). The non-rigid registration of 52 shapes finished with a mean squared error of 0.002±0.001 mm in terms of pointwise mesh-to-mesh differences, indicating that the registered shapes showed a high correspondence.

Generating statistical shape models

An SSM can be obtained through principal component analysis on corresponding points of 3D shapes,[20] a dimensionality reduction method to represent variations in terms of a set of orthogonal vectors, maximizing the variance of points in each direction.[21] These vectors, referred to as 'modes' of variation, are placed in descending order, with the first mode describing the most pronounced shape variation. To visualize variations, an SSM was developed using all 26 shapes of Madelung deformity distal radius bones. While SSMs encode characteristic information to establish the mean shape and any statistical variation within a 99.7% confidence interval (-3 SD to +3 SD), we visualized the 95% confidence interval (-2 SD to +2 SD) to limit the effect of rare outliers.

Determining coefficients

For each Madelung deformity shape, an individual SSM was developed after excluding that shape from the dataset of Madelung deformity shapes (n=26), ensuring that the resulting model did not contain characteristic information of the excluded shape. The generated SSMs were then fitted to the excluded shape, resulting in a set of calculated coefficients for each SSM mode, best fitting the excluded shape. The combination of all modes' coefficients effectively quantified a 3D shape and was determined for each shape to detect any potential grouping within Madelung deformity. Grouping was investigated by analyzing whether coefficient data were distributed normally or in a multinomial manner, with a potential binomial distribution indicating two distinct groups.

The same procedure was performed for each of the 3D shapes in a combined dataset of Madelung deformity and healthy radius bones (n=52), generating 'mixed' SSMs after excluding a shape, fitting the model to that shape, and determining its coefficients. These coefficients, which were determined for all Madelung deformity and healthy distal radius bones, were used to assess a shapes' predictive ability.

Statistical analysis

The Kolmogorov-Smirnov test for normality was performed to detect multinomial distributions of coefficients for the modes in our Madelung deformity SSM. Multiple binary logistic regression models were developed using the coefficients of our 'mixed' SSMs as continuous covariates and a shape's origin as a binary outcome (0 = healthy, 1 = Madelung deformity). To avoid overfitting, 70% of our combined dataset (36 randomly selected shapes) was used as a training set and the remaining 30% (sixteen shapes) as a testing set. Both sets contained equal numbers of Madelung deformity and healthy wrists. Model performance was expressed using the metrics: sensitivity, specificity, accuracy, precision, and F1-score. Accuracy was defined as the ratio of correctly classified shapes relative to all shapes and was used to rank performance. Precision was defined as the weighted average of: correct percentage of classified Madelung deformity shapes and the correct percentage of classified healthy shapes. F1-score was defined as the 'harmonic' average of precision and sensitivity, using the formula:

$$F_1 = 2 \cdot \frac{precision \cdot sensivity}{precision + sensivity}$$

Analyses were done in Python using the SciPy (1.3.1) and scikit-learn (0.21.3) packages, open-source libraries used for scientific computing and machine learning, respectively.

Table 1. Study characteristics.

	Madelung deformity wrists (n=26)	**Healthy wrists (n=26)**
Age at CT scan, y	19.2±6.6	22.0±5.2
Female	26 (100%)	26 (100%)
Right-hand side	15 (58%)	15 (58%)
Bilateral deformity	23 (88%)	—
Confirmed genetic cause	8 (31%)	—

Table 2. First five modes of variation for a statistical shape model of the distal radius in Madelung deformity wrists.

Mode	**Description**	**Explained variance**	**Kolmogorov-Smirnov statistic**	**P**
1	Ulnar-Sided Collapse	37%	0.077	0.998
2	Coronal Width	18%	0.158	0.494
3	Sigmoid Notch Axial Rotation	13%	0.118	0.865
4	Volar Tilt	9%	0.223	0.129
5	Lunate Fossa Angle	5%	0.187	0.287

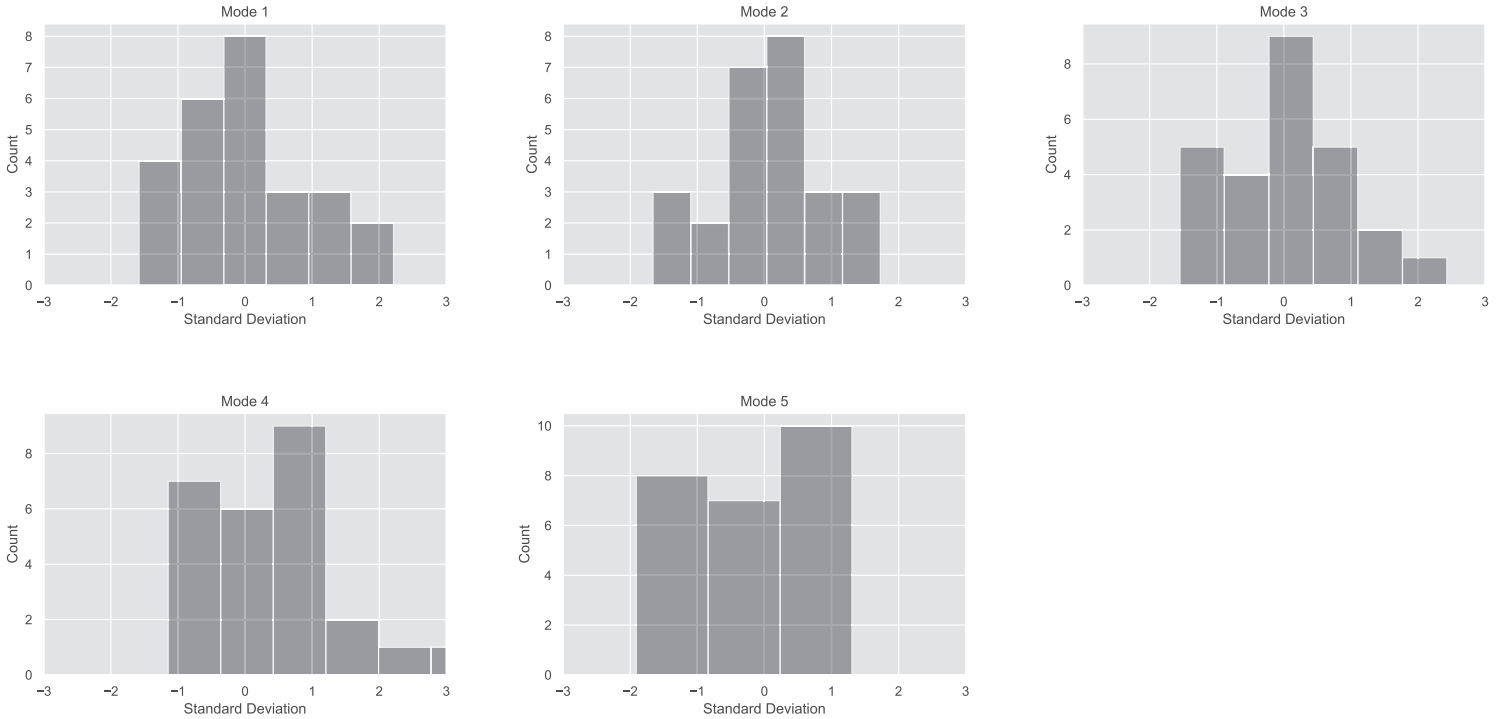

Figure 2. Shape variations of the distal radius in Madelung deformity. The -2SD, mean, and +2SD of the first five modes are visualized.

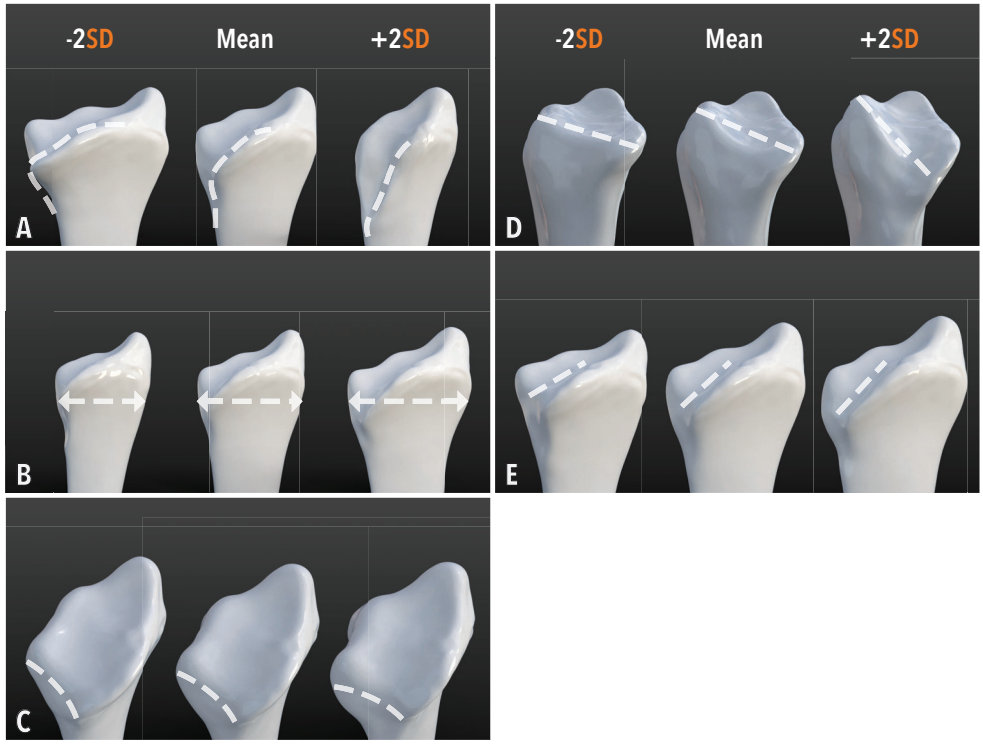

Figure 3. Distribution of shape parameters for the first five modes in a Madelung deformity statistical shape model: (A) Ulnar-Sided Collapse; (B) Coronal Width; (C) Sigmoid Notch Axial Rotation; (D) Volar Tilt; and (E) Lunate Fossa Angle.

Table 3. Performance metrics of binary logistic regression models.

Mode(s)	Sensitivity	Specificity	Accuracy	Precision	F1 Score
1	0.857	0.889	0.875	0.875	0.875
2	0.714	0.333	0.500	0.536	0.484
3	0.714	0.333	0.500	0.536	0.484
4	0.571	0.444	0.500	0.516	0.500
5	1.000	0.000	0.438	0.191	0.266
1, 2	0.857	1.000	0.938	0.944	0.937
1, 3	1.000	0.778	0.875	0.903	0.875
2, 3	0.857	0.444	0.625	0.689	0.613

RESULTS

Madelung deformity wrists (n=26) were scanned at a mean age of 19.2±6.6 years; healthy wrists (n=26) were scanned at a mean age of 22.0±5.2 years. All wrists belonged to female patients. Study characteristics are shown in Table 1.

The first five modes of variation (37%, 18%, 13%, 9%, and 5%), cumulatively explain up to 82% of the statistical shape variation seen in Madelung deformity and are described in Table 2. The distribution of shape parameters in Madelung deformity distal radius bones is shown for each mode in Figure 2. Each of the five modes followed a normal distribution, and there were no clear groupings. The 3D models corresponding with these modes' various values are shown in Figure 3, visualizing the statistical variation that exists within a 95% confidence interval.

The performance of our binary logistic regression models using various combinations of the modes of variation from a mixed SSM is described in Table 3. The highest performance was seen in a model using modes 1 and 2 (Sensitivity 0.857, Specificity 1.000, Accuracy 0.938, Precision 0.944, and F1 Score 0.937).

DISCUSSION

In this study, we developed an SSM of the distal radius in Madelung deformity to statistically quantify and visualize shape variations. The first five modes of this SSM, explaining up to 82% of the observed variation in shape, did not show any distinct groupings. A mixed SSM was developed containing distal radius shapes of both Madelung deformity and healthy bones. After fitting this model to each shape, the resulting coefficients were used to classify shapes as belonging to a Madelung deformity wrist or a healthy wrist with high accuracy (up to 94%).

Shape variations of the distal radius

Previous studies have developed SSMs of the distal radius in healthy volunteers and in cadaveric settings to assess morphometric data, predict pre-traumatic healthy shapes, and investigate shape differences between males and females.[22-24] In contrast, Madelung deformity's distal radius shape has only been described qualitatively in clinical and medical imaging studies.[6,12,25-27] To the best of our knowledge, this is the first study that established an SSM for Madelung deformity, enabling us to quantify and visualize a full spectrum of existing variations (Supplemental Video 1). We subjectively described the most prominent visible change for each mode of variation when adjusting the coefficients of that mode (from -3SD to +3SD). Mode 1 was described as the ulnar-sided collapse of the distal radius, showing increasing levels of collapse of both the radiocarpal and the distal radioulnar (DRU) joint while nearing the +3 SD value. Mode 2 was described as coronal width, showing variations in distal radial bone width in the coronal plane, with some minor differences in lunate fossa concavity and DRUJ concavity. Mode 3 was described as the axial rotation of the sigmoid notch. Mode 4 was described as volar tilt, a parameter that has been previously introduced to potentially quantify the deformity,[6] but not used in the current work-up due to its unfeasibility to be reliably measured on lateral x-rays.[5,6,28] Lastly, we described mode 5 as lunate fossa angle,[6] showing an increased ulnar angulation of the lunate fossa combined with a slight protrusion of the DRU joint while nearing the -3 SD value. Of these five modes mentioned above, four seem to manipulate the shape of the DRU joint, which is known to be crucial for forearm pronation and supination.[29] Interestingly, of all the range of motion measurements, pronation and supination are the most limited in Madelung deformity patients.[30-32] Nevertheless, current surgical

treatment options are mainly focused on the radiocarpal joint;[11] this is noteworthy, since ignoring an abnormal DRU joint could lead to suboptimal outcomes following surgery.[17,32,33] Some studies have performed the 'Sauvé-Kapandji' procedure,[34,35] which does address the DRU joint but has been reported to cause postoperative instability in some cases.[36-38] Therefore, it might be beneficial to explore alternative surgical treatment options for a subset of patients in which the DRU is too deformed.

Towards a classification framework

The Dannenberg criteria were the first published criteria for the diagnosis of Madelung deformity,[39] describing radiographic abnormalities mainly of the radius bone, but also of the ulna and carpal bones.[4] McCarroll et al. defined four parameters of the distal radius for use in the diagnostic work-up, to monitor changes in time, and to quantify pre- and postoperative differences.[6] These measurements reduce the complex anatomy to two angles and two linear measurements,[10] with each measurement showing a considerable amount of dispersion.[9] Zebala et al. identified two groups within Madelung deformity patients: patients with involvement of the distal radius only and patients with involvement of the entire radius. The latter group was reported to have increased values of the McCarroll parameters and a significantly higher occurrence of dyschondrosteosis (100% vs. 64%) in comparison to patients with distal involvement only.[8] Given the combination of Madelung deformity's anomalous spectrum, the wide range of etiological causes,[25,40,41] and the absence of a surgical treatment protocol,[11] it is not surprising that clinicians have attempted to develop a classification. In this study, we visualized 3D shapes on both ends of the spectrum (Figure 2) and everything in between, through the development of an SSM, which is being increasingly used in imaging studies.[14,24,42-44] Next, we attempted to establish a classification using statistically sound methods to determine shape variability. Unfortunately, in our limited dataset (n=26) which focused on the distal aspect of the radius bone, we did not find any evidence of distinct Madelung deformity groups based on shape (Figure 2, Table 2).

Diagnostic potential

The diagnosis of Madelung deformity is unreliable for mild cases, with a low agreement between hand surgeons independent of rater confidence, place of practice, and a surgeons' professional experience.[13] Also, there is considerable overlap between Madelung deformity wrists and healthy wrists for current 2D and newly proposed 3D measurements.[9,10,12] Since our 'mixed' SSM, containing both Madelung deformity and healthy shapes, quantifies all 3D shape information instead of manually measuring lengths and angles, it would be interesting to investigate its potential to distinguish between deformed and healthy. Every shape in our dataset was quantified using the coefficients of the modes of variation. After division into a training and a testing set, we tested the performance of several regression models. Combining the first two modes, we were able to accurately (94%) classify a distal radius either as belonging to a Madelung deformity patient or a healthy volunteer. While there seems to be potential for predictive modeling, it should be noted that our testing dataset was quite limited (n=16), limiting firm conclusions regarding future diagnostic efficacy.

Future applications

Studies have used SSMs to reconstruct bony defects,[45] predict cartilage shape from bone shape,[46] and to associate anatomy with kinematics.[47] Using a SSM as a guideline for reconstruction could be especially beneficial in settings where the contralateral side cannot be used, such as in patients with bilaterally affected anatomy like Madelung deformity.[17] Since the entire radius can be affected, and both radial length and curvature have been suggested in radiographic criteria,[4,8] it could be of interest to create an SSM of the forearm. This could increase predictive performance and enable classifying different types of Madelung deformity. Also, including early Madelung deformity cases in the SSM could ultimately enable diagnosis at an early stage of development, where proper treatment could prevent excessive bone deformation.[5,41] In general, SSMs can increase our knowledge of anatomy and statistically likely variations, even if the absolute number of shapes is relatively small.[48] This could be particularly useful in comprehending other rare congenital conditions, where clinicians' severely limited exposure has limited their anatomical understanding.

Strengths & Limitations

This study's main limitation was that our retrospective dataset predominantly contained wrist CT scans in which only the distal radius bone was captured. Especially since SSMs can only describe shapes similar to what has been 'seen', this would limit the spectrum as visualized and quantified in this study, affecting our ability to find a potential classification and optimize prediction models. Also, a relatively low number of Madelung deformity wrists were included. A similar study investigating healthy scaphoid and lunate bones showed that using 25 and ten shapes for scaphoid and lunate, respectively, was sufficient to describe statistical variations.[48] While we included 26 shapes, there is probably more variation in the distal radius of an anatomically complex deformity in comparison to the scaphoid and lunate bones of healthy wrists. Another limitation was the manual selection of landmarks for the initial alignment. However, we expect the effect on our results to be negligible, as these landmarks were only used for the initial 'rough' alignment, after which an automatic alignment was performed using an ICP algorithm. Lastly, there was potential for misclassification of Madelung deformity patients, even though we reviewed each patient chart. It has been argued that a distinction can be made between 'true' Madelung deformity and 'Madelung-like' deformities; this is a critical and ongoing discussion, but unfortunately, there is still no consensus on how to make the distinction accurately.[2,7,41,49] That being said, we excluded 'post-traumatic' patients[41] as not to contaminate our dataset.

Conclusion

In this study, we statistically quantified and visualized the five most crucial shape variations of Madelung deformity in 3D, highlighting the spectrum in which the distal radius can present. Madelung deformity patients' distal radius shape is both visibly and quantitatively different in comparison to healthy volunteers, and we demonstrated the promising efficacy of using this information in predictive models to distinguish Madelung deformity from healthy.

REFERENCES

1. Madelung O. Die spontane Subluxation der Hand nach vorne. ***Verh Dtsch Ges Chir.*** 1878;7:259-276.
2. Anton JI, Reitz GB, Spiegel MB. MADELUNG'S DEFORMITY. ***Ann Surg.*** 1938;108(3):411-439.
3. Flatt AE. ***The care of congenital hand anomalies.*** Mosby St Louis; 1977.
4. Dannenberg M, Anton J, Spiegel M. Madelung's deformity: consideration of its roentgenological diagnostic criteria. ***Am J Roentgenol.*** 1939;42:671-676.
5. Vickers D, Nielsen G. Madelung deformity: surgical prophylaxis (physiolysis) during the late growth period by resection of the dyschondrosteosis lesion. ***J Hand Surg Br.*** 1992;17(4):401-407.
6. McCarroll HR, Jr., James MA, Newmeyer WL, 3rd, Molitor F, Manske PR. Madelung's deformity: quantitative assessment of x-ray deformity. ***J Hand Surg Am.*** 2005;30(6):1211-1220.
7. Hanson TJ, Murthy NS, Shin AY, Kakar S, Collins MS. MRI appearance of the anomalous volar radiotriquetral ligament in true Madelung deformity. ***Skeletal Radiol.*** 2018.
8. Zebala LP, Manske PR, Goldfarb CA. Madelung's deformity: a spectrum of presentation. ***J Hand Surg Am.*** 2007;32(9):1393-1401.
9. McCarroll HR, James MA, Newmeyer WL, 3rd, Manske PR. Madelung's deformity: quantitative radiographic comparison with normal wrists. ***J Hand Surg Eur Vol.*** 2008;33(5):632-635.
10. McCarroll HR, Jr., James MA, Newmeyer WL, 3rd, Manske PR. Madelung's deformity: diagnostic thresholds of radiographic measurements. ***J Hand Surg Am.*** 2010;35(5):807-812.
11. Peymani A, Johnson AR, Dowlatshahi AS, et al. Surgical Management of Madelung Deformity: A Systematic Review. ***Hand (N Y).*** 2019;14(6):725-734.
12. Peymani A, Dobbe JGG, Streekstra GJ, McCarroll HR, Strackee SD. Quantitative three-dimensional assessment of Madelung deformity. ***J Hand Surg Eur Vol.*** 2019;44(10):1041-1048.
13. Farr S, Guitton TG, Ring D, Science of Variation G. How Reliable is the Radiographic Diagnosis of Mild Madelung Deformity? ***J Wrist Surg.*** 2018;7(3):227-231.
14. Vlachopoulos L, Luthi M, Carrillo F, Gerber C, Szekely G, Furnstahl P. Restoration of the Patient-Specific Anatomy of the Proximal and Distal Parts of the Humerus: Statistical Shape Modeling Versus Contralateral Registration Method. ***J Bone Joint Surg Am.*** 2018;100(8):e50.
15. Dobbe JGG, de Roo MGA, Visschers JC, Strackee SD, Streekstra GJ. Evaluation of a Quantitative Method for Carpal Motion Analysis Using Clinical 3-D and 4-D CT Protocols. ***IEEE Trans Med Imaging.*** 2019;38(4):1048-1057.
16. Lüthi M, Gerig T, Jud C, Vetter T. Gaussian process morphable models. ***IEEE transactions on pattern analysis and machine intelligence.*** 2017;40(8):1860-1873.
17. Ghatan AC, Hanel DP. Madelung deformity. ***J Am Acad Orthop Surg.*** 2013;21(6):372-382.
18. Besl PJ, McKay ND. Method for registration of 3-D shapes. Paper presented at: Sensor fusion IV: control paradigms and data structures1992.
19. Salhi A, Mutsvangwa T, Chimhundu C, Borotikar B, Burdin V. O49. A comparison of two model fitting methods for transferring mesh correspondences: Implications to scapular bone using statistical shape modelling. ***Physica Medica.*** 2016;32:157.
20. Gioia F, Lauro CN. Principal component analysis on interval data. ***Computational Statistics.*** 2006;21(2):343-363.

21. Lindner C. Automated image interpretation using statistical shape models. In: ***Statistical Shape and Deformation Analysis.*** Elsevier; 2017:3-32.

22. Oppermann J, Bredow J, Beyer F, et al. Distal radius: anatomical morphometric gender characteristics. Do anatomical pre-shaped plates pay attention on it? ***Arch Orthop Trauma Surg.*** 2015;135(1):133-139.

23. Baumbach SF, Binder J, Synek A, et al. Analysis of the three-dimensional anatomical variance of the distal radius using 3D shape models. ***BMC Med Imaging.*** 2017;17(1):23.

24. Mauler F, Langguth C, Schweizer A, et al. Prediction of normal bone anatomy for the planning of corrective osteotomies of malunited forearm bones using a three-dimensional statistical shape model. ***J Orthop Res.*** 2017;35(12):2630-2636.

25. Henry A, Thorburn MJ. Madelung's deformity. A clinical and cytogenetic study. ***J Bone Joint Surg Br.*** 1967;49(1):66-73.

26. Cook PA, Yu JS, Wiand W, et al. Madelung deformity in skeletally immature patients: morphologic assessment using radiography, CT, and MRI. ***J Comput Assist Tomogr.*** 1996;20(4):505-511.

27. Schmidt-Rohlfing B, Schwobel B, Pauschert R, Niethard FU. Madelung deformity: clinical features, therapy and results. ***J Pediatr Orthop B.*** 2001;10(4):344-348.

28. Felman AH, Kirkpatrick JA, Jr. Madelung's deformity: observations in 17 patients. ***Radiology.*** 1969;93(5):1037-1042.

29. Hagert CG. The distal radioulnar joint in relation to the whole forearm. ***Clin Orthop Relat Res.*** 1992(275):56-64.

30. Ranawat CS, DeFiore J, Straub LR. Madelung's deformity. An end-result study of surgical treatment. ***J Bone Joint Surg Am.*** 1975;57(6):772-775.

31. Murphy MS, Linscheid RL, Dobyns JH, Peterson HA. Radial opening wedge osteotomy in Madelung's deformity. ***J Hand Surg Am.*** 1996;21(6):1035-1044.

32. dos Reis FB, Katchburian MV, Faloppa F, Albertoni WM, Laredo Filho J, Jr. Osteotomy of the radius and ulna for the Madelung deformity. ***J Bone Joint Surg Br.*** 1998;80(5):817-824.

33. Coffey MJ, Scheker LR, Thirkannad SM. Total distal radioulnar joint arthroplasty in adults with symptomatic Madelung's deformity. ***Hand (N Y).*** 2009;4(4):427-431.

34. Angelini LC, Leite VM, Faloppa F. Surgical treatment of Madelung disease by the Sauve-Kapandji technique. ***Ann Chir Main Memb Super.*** 1996;15(4):257-264.

35. Eid A, Abdel Salam MA, Elgawhary S. Management of idiopathic Madelung deformity with the Sauve-Kapandji procedure. ***Current orthopaedic practice.*** 2018;29(5):491-496.

36. Vincent KA, Szabo RM, Agee JM. The Sauve-Kapandji procedure for reconstruction of the rheumatoid distal radioulnar joint. ***J Hand Surg Am.*** 1993;18(6):978-983.

37. Daecke W, Martini AK, Schneider S, Streich NA. [Clinical results after Sauve-Kapandji procedure in relation to diagnosis]. ***Unfallchirurg.*** 2004;107(11):1057-1064.

38. Guo Z, Wang Y, Zhang Y. Modified Sauve-Kapandji Procedure for Patients with Old Fractures of the Distal Radius. ***Open Med (Wars).*** 2017;12:417-423.

39. Dubey A, Fajardo M, Green S, Lee SK. Madelung's deformity: a review. ***J Hand Surg Eur Vol.*** 2009;35(3):174-181.

40. Belin V, Cusin V, Viot G, et al. SHOX mutations in dyschondrosteosis (Leri-Weill syndrome). ***Nat Genet.*** 1998;19(1):67-69.

41. Ali S, Kaplan S, Kaufman T, Fenerty S, Kozin S, Zlotolow DA. Madelung deformity and Madelung-type deformities: a review of the clinical and radiological characteristics. ***Pediatr Radiol.*** 2015;45(12):1856-1863.

42. Lotjonen J, Kivisto S, Koikkalainen J, Smutek D, Lauerma K. Statistical shape model of atria, ventricles and epicardium from short- and long-axis MR images. ***Med Image Anal.*** 2004;8(3):371-386.

43. Heimann T, Meinzer HP. Statistical shape models for 3D medical image segmentation: a review. ***Med Image Anal.*** 2009;13(4):543-563.

44. Gielis WP, Weinans H, Welsing PMJ, et al. An automated workflow based on hip shape improves personalized risk prediction for hip osteoarthritis in the CHECK study. ***Osteoarthritis Cartilage.*** 2020;28(1):62-70.

45. Plessers K, Vanden Berghe P, Van Dijck C, et al. Virtual reconstruction of glenoid bone defects using a statistical shape model. ***J Shoulder Elbow Surg.*** 2018;27(1):160-166.

46. Van Dijck C, Wirix-Speetjens R, Jonkers I, Vander Sloten J. Statistical shape model-based prediction of tibiofemoral cartilage. ***Comput Methods Biomech Biomed Engin.*** 2018:1-11.

47. Smoger LM, Fitzpatrick CK, Clary CW, et al. Statistical modeling to characterize relationships between knee anatomy and kinematics. ***J Orthop Res.*** 2015;33(11):1620-1630.

48. van de Giessen M, Foumani M, Streekstra GJ, et al. Statistical descriptions of scaphoid and lunate bone shapes. ***J Biomech.*** 2010;43(8):1463-1469.

49. Brooks TJ. Madelung Deformity in a Collegiate Gymnast: A Case Report. ***J Athl Train.*** 2003;36(2):170-173.

SUPPLEMENTAL DATA

Supplemental Video 1. Scan the QR code to view the video.

8

MADELUNG DEFORMITY: RADIOSCAPHOLUNATE ARTHRODESIS WITH A NEO-DRUJ

A. Peymani[1,2], A.R. Piek[1,2], J.G.G. Dobbe[2],
G.A. Buijze[3,4], M. Chammas[4],
G.J. Streekstra[2,5], S.D. Strackee[1]

[1] Department of Plastic, Reconstructive and Hand Surgery, Amsterdam UMC, University of Amsterdam, Amsterdam, The Netherlands.
[2] Department of Biomedical Engineering and Physics, Amsterdam UMC, University of Amsterdam, Amsterdam, The Netherlands.
[3] Department of Orthopedic Surgery, Amsterdam UMC, University of Amsterdam, Amsterdam, The Netherlands.
[4] Hand and Upper Extremity Surgery Unit, CHU Lapeyronie, University of Montpellier, Montpellier, France.
[5] Department of Radiology and Nuclear Medicine, Amsterdam UMC, University of Amsterdam, Amsterdam, The Netherlands.

Submitted.

ABSTRACT

Madelung deformity is a rare wrist anomaly that causes considerable pain while restricting function. In this study, we describe a radioscapholunate (RSL) arthrodesis with a neo-DRUJ in Madelung deformity patients with an abnormal sigmoid notch and compare results to patients after a reverse wedge osteotomy. Six wrists underwent RSL-arthrodesis with a neo-DRUJ in a two-phase approach: (1) modified RSL-arthrodesis with triquetrectomy; (2) distal scaphoidectomy. Seven wrists underwent a reverse wedge osteotomy procedure. There were no differences found in postoperative pain, grip strength, or range of motion (ROM), apart from extension, which was decreased after RSL-arthrodesis with a neo-DRUJ. Quality of life (EQ-5D-5L) and Michigan Hand Outcomes Questionnaire (MHQ) scores were similar. An RSL-arthrodesis with a neo-DRUJ could provide an alternative treatment option for a subset of patients with a severely affected sigmoid notch; while short-term postoperative outcomes seem satisfactory, more comprehensive follow-up studies will be required to confirm the procedure's durability.

INTRODUCTION

Madelung deformity is a rare wrist anomaly characterized by shortening and angulation of the distal radius articular surface, a palmar subluxation of the hand, and a prominent distal ulna.[1,2] Presentation is often bilateral and includes the presence of abnormally thickened ligaments from the distal radius to the lunate and triquetral bones.[3]

In the diagnostic work-up of Madelung deformity, the radiological criteria as proposed by McCarroll are often used in the quantification, early identification, monitoring of progression, and assessment after corrective surgery.[4] Indications for surgical treatment include wrist pain, restricted range of motion, loss of grip strength, and cosmetic deformity.[1,5,6] Currently, there is no standardized surgical method.[1,5] When evaluating the range of surgical treatment options, the spotlight has been placed on correcting length and angles to obtain a 'near-normal' anatomical configuration, with a majority of case series performing osteotomies of radius and/or ulna.[5,7] However, in some patients, a large discrepancy between the ulna and proximal carpal row can be found on preoperative computed tomography (CT) imaging. Additionally, the sigmoid notch can be severely underdeveloped, leaving the ulnar head with nothing to articulate with.[8,9] For these patients, an osteotomy procedure could be suboptimal. The new surgical approach as introduced in this study aims to offer a solution for this subset of patients.

The primary objective of this case series study is to describe a new surgical approach to Madelung deformity, consisting of a radioscapholunate (RSL) arthrodesis and construction of a neo-distal radioulnar joint (DRUJ). Preliminary results are reported through clinical outcomes: pain intensity levels, range of motion (ROM), and grip strength measurements; functional outcomes are assessed using patient-reported outcome measures (PROMs). To determine its position in the current treatment landscape, we compared outcomes after the new surgical approach to outcomes after a reverse wedge osteotomy.

MATERIALS AND METHODS

Setting and study population

Patients diagnosed with Madelung deformity were identified by a search of our two academic tertiary referral institutions' electronic medical record databases, using the International Classification of Diseases, Ninth Revision, Clinical Modification (ICD-9-CM) code: 755.54. Medical record review showed that the McCarroll criteria were used in the diagnostic work-up.[4] Initially, the McCarroll criteria[4] were used to confirm the diagnosis of Madelung deformity. As part of the surgical decision-making process, preoperative CT scans were reviewed; in some patients, little to no sigmoid notch was visible, leaving the ulnar head with nothing to articulate (Figure 1). In these cases, surgeons chose to use the alternative surgical technique, aimed to remove the discrepancy between the ulna and the proximal carpal row. Patients with a 'post-traumatic' Madelung deformity[10] or history of corrective wrist surgery other than an RSL-arthrodesis with a neo-DRUJ or reverse wedge osteotomy were excluded; pregnancy and age under 18 at time of follow-up were additional exclusion criteria. A total of twelve patients were identified that had previously undergone RSL-arthrodesis with construction of a neo-DRUJ or a reverse wedge osteotomy[11] between 2005 and

2019. Of these, nine agreed to participate in the study. Four patients (six wrists) had undergone RSL-arthrodesis with a neo-DRUJ and five patients (seven wrists) had undergone a reverse wedge osteotomy. Patients were evaluated between April 2019 and February 2020 to assess their clinical and radiographic outcomes. Written informed consent was obtained from all patients.

Radioscapholunate arthrodesis with construction of a neo-DRUJ

This two-stage surgery, which addresses the abnormal DRUJ, consists of: (1) a modified radioscapholunate (RSL) arthrodesis and triquetrectomy; and (2) a distal scaphoidectomy and removal of osteosynthetic material. The time between both surgeries is imperative since the scaphoid receives the majority of its blood supply from distal branches,[12] and a waiting interval of 6 months to 1 year assures an adequate formation of collaterals before the distal scaphoidectomy is performed.[13] In the first operation (Figure 2a, 2b), a longitudinal dorsal incision is made over the fourth to fifth dorsal extensor compartment. The involved structures are released and access to the joint capsule is obtained. On the ulnar side of the fifth extensor compartment, a capsular flap is created, after which the lunate, scaphoid and triquetrum bones are identified. Next, the radius is shortened by carving out the distal bone while leaving the radial side of the radius (containing the radial styloid) intact for stability and maintenance of vascularization. The triquetrum bone is released and excised. The scaphoid and lunate are positioned in a more dorsal stance in order to correct the volar dislocation of the hand and are fixated to the radius with a 2.4 mm dorsal L-plate and locking screws. Since the sigmoid notch in Madelung deformity is underdeveloped, a new articular surface for the ulnar head is needed; removing the triquetrum creates space for the ulnar head. By repositioning the scaphoid and lunate more dorsally before fixation, the ulnar side of the lunate bone is allowed to articulate with the ulnar head as they now form a 'neo-DRUJ' (Figure 2b). Stability is achieved by suturing (Vicryl 2-0) the palmar and dorsal distal radioulnar ligaments

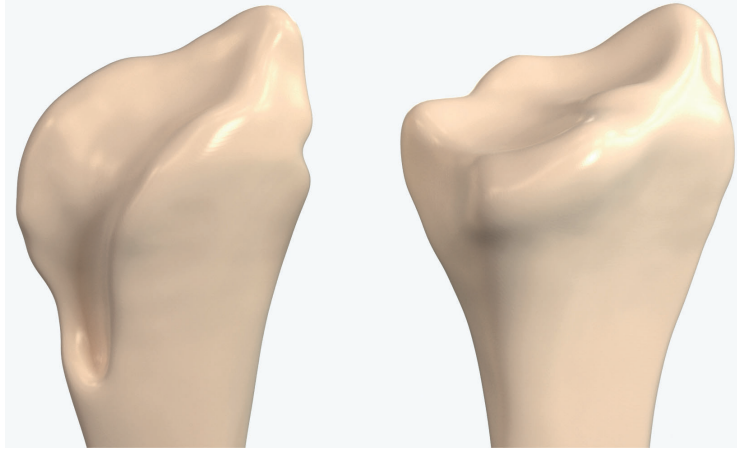

Figure 1. Preoperative DRUJ of a patient who underwent radioscapholunate arthrodesis with a neo-DRUJ (left) and preoperative DRUJ of a patient who underwent reverse wedge osteotomy (right).

of the triangular fibrocartilage complex (TFCC); palmarly, to the remnants of the lunotriquetral ligament and dorsally to the soft tissues of the lunate. Removal of the cartilage on the radio-lunar articular surface does not pose a risk of damaging the LT ligament palmarly, granted that solely the contact surface of the desired arthrodesis is stripped of its cartilage. Furthermore, the cranial part of the lunate (i.e., where the ligamentous part of the LT ligament attaches) is spared. The dorsal DRUJ capsule and the radiocarpal joint capsule of the fifth extensor compartment are closed; the extensor digiti minimi remains in an extra-anatomical position. Repositioning and fixation of the structures were adjusted and confirmed using intraoperative x-ray imaging. The wrist is immobilized for six weeks in a below-elbow cast, using a neutral position of rotation with a slight cock-up of the wrist. The range of motion after consolidation of the RSL-arthrodesis is limited to a dart-throwing motion pattern with only limited flexion, extension, and radioulnar deviation.

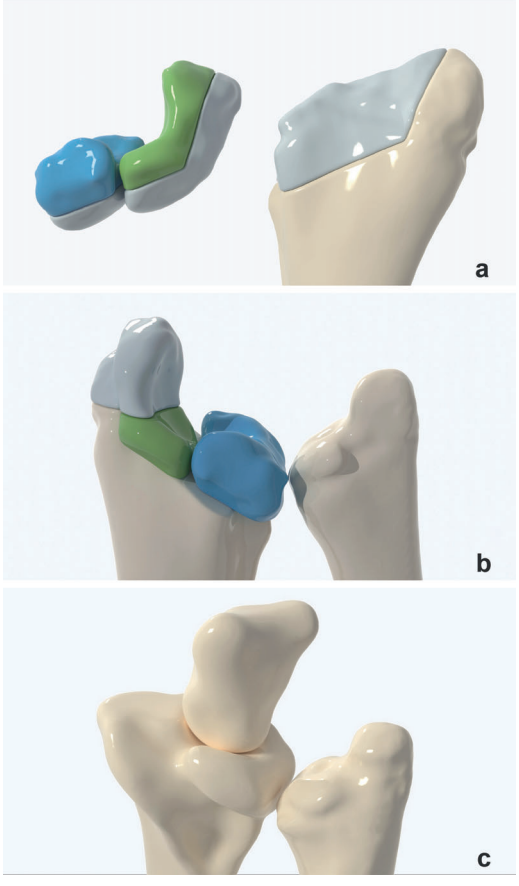

Figure 2. (a) The distal radius is shortened by carving out a piece of bone and replacing it by the scaphoid and lunate. The proximal articular surfaces of the lunate and scaphoid are dechondrified. The triquetrum is released and excised. (b) The scaphoid and lunate are fixated to the dorsal radius using a L-plate 2.4 and locking screws. The ulnar side of the lunate will articulate with the ulnar head as a neo-DRU-joint. (c) Neo-DRUJ showing articulation with the capitate and ulnar bone. Note that the distal pole of the scaphoid has been excised.

After confirmation of full consolidation of the partial arthrodesis on postoperative CT-scans, the distal pole of the scaphoid is excised, to improve the range of motion of the remaining joint. In this second surgery (Figure 2c), the scar from the first surgery is also excised. The structures of the third and fourth extensor compartment are released and access to the osteosynthesis plate is acquired. The plate and screws are removed, the midcarpal joint is identified and the distal scaphoid pole is exposed. The distal pole of the scaphoid is removed with a saw and extracted using a rongeur; loose fragments are removed. The wound is closed using absorbable sutures, after which a pressure bandage is applied. All patients start hand therapy one week postoperatively for a total of twelve weeks.

Clinical and radiographic evaluation

Patients were examined at our outpatient clinic to assess pain, ROM, and grip strength. Pain intensity levels were measured using a Visual Analogue Scale (VAS) (range 0-10; lower is better). ROM was measured in degrees using a goniometer for the following motions: flexion, extension, radial deviation, ulnar deviation, pronation, and supination. Grip strength was assessed with a dynamometer, following AMA guidelines.[14] Instability of the DRUJ was assessed pre- and postoperatively by testing for anterior-posterior translation. PROMs were assessed using the five-level EQ-5D-5L questionnaire (range 1-5; higher is better),[15] and the Michigan Hand Outcomes Questionnaire (MHQ) (range 0-100; higher is better).[16] Follow-up for the neo-DRUJ group was defined as time since the second surgery.

Pre- and postoperative x-ray images were obtained for both patient groups (Figure 3, Figure 4), with patients being evaluated one week and six weeks after surgery. The degree of deformity was radiographically quantified using the McCarroll criteria,[4] measuring: ulnar tilt, lunate subsidence, lunate fossa angle, palmar tilt, and palmar carpal displacement. Postoperative measurements could not be performed in RSL-arthrodesis patients as the anatomical configuration was radically altered. At six weeks, all osteotomy cases showed partial consolidation on x-ray imaging, after which bone healing was not further evaluated. In the neo-DRUJ group, bone healing was actively monitored at six months on CT imaging due to the procedure's novelty and the inability to assess consolidation of the RSL-arthrodesis on x-ray imaging accurately. If the partial arthrodesis was not fully consolidated, CT imaging was repeated at nine months; full consolidation was seen after an average of 7.5±1.9 months.

Statistical analysis

Mean postoperative outcomes of pain, ROM, grip strength, MHQ scores, and EQ-5D-5L scores were compared between the RSL-arthrodesis with a neo-DRUJ and reverse wedge osteotomy groups. Grip strength data was unavailable for two patients. Data distribution was evaluated using a Shapiro-Wilk test to assess normality. Normally distributed variables were analyzed with an independent samples t-test (variances equal) or Welch's test (variances not equal). Equality of variances was assessed using Levene's test. Non-normally distributed variables were compared with a Mann-Whitney U test.

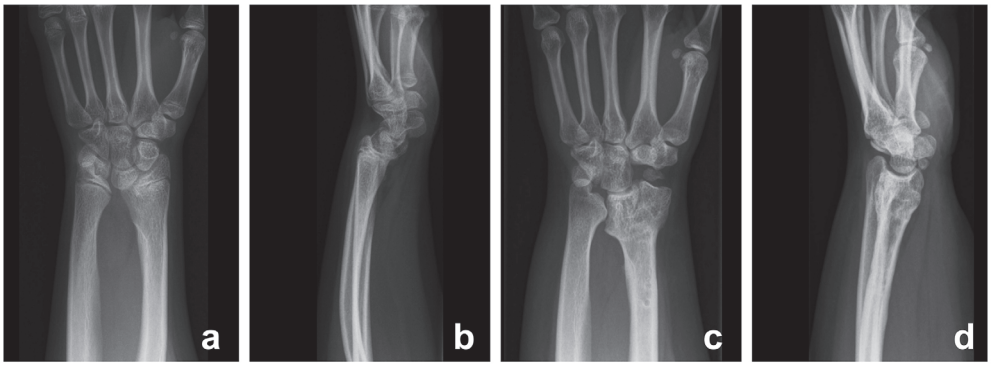

Figure 3. Preoperative AP (a) and lateral (b) radiographs, and postoperative AP (c) and lateral (d) radiographs of a patient that underwent RSL-arthrodesis with a neo-DRUJ.

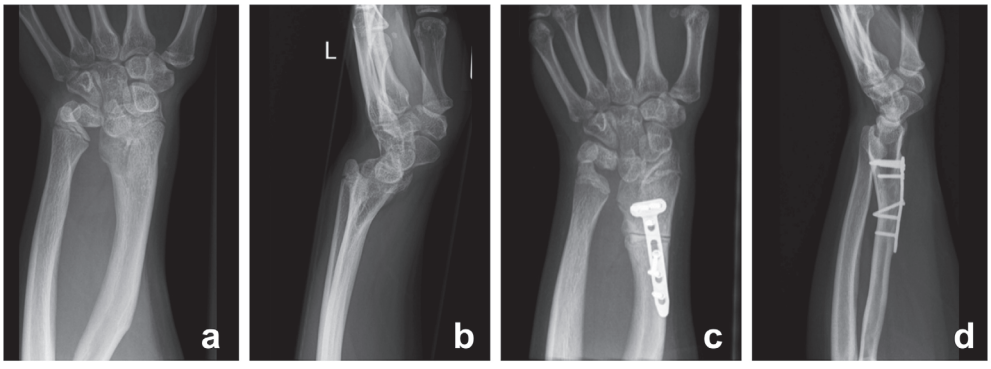

Figure 4. Preoperative AP (a) and lateral (b) radiographs, and postoperative AP (c) and lateral (d) radiographs of a patient that underwent reverse wedge osteotomy.

RESULTS

Patients that had undergone RSL-arthrodesis with a neo-DRUJ (n=4) had a mean age of 15±0.8 years with a follow-up of 47.6±18.6 months; reverse wedge osteotomy patients (n=5) had a mean age of 13.8±2.2 years with a follow-up of 105.4±80.6 months (Table 1). Average time between surgeries in the RSL-arthrodesis group was 10.5±2.0 months.

Primary preoperative complaints included pain, decreased grip strength, and cosmetic deformity. Radiographic evaluation revealed no differences in preoperative measurements (Supplemental Table S1).

No differences in ROM were found between cases after an RSL-arthrodesis with a neo-DRUJ (n=6) and cases after a reverse wedge osteotomy (n=7), except for extension (54.3±11.0 versus 34.2±15.3) (Table 2). In regard to pain, grip strength, and functional outcomes no postoperative differences were found between the two groups (Table 3).

Table 1. Patient characteristics.

	RSL-arthrodesis with a neo-DRUJ (n=4)	Reverse wedge osteotomy (n=5)
Wrists	6	7
Age at (first) surgery, y	15±0.8	13.8±2.2
Follow-up, m (range)	47.6±18 (13-62)	105.4±80.6 (17-174)
Female	4	5
Right dominant hand	4	5
Bilateral deformity	4	5
Confirmed genetic cause	2	0
Additional procedures	1	1

Table 2. Range of motion.

	RSL-arthrodesis with a neo-DRUJ (n=6)	Reverse wedge osteotomy (n=7)	P
Flexion, degrees	55.8±3.8	53.6±10.7	0.63
Extension, degrees	34.2±15.3	54.3±11.0	**0.04**
Radial deviation, degrees	15.0±6.3	17.6±11.1	0.63
Ulnar deviation, degrees	23.3±6.1	28.4±8.2	0.23
Pronation, degrees	79.2±9.7	77.1±10.7	0.73
Supination, degrees	82.0±10.9	76.6±17.5	0.45

Table 3. Pain, grip strength, and functional outcomes.

	RSL-arthrodesis with a neo-DRUJ (*n*=6)	Reverse wedge osteotomy (*n*=7)	P
Pain (VAS)	3.9±3.7	2.3±1.9	0.30
Grip strength, kg	22.6±1.8	17.0±10.3	0.29
Michigan score	71.3±15.9	66.8±11.5	0.58
EQ-5D-5L	0.86±0.1	0.89±0.1	0.67
EQ (VAS)	81.0±14.3	88.3±13.1	0.46

DISCUSSION

This case-control study describes early outcomes of an RSL-arthrodesis with a neo-DRUJ, a new surgical technique for the corrective treatment of Madelung deformity. The described surgical approach offers an alternative for patients with a severely affected sigmoid notch. Short-term results were compared to a group that underwent a reverse wedge osteotomy. In regard to clinical and radiographic parameters, the results were similar. Compared to reverse wedge osteotomy patients, patients after RSL-arthrodesis and construction of a neo-DRUJ had similar grip strength

measurements and ROM, except for extension, which was lower in the latter group. Quality of life (EQ-5D-5L) and overall MHQ scores were similar.

A strength of this study is that we used a structured protocol to report on postoperative outcomes.[5] A limitation was the small number of cases; low statistical power limited detecting differences that might prove clinically relevant. In addition, differences in preoperative anatomical configuration and follow-up between the two groups could lead to significant confounding. That being said, the purpose of this study was to introduce a new surgical approach rather than determining the best treatment by comparing outcomes. Another limitation was that preoperative measurements were not performed consistently; therefore, comparisons between the pre- and postoperative anatomical configurations were not possible, preventing the assessment of relative improvement. Lastly, while sufficient time elapsed for proper bone healing[17] our study's follow-up was relatively limited.

The mean range of motion in the RSL-arthrodesis with a neo-DRUJ group was similar compared to the reverse wedge osteotomy group, except for extension which was lower. During extension, the radiocarpal joint contributes to 66.5%, and the midcarpal joint to 33.5% of the total motion pattern.[18] In contrast, during flexion, this balance shifts to 60% and 40% for radiocarpal and midcarpal, respectively. Therefore, it is not unexpected that after fixation of the proximal carpal row, flexion would be less affected after fusion, which corresponds with the results of both our study (55.8 and 53.6 degrees in respective groups) and previous studies reporting outcomes after osteotomy procedures.[6,19] Notable were the relatively intact pronation and supination measurements in both groups compared to normal reference values.[20] Other studies reported a mean supination of 75 degrees after distal radial dome osteotomy[19] and 72 degrees[6] after various osteotomies of the distal radius.

Mean postoperative pain was similar and considered 'mild' for both groups.[21] Pain was mainly localized to the areas between the distal radius and ulna, and the ulnar side of the wrist. One recent case series study, describing outcomes after a Sauvé-Kapandji procedure,[22] reported mean VAS scores of 2.3±0.6[23] with a mean follow-up of 16 months. Other studies described only the presence or absence of pain without any quantification.[6,11,19]

Regarding grip strength, both groups scored below average reference values for healthy females in the same age range (age 18-19 years, mean grip strength 31.4 kg).[24] Arthrodesis procedures are associated with loss of grip strength,[25] restoring up to 75% of strength at best; the leading causes being a loss of radiocarpal and intercarpal bone movement, relative lengthening of musculotendinous units after bone removal,[25] and a suboptimal wrist position after fusion.[26] The few case series studies that have measured grip strength, report means of 22.1 kg after a combination of an opening wedge osteotomy and modified Darrach,[27] and 24.2 kg after reverse wedge osteotomy;[11] one study reported grip strength as a percentage of expected normal values (68%).[28]

In our study, total MHQ-scores after RSL-arthrodesis were similar to our control group. The use of PROMs in Madelung deformity research has been limited. The few studies that implement PROMs either use the DASH,[29] QuickDASH,[30] or PRW(H)E;[11,19,23,27] overall, patients reported being satisfied with both functional outcomes and esthetics. For future studies, we would recommend using

the Patient Reported Outcomes Measurement Information System (PROMIS), as it has been shown to have high validity and reliability in congenital hand research.[31]

The approach in this study aims to create a neo-DRUJ from the ulnar joint surface of the lunate, in which the relatively long ulna[1,2] can articulate. The DRUJ is responsible for the articulation of the distal ulnar head in the sigmoid notch of the distal radius, enabling rotation of the wrist.[32] Problems can occur due to an uneven surface, bowing of the distal radius, and a smaller sigmoid notch,[33] which have all shown to be abnormal in Madelung deformity wrists.[34] Madelung deformity has a spectrum of presentation, including patients whose anatomy is more severely affected than others.[2,9] Although there were no statistical differences in radiographic measurements, patients who underwent RSL-arthrodesis with a neo-DRUJ appeared to have a more deformed radius in comparison to the control group (Figure 1). In future studies, mathematical quantifications should scientifically prove DRUJ abnormalities, as has been previously done in 3D for other anatomical changes in Madelung deformity.[34] Since existing techniques focus mainly on remodeling the radiocarpal joint, the new approach could provide an alternative treatment option for patients with a severely deformed DRUJ.[8,9] To the best of our knowledge, the approach described in this study is the only procedure that results in a functional sigmoid notch in patients with a preoperatively abnormal DRUJ in Madelung deformity.

While enough time was granted for adequate bone healing[17] the complex anatomical changes can alter biomechanics.[35,36] Therefore, it is paramount to continue observation of the long-term effects of these altered forces on the wrist joint to confirm the benefits of this procedure, primarily since patients are operated on at a young age.[1] Furthermore, inconsistent reporting of outcomes in Madelung deformity has prevented any objective comparisons.[5] Therefore, future studies should adhere to a structured protocol to compare different procedures through meta-analyses. Since the deformity can present on a wide spectrum, the surgical management of Madelung deformity patients will most likely necessitate an individualized treatment algorithm. Quantification of the sigmoid notch could aid in the selection of patients to undergo the new surgical approach. Lastly, it is recommended to perform cost-effectiveness studies, as a two-step approach will be associated with higher initial treatment costs.

In this study, we introduced and assessed a new surgical approach for the corrective treatment of Madelung deformity. Since the DRUJ in Madelung deformity can be severely deformed, this approach could provide an alternative treatment option for a subset of patients. While short-term postoperative outcomes seem satisfactory and similar to outcomes after reverse wedge osteotomy, longer follow-up studies will be required to confirm the procedure's durability.

REFERENCES

1. Arora AS, Chung KC. Otto W. Madelung and the recognition of Madelung's deformity. ***J Hand Surg Am.*** 2006;31(2):177-182.
2. Kozin SH, Zlotolow DA. Madelung Deformity. ***J Hand Surg Am.*** 2015;40(10):2090-2098.
3. Hanson TJ, Murthy NS, Shin AY, Kakar S, Collins MS. MRI appearance of the anomalous volar radiotriquetral ligament in true Madelung deformity. ***Skeletal Radiol.*** 2019;48(6):915-918.
4. McCarroll HR, Jr., James MA, Newmeyer WL, 3rd, Molitor F, Manske PR. Madelung's deformity: quantitative assessment of x-ray deformity. ***J Hand Surg Am.*** 2005;30(6):1211-1220.
5. Peymani A, Johnson AR, Dowlatshahi AS, Dobbe JGG, Lin SJ, Upton J, et al. Surgical Management of Madelung Deformity: A Systematic Review. ***Hand (N Y).*** 2019;14(6):725-734.
6. Saffar P, Badina A. Treatment of Madelung's deformity. ***Chir Main.*** 2015;34(6):279-285.
7. Ali S, Kaplan S, Kaufman T, Fenerty S, Kozin S, Zlotolow DA. Madelung deformity and Madelung-type deformities: a review of the clinical and radiological characteristics. ***Pediatr Radiol.*** 2015;45(12):1856-1863.
8. Coffey MJ, Scheker LR, Thirkannad SM. Total distal radioulnar joint arthroplasty in adults with symptomatic Madelung's deformity. ***Hand (N Y).*** 2009;4(4):427-431.
9. Ghatan AC, Hanel DP. Madelung deformity. ***J Am Acad Orthop Surg.*** 2013;21(6):372-382.
10. Knutsen EJ, Goldfarb CA. Madelung's Deformity. ***Hand (N Y).*** 2014;9(3):289-291.
11. Mallard F, Jeudy J, Rabarin F, Raimbeau G, Fouque PA, Cesari B, et al. Reverse wedge osteotomy of the distal radius in Madelung's deformity. ***Orthop Traumatol Surg Res.*** 2013;99(4 Suppl):S279-283.
12. Handley RC, Pooley J. The venous anatomy of the scaphoid. ***J Anat.*** 1991;178:115-118.
13. LaStayo PC, Winters KM, Hardy M. Fracture healing: bone healing, fracture management, and current concepts related to the hand. ***J Hand Ther.*** 2003;16(2):81-93.
14. Brigham CR. AMA guides to the evaluation of permanent impairment. 2006.
15. Herdman M, Gudex C, Lloyd A, Janssen M, Kind P, Parkin D, et al. Development and preliminary testing of the new five-level version of EQ-5D (EQ-5D-5L). ***Qual Life Res.*** 2011;20(10):1727-1736.
16. Chung KC, Pillsbury MS, Walters MR, Hayward RA. Reliability and validity testing of the Michigan Hand Outcomes Questionnaire. ***J Hand Surg Am.*** 1998;23(4):575-587.
17. Islam O, Soboleski D, Symons S, Davidson LK, Ashworth MA, Babyn P. Development and duration of radiographic signs of bone healing in children. ***AJR Am J Roentgenol.*** 2000;175(1):75-78.
18. Sarrafian SK, Melamed JL, Goshgarian GM. Study of wrist motion in flexion and extension. ***Clin Orthop Relat Res.*** 1977(126):153-159.
19. Steinman S, Oishi S, Mills J, Bush P, Wheeler L, Ezaki M. Volar ligament release and distal radial dome osteotomy for the correction of Madelung deformity: long-term follow-up. ***J Bone Joint Surg Am.*** 2013;95(13):1198-1204.
20. Soucie JM, Wang C, Forsyth A, Funk S, Denny M, Roach KE, et al. Range of motion measurements: reference values and a database for comparison studies. ***Haemophilia.*** 2011;17(3):500-507.
21. Jensen MP, Chen C, Brugger AM. Interpretation of visual analog scale ratings and change scores: a reanalysis of two clinical trials of postoperative pain. ***J Pain.*** 2003;4(7):407-414.

22. Taleisnik J. The Sauve-Kapandji procedure. ***Clin Orthop Relat Res.*** 1992(275):110-123.

23. Eid A, Abdel Salam MA, Elgawhary S. Management of idiopathic Madelung deformity with the Sauve-Kapandji procedure. ***Current orthopaedic practice.*** 2018;29(5):491-496.

24. Werle S, Goldhahn J, Drerup S, Simmen BR, Sprott H, Herren DB. Age- and gender-specific normative data of grip and pinch strength in a healthy adult Swiss population. ***J Hand Surg Eur Vol.*** 2009;34(1):76-84.

25. Bhardwaj P, Nayak SS, Kiswar AM, Sabapathy SR. Effect of static wrist position on grip strength. ***Indian J Plast Surg.*** 2011;44(1):55-58.

26. O'Driscoll SW, Horii E, Ness R, Cahalan TD, Richards RR, An KN. The relationship between wrist position, grasp size, and grip strength. ***J Hand Surg Am.*** 1992;17(1):169-177.

27. Kampa R, Al-Beer A, Axelrod T. Madelung's deformity: radial opening wedge osteotomy and modified Darrach procedure using the ulnar head as trapezoidal bone graft. ***J Hand Surg Eur Vol.*** 2010;35(9):708-714.

28. Murphy MS, Linscheid RL, Dobyns JH, Peterson HA. Radial opening wedge osteotomy in Madelung's deformity. ***J Hand Surg Am.*** 1996;21(6):1035-1044.

29. Hudak PL, Amadio PC, Bombardier C. Development of an upper extremity outcome measure: the DASH (disabilities of the arm, shoulder and hand) [corrected]. The Upper Extremity Collaborative Group (UECG). ***Am J Ind Med.*** 1996;29(6):602-608.

30. Beaton DE, Wright JG, Katz JN, Upper Extremity Collaborative G. Development of the QuickDASH: comparison of three item-reduction approaches. ***J Bone Joint Surg Am.*** 2005;87(5):1038-1046.

31. Waljee JF, Carlozzi N, Franzblau LE, Zhong L, Chung KC. Applying the Patient-Reported Outcomes Measurement Information System to Assess Upper Extremity Function among Children with Congenital Hand Differences. ***Plast Reconstr Surg.*** 2015;136(2):200e-207e.

32. Arias DG, Varacallo M. Anatomy, Shoulder and Upper Limb, Distal Radio-Ulnar Joint. In: ***StatPearls.*** Treasure Island (FL)2019.

33. Bruno RJ, Blank JE, Ruby LK, Cassidy C, Cohen G, Bergfield TG. Treatment of Madelung's deformity in adults by ulna reduction osteotomy. ***J Hand Surg Am.*** 2003;28(3):421-426.

34. Peymani A, Dobbe JGG, Streekstra GJ, McCarroll HR, Strackee SD. Quantitative three-dimensional assessment of Madelung deformity. ***J Hand Surg Eur Vol.*** 2019;44(10):1041-1048.

35. Eschweiler J, Hawlitzky J, Quack V, Tingart M, Rath B. Biomechanical model based evaluation of Total Hip Arthroplasty therapy outcome. ***J Orthop.*** 2017;14(4):582-588.

36. Friedman RJ. Biomechanics of total shoulder arthroplasty: a preoperative and postoperative analysis. ***Semin Arthroplasty.*** 1995;6(4):222-232.

SUPPLEMENTAL DATA

Supplemental Table S1. Radiographic measurements.

	RSL-arthrodesis with a neo-DRUJ (*n*=6)	Reverse wedge osteotomy (*n*=7)	
	Preoperative	Preoperative	Postoperative
Ulnar tilt, degrees	53.2±4.1	47.3±9.8	40.2±16.2
Lunate subsidence, mm	2.0±6.6	7.7±6.7	1.7±5.4
Lunate fossa angle, degrees	53.7±9.7	48.8±12.3	39.5±14.5
Palmar tilt, degrees	33.0±11.1	25.1±7.1	8.7±7.3
Palmar carpal displacement, mm	54.8±8.2	44.8±14.9	42.8±18.9

IV

GENERAL DISCUSSION AND SUMMARY

9

GENERAL DISCUSSION AND FUTURE PERSPECTIVES

OVERVIEW

The research presented in this thesis provides an overview of our current understanding of Madelung deformity, both from the clinician's and the patient's perspective. Throughout, several knowledge gaps were revealed in the deformity's assessment, anatomical understanding, diagnostic work-up, surgical approach, and reporting of outcomes. Therefore, this thesis aimed to introduce several solutions to these issues by using the most current clinical and technological tools at our disposal. In this section, each of the previous chapters will be discussed to finally conclude with some reflections on the future of Madelung deformity research.

CURRENT STATE OF AFFAIRS

The very first step in this journey to increase our understanding of Madelung deformity was to explore the scientific literature through a systematic review. While the main objective was to identify the optimal surgical treatment option by comparing clinical and functional outcomes, we learned many essential questions to remain unanswered. As Otto Wilhelm Madelung published his findings before the discovery of x-ray imaging,[1-3] the most fundamental question was: what is Madelung deformity? Is it a condition purely diagnosed using radiological findings using pre-determined criteria,[4] or does an accurate diagnosis necessitate a combination of both clinical and genetic abnormalities in addition to the abnormal findings on imaging? The answer will probably be the latter for a significant proportion of patients, as the deformity can present on a spectrum and there are no absolute cut-off values for radiographic measurements.[5-7] Several authors have hypothesized 'true' Madelung deformity can only be established in: (1) patients with an underlying diagnosis of Léri-Weill dyschondrosteosis (LWD); or (2) patients with a presence of Vickers ligament or anomalous radiotriquetral ligament.[8-12] Interestingly, there is still no consensus on this definition of 'true' Madelung deformity and it remains an ongoing discussion. Even though the hypothesis mentioned earlier has not been scientifically proven, findings from current small-powered studies seem to indicate it to be valid. In Chapter 2 we investigated 25 case series studies.[13] While not systematically reported in every study, several characteristic findings repeatedly appear: the bilateral occurrence, an underlying genetic disorder, decreased patient height, and an increased BMI. The few imaging studies on Madelung deformity, describing soft-tissue anomalies in addition to the skeletal deformities, indicate there to be a strong association with the presence of an abnormal radiolunate (Vickers) and radiotriquetral ligament.[14-16] Again, and this limitation is mentioned throughout this thesis, these conclusions are based on small patient numbers, and therefore not entitled to be assumed true. The only way to confirm with certainty is through future studies, most likely requiring multicenter collaborations. Until then, reporting findings such as underlying genetic disorders and the presence of ligamentous anomalies in future small-powered studies could increase our collective understanding. Therefore, in each patient where there is a suspicion of congenital Madelung deformity (i.e., not caused by a traumatic event), we recommend taking a complete family history, obtaining genetic material for testing and storage (blood smears),[17] and appropriate imaging (e.g., MRI) to visualize anomalous ligaments. Hopefully, if we can collect this data for a significant number of patients, we can solve one of the core mysteries

surrounding the condition. Also, while associated mutations in the short stature homeobox-containing gene (SHOX) gene have been previously discovered, researchers must consider that there could very well be other undiscovered genotypes leading to a similar phenotype.[18-20]

In the optimization of patient care, it is necessary to determine which treatment best serves the individual. One way of doing this is by comparing the outcomes of different surgical approaches. In Chapter 2, we gain a broad overview of Madelung deformity's current treatment options. After an extensive review of published case series studies, it seems outcomes regarding pain and range of motion (ROM) after osteotomies are satisfactory. Yet, most studies did not report outcomes in a consistent and protocolized manner. Therefore, methodological sound comparisons will only be possible if prospective small-powered studies start using a standardized reporting methodology. Since long-term follow-up studies are gradually being published, implementing these guidelines could finally answer questions about what defines 'optimal' surgical treatment.[21-24] To this end, we introduced a protocol for use in future patient work-up and prospective studies, proposing multiple changes that could serve as the basis for new clinical guidelines. In short, the protocol involves extensively documenting patient history, a thorough pre- and postoperative evaluation, and reporting any perioperative anatomical findings. Also, while we learned that most surgeons are performing osteotomies of radius and ulna, there is a lack of quantitative outcomes in a majority of current studies. These facts should make us realize that there is no gold standard for Madelung deformity treatment, thus demonstrating the need to keep contemplating alternative surgical treatment options.

In our proposed protocol, we recognize the use of the Michigan Hand Outcomes Questionnaire (MHOQ) and the Patient-Rated Wrist Evaluation (PRWE) questionnaire as robust instruments in the assessment of patient-reported outcome measures (PROMs).[25,26] Recently, the universal Patient-Reported Outcomes Measure Information System (PROMIS) has been shown to be even more applicable, specifically in patients with congenital upper limb anomalies.[27,28] This highlights the importance of continuously evaluating and reiterating our approach to the work-up of Madelung deformity, as our knowledge base also grows in the context of congenital hand and upper limb anomalies as a whole.

SEEKING THE PATIENT PERSPECTIVE

Today, a shift is visible from provider-focused healthcare to a more patient-centered healthcare system, evident from the development of personal health records, the importance of patient perception, and an increasing focus on patient-provider communication.[29] In Chapter 2, we reported on the inadequate coverage of the patient experience and aimed to tackle this issue by protocolizing the structural use of PROMs. Even after implementing routine use of PROMs in patient care, the knowledge gained from any single-center research setting will most likely be limited due to low patient numbers. Noteworthy in this regard are the efforts of the team behind the Congenital Upper Limb Differences (CoULD) Registry (www.kidshandregistry.com), who have been developing a multicenter registry for congenital upper limb differences. The CoULD Registry is prospectively creating a database focused on patient-centered outcomes, intending to

improve patient care quality through collaborative research. These initiatives will enable collecting significant amounts of data through its multicenter design even in rare congenital conditions, hopefully leading to sufficiently powered studies on patient characteristics and outcomes. Until then, despite its intrinsic limitations (e.g., self-reporting bias, recall bias), survey studies could be used as a worthy placeholder to understand the patient perspective.

Patients are increasingly using the internet to share and rate their health care experiences, connecting with others having similar illnesses, and beginning to manage their conditions by leveraging these technologies.[30] In Chapter 3, we described a novel approach to the patient perspective of a rare disease, utilizing social media to engage in online Madelung deformity communities. We posted a message on several social media platforms providing a direct link to our survey. In this message, we also addressed the following questions: (1) who is doing the research; (2) why are we doing this study; (3) is any identifiable information being collected; and (4) what previous research have we done. In addition to increasing credibility, we believe that providing this information is fundamental to maximize engagement as privacy concerns are one of the main barriers of patients.[31] Lastly, we provided participants with the ability to contact us regarding any non-medical questions specific to this study. Throughout this process, several concerned patients reached out to our research team, sharing their everyday health care experiences. Anecdotally, patients reported not being taken seriously regarding pain levels and limited functioning, with some primary care providers not ever having heard of Madelung deformity. In turn, this would lead to a delayed referral to tertiary and quaternary centers. Therefore, we believe our study findings are a comparative reference for prospective patient-reported outcome studies and as an educational resource for clinicians to understand better the person sitting across from them during an outpatient visit.

TRANSFORMING ANATOMY TO NUMBERS

In the mid-1980s, digital radiography was introduced, converting the x-ray energy pattern into digital signals through laser-stimulated luminescence.[32] The modern radiologist now loads a digital x-ray from their department's picture archiving and communication systems (PACS) into their radiology information system.[33] Despite our technological advancements, clinicians often still quantify skeletal abnormalities by measuring lengths and angles.[4-6] Albeit in a digital environment, the points, lines, and rulers are placed manually, after which various (simple) calculations are done automatically. Although this has proven to be sufficient for many diagnostic and research settings, the inherent methodology is suboptimal and prone to error. The manual aspect of the measurements results in inter-and intra-rater measurement differences. To exemplify, the lengths and angles measured by radiologist 'A' will differ from the measurements taken by him or her a week from now. The same measurements will also vary between radiologist 'A' and radiologist 'B'.[34,35] Lastly, as the 2D visualizations are highly dependent on the orientation and position of the 3D subject in question (e.g., a wrist) relative to the x-ray detector, measurement values can be consequently affected.[36]

By adding an extra dimension to our 2D assessment, we eradicate any inaccuracies in our measured values due to translational or rotational parameters, as we now evaluate 3D information in 3D. More interestingly, this provides us with the opportunity for automation. After the segmentation of bones on a CT scan, we acquire a virtual representation of that bone in 3D space. Now it is possible to perform measurements on this virtual model in an automatic manner, nullifying any inter- and intra-rater measurement differences. While the calculations are simple (e.g., distances between coordinates or angles between lines), several challenges remain in the automatic detection of anatomical landmarks. Even relatively straight-forward bony landmarks such as the radial styloid process require us to 'think like a programmer'. To exemplify, to determine the coordinates of the radial styloid process, we can first load a virtual model of the radius in 3D space with a Cartesian ***XYZ***-coordinate system (Figure 1, red). Next, we adopt a 3D shape alignment method known as 'principal component analysis', determining the direction of largest variance in a dataset, and aligning the virtual model accordingly (Figure 1, orange).[37] Lastly, we take 10% of both ends of the bone and calculate the surface area or volume. The distal part of the radius is generally larger than the proximal portion. Thus, applying this knowledge, we can determine which side is distal and which side is proximal, and transform the virtual model to obtain the final result (Figure 1, green).

The first studies on Madelung deformity's anatomical changes used x-ray imaging, showing the earliest roentgenographic changes at the distal radial epiphyseal line.[9,38,39] Applying the technological advancements described in the previous paragraph to Madelung deformity not only allows us to perform measurements in an objective and automatic manner, but also

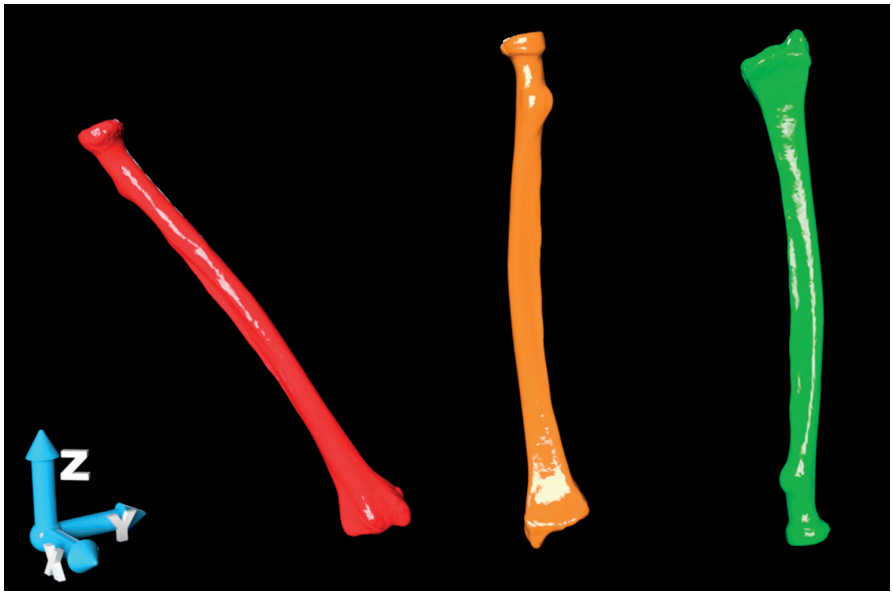

Figure 1. Virtual models of the radius in 3D space, showing an unaligned imported bone (red), the result after alignment on the Z-axis of the coordinate system (orange), and the result after subsequent detection of proximal and distal parts (green).

enables us to quantify previously described clinical findings. In Chapter 5, we choose to quantify the proximal row by calculating 3D lines using the centroid coordinates of the scaphoid, lunate, and triquetral bones. This quantification was based on known clinical findings, describing the proximal row configuration as 'V-shaped' or triangular.[14,40-42] It is also possible that a range of undiscovered abnormalities exists, never described because they are too subtle for a clinician to notice or hidden away within the complex multidimensional anatomy. Chapter 5 evaluated the shape of the lunate fossa using new parameters, including surface area, concavity, and irregularity. As these parameters have never been reported in a quantitative or even qualitative manner yet show significant differences with healthy wrists, the need to diversify our diagnostic arsenal is highlighted. Therefore, in conjunction with using previous studies' clinical findings, we need to continually reflect on our understanding of anatomical changes and their subsequent effects on wrist biomechanics. This mindset could often bring to light new structural flaws and pathogenic mechanisms, previously invisible to the naked eye.

THE 4TH DIMENSION

A 4D space is a mathematical extension of the concept of 3D space. While there are multiple definitions, we used the definition described by Joseph-Louis Lagrange (1788-1789) in his 'Mécanique analytique', viewing 4D space as 3 dimensions of space and 1 dimension of time.[43]

Although we have been applying 4D imaging for over ten years in research and clinical settings,[44-46] 4D or 'dynamic CT' imaging is relatively new, implemented in only a few academic centers worldwide. While some of these studies are in-vivo,[47] most are done in-vitro, using cadaveric models.[48-50] It is not surprising that the first pilot studies of 4D imaging were done in academic laboratories, optimizing the accuracy and resolution while minimizing the exposure to low-dose radiation.[51] Thereafter, curious scientists seek to use this technology to answer lingering research questions in the back of their minds. The introduction of 4D imaging to the fields of surgery and musculoskeletal medicine specifically, allows us to answer two critical questions: (1) what are the differences between patients and healthy volunteers; and (2) what is the effect of an intervention (i.e., surgery)? While the 2nd question will require prospective studies with sufficient follow-up,[52] we could partly answer the 1st question in Chapter 6 for two motion patterns: flexion-extension and radio-ulnar deviation. Previous imaging studies in Madelung deformity have detected abnormal wrist ligaments in patients, shedding more light on the pathophysiology that has led to the symptoms.[8,14-16,38] Knowing that patients have limited ROM, it is not surprising that we sought to investigate further the differences between patients and healthy volunteers during motion. Interestingly, we found decreased kinematics precisely in those two carpal bones for which abnormal ligaments have been previously found: the lunate bone, tethered to the radius with the radiolunate ligament, and the triquetral bone, tethered to the radius through the radiotriquetral ligament. However, the reader should keep in mind that the only way to prove a causative association would be to investigate carpal kinematics using 4D after ligament release.

In Madelung deformity research, the most significant decreases in ROM have been described for pronation and supination.[7,23,53,54] In Chapter 6, an accurate evaluation during pronation-supination

was not possible due to technical limitations of our radiological CT protocol, which started showing motion artifacts due to the relatively large translocations occurring during pronation-supination. At our institute, we have been maturing both our CT protocol and the custom-made positioning device used to limit participants' wrist mobility to specific movement patterns. These improvements will be incredibly beneficial in Madelung deformity research. Additionally, this will open possibilities to analyze the distal radioulnar joint, which can be significantly affect ed in some Madelung deformity patients, as shown in this thesis (Chapters 5, 7, and 8).

EVOLVING ANATOMICAL ANALYSES

Diagnostics in Madelung deformity have advanced significantly but remain suboptimal and unreliable in mild deformity cases.[55,56] There is an overlap of measurement values (e.g., ulnar tilt) between patients and healthy volunteers, hypothesized to be due to the 2D nature of the criteria and inter- and intra-rater measurement differences.[5,6] In Chapter 5, we developed new 3D criteria and automated both 2D and 3D measurements, but overlap with healthy wrists remained in our study. What if the problem is not the quality of measurements but the concept behind these measurements? Even though we converted 'classic' 2D parameters to 3D and developed several new 3D parameters (e.g., fossa concavity, fossa irregularity, and scapholunotriquetral angle), each parameter is based on our human interpretation of which anatomical aspects are most likely abnormal in patients.

In rare conditions such as Madelung deformity, a clinicians' exposure is severely limited; at most, surgeons will see a handful of patients during their careers. Therefore, maybe the decision regarding anatomical points-of-interest should not be based on our own limited experiences, but instead, be 'outsourced' to computer algorithms that can statistically analyze all the shapes in relation to each other. To this end, in Chapter 7, we developed a statistical shape model (SSM), a computer-generated model that can determine shape variations and quantify shape. We used SSMs to visualize and describe the most important shape variations of the distal radius in Madelung deformity. Also, converting shapes into numbers made it possible to 'diagnose' if a virtual model of the distal radius belonged to a patient or healthy volunteer. Interestingly, this technology could be highly applicable for use in other rare conditions (e.g., radial dysplasia), as the performance is satisfactory even with a relatively limited number of shapes.[57]

One application of SSMs we did not explore in Chapter 7 is its use in preoperative planning.[58] Currently, when planning a surgical correction for a unilateral fracture, malunion, or trauma case, we use the contralateral healthy side as a reference. After segmentation of the healthy bone on a CT scan, we can mirror the resulting virtual model to visualize how an anatomical configuration should be.[59] Unfortunately, in bilateral Madelung deformity, this mirroring technique can not be used as there is no healthy reference. However, in 'post-traumatic' or 'pseudo' Madelung deformity, which often necessitates a corrective osteotomy, the pathology is limited to one side, allowing us to mirror the contralateral healthy side for the preoperative planning process.[8,53,60] Interestingly, recent studies have shown that the use of SSMs leads to a more precise reconstruction of defects in comparison to mirroring procedures.[61] The rationale behind this increased precision is that human

anatomy is less symmetrical than our instinct would tell us, and SSMs take these asymmetrical properties into account when statistically determining a reconstructive plan.[62-66]

PERSONALIZING OUR SURGICAL APPROACH

The pathophysiology of Madelung deformity involves a premature growth plate arrest at the ulnar end of the distal radius,[67] which gives rise to two anatomical structures crucial to the wrist joint: the radiolunate joint and the distal radioulnar (DRU) joint. This pathological process leads to a volar and ulnar tilted distal radial articular surface.[68,69] We learned in Chapter 2 that most surgeons perform osteotomies of radius and ulna to correct these angles. In Chapter 3, we observed the significant patient-reported health burden that remains despite surgical treatment. Chapter 5 highlighted the abnormal radiolunate joint, with lunate fossa shape in patients showing a decreased surface area with increased levels of concavity and irregularity. In Chapter 7, we also witnessed the spectrum of variation in the distal radius, which in some cases results in a severely affected DRU joint. Given these findings, it is reasonable to contemplate what this means for our surgical treatment strategies. We started this journey over 3 years ago in search of the 'optimal' surgical treatment. However, given the repeatedly proven fact that Madelung deformity presents on a broad spectrum,[5-7,70] maybe one size does not fit all. A novel surgical approach is introduced in Chapter 8, that does address the DRU joint. While we described the preliminary outcomes of a new approach, only long-term studies will determine the feasibility of this two-stage procedure that drastically alters the wrist's anatomical configuration.

FUTURE PERSPECTIVES

Several key concepts should be addressed to tackle the challenges of research in rare congenital hand anomalies. First, there is a need to reach consensus and devise a standardized protocol for patients' work-up in clinical and research settings. This will enable the pooling of data in more prominent studies and multicenter collaborations. Second, it is highly recommended to implement PROMs in outcome research, using validated and reliable measurement instruments. Currently, PROMIS seems the most suitable to assess upper extremity functioning in Madelung deformity patients.[27,28]

Increasing our anatomical knowledge of very rare conditions will bring its own challenges. To decrease the tainting of data and quantifications due to inter- and intra-rater differences, it would be advantageous to implement automated and objective quantifications. We urge clinicians and scientists to use the latest technologies at their disposal. Most of the software programs used throughout this thesis were developed from scratch. However, in nearly every instance, we expanded on existing free and open-source software packages. Increasing the dimensionality of both our imaging and evaluation of complex anatomy, might compensate for the lack of anatomical exposure of rare conditions. For Madelung deformity specifically, it is evident that it is not just the distal radius that is affected.[7] To allow for meaningful analyses in the future (e.g., proximal radioulnar joint anomalies, SSMs of the entire radius) it is recommended to build databases with CT scans of the whole forearm. Studies should also investigate any abnormalities of the carpal bones,

as the altered biomechanics in Madelung deformity probably affect anatomical wrist structures other than the radius and ulna.

Madelung deformity patients will require a personalized and multidisciplinary approach. Each patient will need an extensive work-up and for clinicians to determine which elements of the wrist anatomy are abnormal and which are not. Assessments through 3D and 4D imaging can play an essential role by automatically quantifying several anatomical aspects and providing us with a dynamic view of the situation within. If the sigmoid notch is intact, an osteotomy could be the right option; if the sigmoid notch is severely affected by the growth arrest, alternative treatment options could be better suited to achieve a functional and pain-free DRU joint. Future investigations of the described abnormal ligaments could help us further appreciate the pathophysiology and anatomical arrangements in Madelung deformity.[8,14,15,38] In healthy wrists, the radiotriquetral ligament at its origin can not easily be morphologically distinguished from other ligaments.[71] This begs the question if the 'anomalous' radiotriquetral ligament as reported in literature is indeed the result of compensatory hypertrophy,[14] or that we are looking at a different ligamentous structure (e.g., palmar triangular fibrocartilage complex) that is tethering part of the proximal carpal row.

Finally, it is noteworthy to mention one problem that I was not able to further explore in this thesis. During the extensive literature review, I noticed a few reports regarding a subset of patients with a unique Madelung deformity variation. This substantially rarer condition was referred to as 'reverse' Madelung deformity.[16,72-74] In reverse Madelung deformity, the radius is bowed dorsally instead, displacing the distal ulna palmarly with a dorsal shift of the carpus. On the off chance that the latter has sparked a young researcher's interest, my advice would be to look up the studies cited in this paragraph and start his or her journey...

REFERENCES

1. Madelung O. Die spontane Subluxation der Hand nach vorne. ***Verh Dtsch Ges Chir.*** 1878;7:259-276.
2. Arora AS, Chung KC. Otto W. Madelung and the recognition of Madelung's deformity. ***J Hand Surg Am.*** 2006;31(2):177-182.
3. Spiegel PK. The first clinical X-ray made in America--100 years. ***AJR Am J Roentgenol.*** 1995;164(1):241-243.
4. McCarroll HR, Jr., James MA, Newmeyer WL, 3rd, Molitor F, Manske PR. Madelung's deformity: quantitative assessment of x-ray deformity. ***J Hand Surg Am.*** 2005;30(6):1211-1220.
5. McCarroll HR, James MA, Newmeyer WL, 3rd, Manske PR. Madelung's deformity: quantitative radiographic comparison with normal wrists. ***J Hand Surg Eur Vol.*** 2008;33(5):632-635.
6. McCarroll HR, Jr., James MA, Newmeyer WL, 3rd, Manske PR. Madelung's deformity: diagnostic thresholds of radiographic measurements. ***J Hand Surg Am.*** 2010;35(5):807-812.
7. Zebala LP, Manske PR, Goldfarb CA. Madelung's deformity: a spectrum of presentation. ***J Hand Surg Am.*** 2007;32(9):1393-1401.
8. Ali S, Kaplan S, Kaufman T, Fenerty S, Kozin S, Zlotolow DA. Madelung deformity and Madelung-type deformities: a review of the clinical and radiological characteristics. ***Pediatr Radiol.*** 2015;45(12):1856-1863.
9. Felman AH, Kirkpatrick JA, Jr. Madelung's deformity: observations in 17 patients. ***Radiology.*** 1969;93(5):1037-1042.
10. Golding JS, Blackburne JS. Madelung's disease of the wrist and dyschondrosteosis. ***J Bone Joint Surg Br.*** 1976;58(3):350-352.
11. Herdman RC, Langer LO, Good RA. Dyschondrosteosis. The most common cause of Madelung's deformity. ***J Pediatr.*** 1966;68(3):432-441.
12. Plafki C, Luetke A, Willburger RE, Wittenberg RH, Steffen R. Bilateral Madelung's deformity without signs of dyschondrosteosis within five generations in a European family--case report and review of the literature. ***Arch Orthop Trauma Surg.*** 2000;120(1-2):114-117.
13. Peymani A, Johnson AR, Dowlatshahi AS, et al. Surgical Management of Madelung Deformity: A Systematic Review. ***Hand (N Y).*** 2019;14(6):725-734.
14. Stehling C, Langer M, Nassenstein I, Bachmann R, Heindel W, Vieth V. High resolution 3.0 Tesla MR imaging findings in patients with bilateral Madelung's deformity. ***Surg Radiol Anat.*** 2009;31(7):551-557.
15. Hanson TJ, Murthy NS, Shin AY, Kakar S, Collins MS. MRI appearance of the anomalous volar radiotriquetral ligament in true Madelung deformity. ***Skeletal Radiol.*** 2019;48(6):915-918.
16. Vickers D, Nielsen G. Madelung deformity: surgical prophylaxis (physiolysis) during the late growth period by resection of the dyschondrosteosis lesion. ***J Hand Surg Br.*** 1992;17(4):401-407.
17. Binder G, Rappold GA. SHOX Deficiency Disorders. In: Adam MP, Ardinger HH, Pagon RA, et al., eds. ***GeneReviews((R)).*** Seattle (WA)1993.
18. Belin V, Cusin V, Viot G, et al. SHOX mutations in dyschondrosteosis (Leri-Weill syndrome). ***Nat Genet.*** 1998;19(1):67-69.
19. Clement-Jones M, Schiller S, Rao E, et al. The short stature homeobox gene SHOX is involved in skeletal abnormalities in Turner syndrome. ***Hum Mol Genet.*** 2000;9(5):695-702.
20. Rappold GA, Fukami M, Niesler B, et al. Deletions of the homeobox gene SHOX (short stature homeobox) are an important cause of growth failure in children with short stature. ***J Clin Endocrinol Metab.*** 2002;87(3):1402-1406.

21. Del Core M, Beckwith T, Phillips L, Ezaki M, Stutz C, Oishi SN. Long-term Outcomes Following Vickers Ligament Release and Growth Modulation for the Treatment of Madelung Deformity. ***J Pediatr Orthop.*** 2020;40(4):e306-e311.

22. Steinman S, Oishi S, Mills J, Bush P, Wheeler L, Ezaki M. Volar ligament release and distal radial dome osteotomy for the correction of Madelung deformity: long-term follow-up. ***J Bone Joint Surg Am.*** 2013;95(13):1198-1204.

23. Salon A, Serra M, Pouliquen JC. Long-term follow-up of surgical correction of Madelung's deformity with conservation of the distal radioulnar joint in teenagers. ***J Hand Surg Br.*** 2000;25(1):22-25.

24. Potenza V, Farsetti P, Caterini R, Tudisco C, Nicoletti S, Ippolito E. Isolated Madelung's deformity: long-term follow-up study of five patients treated surgically. ***J Pediatr Orthop B.*** 2007;16(5):331-335.

25. Chung KC, Pillsbury MS, Walters MR, Hayward RA. Reliability and validity testing of the Michigan Hand Outcomes Questionnaire. ***J Hand Surg Am.*** 1998;23(4):575-587.

26. MacDermid JC, Turgeon T, Richards RS, Beadle M, Roth JH. Patient rating of wrist pain and disability: a reliable and valid measurement tool. ***J Orthop Trauma.*** 1998;12(8):577-586.

27. Waljee JF, Carlozzi N, Franzblau LE, Zhong L, Chung KC. Applying the Patient-Reported Outcomes Measurement Information System to Assess Upper Extremity Function among Children with Congenital Hand Differences. ***Plast Reconstr Surg.*** 2015;136(2):200e-207e.

28. Wall LB, Vuillermin C, Miller PE, Bae DS, Goldfarb CA, Co ULDSG. Convergent Validity of PODCI and PROMIS Domains in Congenital Upper Limb Anomalies. ***J Hand Surg Am.*** 2020;45(1):33-40.

29. DuPree E, Anderson R, Nash IS. Improving quality in healthcare: start with the patient. ***Mt Sinai J Med.*** 2011;78(6):813-819.

30. Rozenblum R, Bates DW. Patient-centred healthcare, social media and the internet: the perfect storm? ***BMJ Qual Saf.*** 2013;22(3):183-186.

31. Antheunis ML, Tates K, Nieboer TE. Patients' and health professionals' use of social media in health care: motives, barriers and expectations. ***Patient Educ Couns.*** 2013;92(3):426-431.

32. Sonoda M, Takano M, Miyahara J, Kato H. Computed radiography utilizing scanning laser stimulated luminescence. ***Radiology.*** 1983;148(3):833-838.

33. Bansal GJ. Digital radiography. A comparison with modern conventional imaging. ***Postgrad Med J.*** 2006;82(969):425-428.

34. Gstoettner M, Sekyra K, Walochnik N, Winter P, Wachter R, Bach CM. Inter- and intraobserver reliability assessment of the Cobb angle: manual versus digital measurement tools. ***Eur Spine J.*** 2007;16(10):1587-1592.

35. Smith TO, Cogan A, Patel S, Shakokani M, Toms AP, Donell ST. The intra- and inter-rater reliability of X-ray radiological measurements for patellar instability. ***Knee.*** 2013;20(2):133-138.

36. Pennock AT, Phillips CS, Matzon JL, Daley E. The effects of forearm rotation on three wrist measurements: radial inclination, radial height and palmar tilt. ***Hand Surg.*** 2005;10(1):17-22.

37. Chaouch M, Verroust-Blondet A. Alignment of 3D models. ***Graphical Models.*** 2009;71(2):63-76.

38. Cook PA, Yu JS, Wiand W, et al. Madelung deformity in skeletally immature patients: morphologic assessment using radiography, CT, and MRI. ***J Comput Assist Tomogr.*** 1996;20(4):505-511.

39. Dannenberg M, Anton J, Spiegel M. Madelung's deformity: consideration of its roentgenological diagnostic criteria. ***Am J Roentgenol.*** 1939;42:671-676.

40. Harley BJ, Carter PR, Ezaki M. Volar surgical correction of Madelung's deformity. ***Tech Hand Up Extrem Surg.*** 2002;6(1):30-35.

41. Kosowicz J. The carpal sign in gonadal dysgenesis. ***J Clin Endocrinol Metab.*** 1962;22:949-952.

42. Henry A, Thorburn MJ. Madelung's deformity. A clinical and cytogenetic study. ***J Bone Joint Surg Br.*** 1967;49(1):66-73.

43. de Lagrange JL. ***Mécanique analytique.*** Vol 1: Mallet-Bachelier; 1853.

44. Carelsen B, Bakker NH, Strackee SD, et al. 4D rotational x-ray imaging of wrist joint dynamic motion. ***Med Phys.*** 2005;32(9):2771-2776.

45. Foumani M, Blankevoort L, Stekelenburg C, et al. The effect of tendon loading on in-vitro carpal kinematics of the wrist joint. ***J Biomech.*** 2010;43(9):1799-1805.

46. Foumani M, Strackee SD, Jonges R, et al. In-vivo three-dimensional carpal bone kinematics during flexion-extension and radio-ulnar deviation of the wrist: Dynamic motion versus step-wise static wrist positions. ***J Biomech.*** 2009;42(16):2664-2671.

47. Leng S, Zhao K, Qu M, An KN, Berger R, McCollough CH. Dynamic CT technique for assessment of wrist joint instabilities. ***Med Phys.*** 2011;38 Suppl 1:S50.

48. Tay SC, Primak AN, Fletcher JG, et al. Four-dimensional computed tomographic imaging in the wrist: proof of feasibility in a cadaveric model. ***Skeletal Radiol.*** 2007;36(12):1163-1169.

49. Mat Jais IS, Liu X, An KN, Tay SC. A method for carpal motion hysteresis quantification in 4-dimensional imaging of the wrist. ***Med Eng Phys.*** 2014;36(12):1699-1703.

50. Gondim Teixeira PA, Formery AS, Hossu G, et al. Evidence-based recommendations for musculoskeletal kinematic 4D-CT studies using wide area-detector scanners: a phantom study with cadaveric correlation. ***Eur Radiol.*** 2017;27(2):437-446.

51. Neo PY, Mat Jais IS, Panknin C, et al. Dynamic imaging with dual-source gated Computed Tomography (CT): implications of motion parameters on image quality for wrist imaging. ***Med Eng Phys.*** 2013;35(12):1837-1842.

52. Shores JT, Demehri S, Chhabra A. Kinematic "4 Dimensional" CT Imaging in the Assessment of Wrist Biomechanics Before and After Surgical Repair. ***Eplasty.*** 2013;13:e9.

53. Ranawat CS, DeFiore J, Straub LR. Madelung's deformity. An end-result study of surgical treatment. ***J Bone Joint Surg Am.*** 1975;57(6):772-775.

54. Murphy MS, Linscheid RL, Dobyns JH, Peterson HA. Radial opening wedge osteotomy in Madelung's deformity. ***J Hand Surg Am.*** 1996;21(6):1035-1044.

55. Farr S, Guitton TG, Ring D, Science of Variation G. How Reliable is the Radiographic Diagnosis of Mild Madelung Deformity? ***J Wrist Surg.*** 2018;7(3):227-231.

56. Tuder D, Frome B, Green DP. Radiographic spectrum of severity in Madelung's deformity. ***J Hand Surg Am.*** 2008;33(6):900-904.

57. van de Giessen M, Foumani M, Streekstra GJ, et al. Statistical descriptions of scaphoid and lunate bone shapes. ***J Biomech.*** 2010;43(8):1463-1469.

58. Dobbe JG, Strackee SD, Schreurs AW, et al. Computer-assisted planning and navigation for corrective distal radius osteotomy, based on pre- and intraoperative imaging. ***IEEE Trans Biomed Eng.*** 2011;58(1):182-190.

59. Grewal S, Dobbe JGG, Kloen P. Corrective osteotomy in symptomatic clavicular malunion using computer-assisted 3-D planning and patient-specific surgical guides. ***J Orthop.*** 2018;15(2):438-441.

60. Hove LM, Engesaeter LB. Corrective osteotomies after injuries of the distal radial physis in children. ***J Hand Surg Br.*** 1997;22(6):699-704.

61. Semper-Hogg W, Fuessinger MA, Schwarz S, et al. Virtual reconstruction of midface defects using statistical shape models. ***J Craniomaxillofac Surg.*** 2017;45(4):461-466.

62. Letzer GM, Kronman JH. A posteroanterior cephalometric evaluation of craniofacial asymmetry. ***Angle Orthod.*** 1967;37(3):205-211.

63. Shah SM, Joshi MR. An assessment of asymmetry in the normal craniofacial complex. ***Angle Orthod.*** 1978;48(2):141-148.

64. Farkas LG, Cheung G. Facial asymmetry in healthy North American Caucasians. An anthropometrical study. ***Angle Orthod.*** 1981;51(1):70-77.

65. Kim YH, Sato K, Mitani H, Shimizu Y, Kikuchi M. Asymmetry of the sphenoid bone and its suitability as a reference for analyzing craniofacial asymmetry. ***Am J Orthod Dentofacial Orthop.*** 2003;124(6):656-662.

66. Vlachopoulos L, Luthi M, Carrillo F, Gerber C, Szekely G, Furnstahl P. Restoration of the Patient-Specific Anatomy of the Proximal and Distal Parts of the Humerus: Statistical Shape Modeling Versus Contralateral Registration Method. ***J Bone Joint Surg Am.*** 2018;100(8):e50.

67. Ghatan AC, Hanel DP. Madelung deformity. ***J Am Acad Orthop Surg.*** 2013;21(6):372-382.

68. Kozin SH, Zlotolow DA. Madelung Deformity. ***J Hand Surg Am.*** 2015;40(10):2090-2098.

69. Knutsen EJ, Goldfarb CA. Madelung's Deformity. ***Hand (N Y).*** 2014;9(3):289-291.

70. Peymani A, Dobbe JGG, Streekstra GJ, McCarroll HR, Strackee SD. Quantitative three-dimensional assessment of Madelung deformity. ***J Hand Surg Eur Vol.*** 2019;44(10):1041-1048.

71. Berger RA, Blair WF. The radioscapholunate ligament: a gross and histologic description. ***Anat Rec.*** 1984;210(2):393-405.

72. Rajput R, Bhat RV, Bhansali A. Reverse Madelung deformity. ***J Assoc Physicians India.*** 2005;53:120.

73. Ulici A, Florea DC, Tevanov I, Zaharie D, Carp M. Surgical Treatment of a Rare "Reverse" Madelung Deformity in 11 Years Female Patient. ***Chirurgia (Bucur).*** 2017;112(1):72-76.

74. Sibbel SE, Bauer AS, McCarroll HR. Madelung deformity. In: ***Congenital anomalies of the upper extremity.*** Springer; 2015:317-324.

10

SUMMARY

SUMMARY

From distal to proximal, the hand can be divided into three regions: phalanges, metacarpals, and the wrist. In turn, the wrist consists of eight carpal bones, the distal radius, and the distal ulna. Upper limb development is regulated on a genetic level, and alterations can lead to upper limb anomalies. Over 2000 children per year are born in the United States with congenital hand differences, and they are severely impacted in their physical, mental, and social functioning.

Madelung deformity is a rare congenital hand difference caused by a distal radial growth arrest. This process leads to a bowing of the radius, an ulnar and volar tilt of the distal radius, a triangular proximal carpal row, and a long ulna. The soft-tissue abnormalities include a thickened radiolunate 'Vickers' ligament and radiotriquetral ligament. Initially, Madelung deformity is asymptomatic, but patients can develop symptoms in early adolescence. The diagnosis can be made using x-ray imaging, but some patients can not be reliably diagnosed. As the condition is progressive, it would be beneficial to diagnose early and intervene. Treatment involves lengthening the radius and shortening the ulna, often combined with the release of abnormal ligaments. There are still many unknowns in regard to Madelung deformity. Possibly, our advances in medical imaging and computational analyses can help us better understand the condition.

In Chapter 2, our findings were published after conducting a systematic review of all studies describing surgical interventions for Madelung deformity, the purpose being to fill the knowledge gap concerning surgical management. Our electronic database search resulted in 713 unique records, of which 25 were eligible for inclusion after an extensive screening and filtering process. Patient workup includes assessing pain, range of motion (ROM), grip strength, and aesthetic deformity, with pain being the primary indication for surgery. Surgical treatment options either involve lengthening the radius, shortening the ulna, or a combination of both. Generally, outcomes in regard to pain reduction and mobility improvement seem favorable. However, they are reported inconsistently and in a heterogeneous manner, prohibiting methodologically sound comparisons from being made. Our proposed protocol could increase the quality of evidence in future studies and compensate for the small patient numbers.

Chapter 3 presented patient outcomes on a large scale and described a potential framework for obtaining patient-reported outcomes of rare conditions. The goal of the study was to understand the clinical spectrum of patients and their health burden. The challenging nature of reaching significant patient numbers in a rare disease inspired us to engage patients internationally through the utilization of several social media platforms. Within nine days, we witnessed 133 participants completing the survey, which, to the best of our knowledge, establishes the largest Madelung deformity outcomes study to date. Nearly all participants were female, an overwhelming majority (92%) was bilaterally affected, and mean patient height was below the normal (157 cm). On average, patients are diagnosed at the age of 19 and undergo (multiple) surgeries starting from the age of 21. Patients are significantly impacted in their physical, mental, and social health, even after being subjected to corrective surgical treatment. Using social media, we were able to compensate for Madelung deformity's rarity by engaging an international audience, demonstrating the feasibility to conduct research through it, and providing a global perspective of the disease entity.

In Chapter 4, we advanced our assessment of the wrist through 3D imaging, 4D imaging, and shape analyses. These novel imaging techniques allowed us to evaluate wrist joint kinematics and quantify the surface area and cartilage thickness of various wrist joints. Shape analyses offer a simple way to compare skeletal anatomy and quantifying anatomical changes over time.

Chapter 5 investigated the Madelung deformity wrist by a look from within, using 3D imaging to increase our anatomical understanding of a condition that has been mainly evaluated in 2D. After segmentation of 28 patient wrists and 56 healthy wrists, we measured previous 2D-based and newly developed 3D-based parameters in an automatic manner. The McCarroll criteria embrace solid underlying principles and demonstrate their applicability in 3D, with clinically relevant differences between patients and healthy volunteers. New 3D quantifications show the lunate fossa in Madelung deformity to be more concave and irregular. The angle between the scaphoid, lunate, and triquetrum is decreased, quantifying the previously described 'pyramidization' of the proximal carpal row. These findings validate the underlying principles of current 2D criteria and reveal previously unknown anatomical abnormalities by utilizing novel 3D parameters to quantify the radiocarpal joint.

In Chapter 6, we expanded our 3D assessment of the Madelung deformity wrist to 4D, taking another look from within, but in a dynamic rather than static context. By unveiling the anatomy of the wrist during movement, we were able to kinematically evaluate the deformity's effects in-vivo. Compared to healthy wrists, patients show significantly decreased movement patterns of two carpal bones, the lunate and the triquetrum, while scaphoid bone mobility remains normal. This raises the question of whether the abnormal carpal kinematics are caused by the distorted skeletal configuration, or the anomalous radiolunate and radiotriquetral ligaments previously discovered in patients' wrists. Prospective studies could use a 4D analysis to investigate the biomechanical effects of surgical ligament release.

In Chapter 7, we developed a statistical shape model (SSM) of the distal radius in Madelung deformity. Using wrist CT scans, we developed an SSM that could visualize shape variations and quantify these variations by representing them as 'modes' of variation. Over 80% of variation in the distal radius of Madelung deformity patients can be explained with the five largest modes: ulnar-sided collapse, coronal width, sigmoid notch axial rotation, volar tilt, and lunate fossa angle. While quantifying shapes allows us to detect any potential groupings, no distinct groups are seen in our relatively small study. Converting an anatomical shape into numbers can prove valuable in diagnostics, as we can achieve high accuracy in automatically determining if a shape is from a healthy volunteer or a patient, based on the first two modes. Even if the absolute number of shapes is small SSMs can be applied, making it especially useful in rare congenital conditions where minimal patient numbers have limited clinicians' anatomical exposure.

Chapter 8 describes the preliminary results of a novel surgical approach to Madelung deformity. This case series study compared the outcomes after a radioscapholunate (RSL) arthrodesis and construction of a neo-distal radioulnar joint (n=6), with outcomes after a 'classic' reverse wedge osteotomy (n=7). The novel surgery involves a two-phase approach: (1) modified RSL arthrodesis with triquetrectomy; and (2) distal scaphoidectomy. Adhering to the protocol developed in Chapter 2, we assessed both functional outcomes (PROMs) and clinical outcomes (pain, ROM,

and grip strength). Outcomes between osteotomy and reconstruction are similar, apart from wrist extension, which is not unexpected after a fusion of the RSL joint. If studies with a more comprehensive follow-up can confirm the procedure's durability, it could prove a viable treatment option for a subset of symptomatic patients where an osteotomy simply 'does not cut it'.

Only future studies will be able to answer the question 'What is Madelung deformity?' by using protocolized assessments of prospective patients. We provided several recommendations on what a complete workup should entail, including clinical, genetic, and imaging findings. It would be beneficial to use the Patient-Reported Outcomes Measure Information System (PROMIS) to evaluate the patient perspective. Until we have large multicenter studies, the findings from our survey study can be used as a baseline, showing the severe functional, mental, and social health impacts of Madelung deformity.

Applying our advancements in imaging allows for automatic and objective assessments of the wrist in 3D. Also, we can now witness the biomechanical effects of anatomical changes through 4D imaging. Quantifications of a full shape through SSM can improve our diagnostic process and statistically establish shape variations. Future implementations of SSMs can even be used to develop virtual surgical reconstruction planning.

Combining the imaging findings from our 3D, 4D, and SSM studies, it is evident that the sigmoid notch is severely deformed in some patients. The preliminary results of a new surgical approach seem satisfactory, and if results hold in the long-term, this could provide a solution for a subset of patients.

NEDERLANDSE SAMENVATTING (DUTCH SUMMARY)

Van distaal naar proximaal kan de hand verdeeld worden in drie regio's: de phalangen, de metacarpalen, en de pols. De pols bestaat uit acht handwortelbeentjes, de distale radius, en de distale ulna. De ontwikkeling van de bovenste extremiteit wordt gereguleerd op gen niveau, en fouten in dit proces kunnen leiden tot anomalieën van de bovenste extremiteit. Meer dan 2000 kinderen per jaar in de Verenigde Staten worden geboren met aangeboren handafwijkingen. Deze kinderen ondervinden veel hinder in hun fysiek, mentaal, en sociaal functioneren.

Madelung deformiteit is een zeldzame aangeboren handafwijking en wordt veroorzaakt door een remming van de groei van de distale radius. Dit proces leidt tot een gebogen radius, een ulnaire en volaire kanteling van de distale radius, een driehoekige proximale carpale rij, en een lange ulna. De afwijkingen in de zachte weefsels bestaan uit een verdikt radiolunate 'Vickers' ligament en afwijkingen in het radiotriquetrale ligament. Patiënten met Madelung deformiteit zijn initieel asymptomatisch, maar zij kunnen symptomen ontwikkelen in de vroege adolescentie. De diagnose kan gesteld worden met een röntgenfoto, maar sommige patiënten kunnen hiermee niet betrouwbaar worden gediagnosticeerd. Gezien de progressiviteit van de aandoening, zou het gunstig zijn om vroegtijdig een diagnose te stellen en in te grijpen. De behandeling bestaat uit het verlengen van de radius en het verkorten van de ulna, vaak gecombineerd met het doornemen van abnormale ligamenten.

Er is nog steeds veel onbekend over Madelung deformiteit. Mogelijk kunnen onze innovaties in medische beeldvorming en computeranalyses helpen om de afwijking beter te begrijpen.

Hoofdstuk 2 laat onze bevindingen zien na het uitvoeren van een systematic review van alle studies die een chirurgische interventie van Madelung deformiteit beschrijven. Het doel was om kennis op te doen over de huidige chirurgische mogelijkheden. Onze zoektocht leidde tot 713 unieke artikelen, waarvan 25 geschikt waren voor inclusie. Bij de work-up van Madelung deformiteit worden de volgende aspecten beoordeeld: pijnklachten, Range of Motion (ROM), grijpkracht, en esthetische hinder. Het voorkomen van pijn is de belangrijkste reden voor chirurgische interventie. Chirurgische behandeling bestaat voornamelijk uit het verlengen van de radius, het verkorten van de ulna, of een combinatie van beide. In het algemeen zijn de uitkomsten in het kader van pijnvermindering en verbeteren van mobiliteit redelijk goed. Echter, worden deze uitkomsten vaak inconsistent en heterogeen beschreven. Dit weerhoudt ons ervan om methodologisch correcte vergelijkingen te maken. Ons voorgestelde protocol zou de kwaliteit van de data van toekomstige studies kunnen verbeteren en de kleine aantallen patiënten mogelijk compenseren.

Hoofdstuk 3 presenteerde patiëntuitkomsten op grote schaal en beschreef een potentieel raamplan voor het verkrijgen van patiënt-gerapporteerde uitkomstmaten (PROMs). Het doel van deze studie was om inzicht te verkrijgen in het klinische spectrum van patiënten en hun gezondheidsklachten. In studies naar zeldzame ziektes, is het verzamelen van genoeg patiënten-data een uitdagende taak. Om die reden hebben wij getracht om patiënten internationaal te benaderen, gebruikmakend van verscheidene social media platformen. In 9 dagen werd onze vragenlijst door 133 deelnemers ingevuld. Voor zover wij weten, is dit het grootste onderzoek van patiëntuitkomsten in Madelung deformiteit. Vrijwel alle deelnemers waren vrouw, een

overweldigende meerderheid (92%) was bilateraal aangedaan, en de gemiddelde lengte van patiënten was onder het normale gemiddelde (157 cm). Gemiddeld genomen worden patiënten gediagnosticeerd op een leeftijd van 19 jaar waarna zij meerdere operaties ondergaan vanaf 21-jarige leeftijd. Patiënten ondervinden significante beperkingen in hun fysieke, mentale, en sociale gezondheid, zelfs na het ondergaan van chirurgische behandelingen. Door het gebruik van social media konden wij de zeldzaamheid van Madelung deformiteit compenseren door een internationaal publiek aan te spreken. Tevens presenteerden wij een globaal perspectief van de aandoening.

In Hoofdstuk 4 breidden wij ons onderzoek van de pols uit middels driedimensionale (3D) beeldvorming, vierdimensionale (4D) beeldvorming, en vormanalyses. Met deze nieuwe beeldvormende technieken konden wij de kinematica van het polsgewricht evalueren, en de oppervlakte en kraakbeendikte van verscheidene polsgewrichten kwantificeren. Vormanalyses bieden een eenvoudige oplossing om skeletanatomie te vergelijken en anatomische veranderingen in tijd te kwantificeren.

In Hoofdstuk 5 onderzochten wij polsen van patiënten met Madelung door een blik van binnenuit, gebruikmakend van 3D beeldvorming om het anatomische begrip te vergroten van een aandoening die voornamelijk in 2D is geëvalueerd. Na segmentatie van 28 polsen van patiënten en 56 gezonde polsen, verrichtten wij automatische metingen van eerder ontwikkelde 2D- en nieuw ontwikkelde 3D-parameters. De McCarroll criteria zijn gebaseerd op solide onderliggende principes en tonen hun toepasbaarheid in 3D, met klinisch relevante verschillen tussen patiënten en gezonde deelnemers. Nieuwe 3D parameters demonstreren dat in Madelung deformiteit patiënten, de fossa lunata meer concaaf en onregelmatig is. Tevens is de hoek tussen het scaphoid, lunatum, en het triquetrum aanzienlijk kleiner. Dit kwantificeert de eerder beschreven 'pyramidisering' van de proximale carpale rij. Deze bevindingen valideren de onderliggende principes van de huidige 2D criteria. Tevens worden voorheen onbekende anatomische afwijkingen onthuld door het gebruik van nieuwe 3D parameters om het radiocarpale gewricht te kwantificeren.

In Hoofdstuk 6 breidden we onze 3D beoordeling van de Madelung deformiteit pols uit naar 4D. Dit is wederom een blik van binnenuit, echter nu in een dynamische in plaats van statische context. Door de anatomie van de pols tijdens beweging te analyseren, werd het mogelijk om de kinematische effecten van de deformiteit in-vivo te beoordelen. In vergelijking tot gezonde polsen, vertonen polsen van patiënten een verminderde beweeglijkheid van 2 carpalia, het lunatum en het triquetrum, terwijl de beweeglijkheid van het scaphoid normaal blijft. Dit roept de vraag op of deze abnormale carpale kinematica wordt veroorzaakt door de vervormde skeletconfiguratie, of door de abnormale radiolunate en radiotriquetrale ligamenten die eerder zijn ontdekt in deze patiëntengroep. Prospectieve studies kunnen deze 4D analysemethode gebruiken om het effect na chirurgisch doornemen van deze ligamenten te onderzoeken.

In Hoofdstuk 7 ontwikkelden wij een statistisch vormmodel (SSM) van de distale radius in Madelung deformiteit patiënten. Gebruikmakend van CT-scans van de pols, ontwikkelden wij een SSM dat vormvariaties kon visualiseren. Deze variaties werden vervolgens gekwantificeerd door deze te representeren als 'modes' van variatie. Meer dan 80% van de variatie in de distale radius van patiënten kan worden verklaard, gebruikmakend van de 5 dominante modes van variatie. Deze

modes representeren 'ulnar-sided collapse', 'coronal width', 'sigmoid notch axial rotation', 'volar tilt', en 'lunate fossa angle'. Hoewel het kwantificeren van vormen ons in staat stelt om eventuele subgroepen binnen de Madelung patiëntenpopulatie te detecteren, zagen wij geen groepsvorming in onze relatief kleine studie. Het omzetten van een anatomische vorm in getallen kan waardevol zijn in het diagnostische proces, aangezien een hoge nauwkeurigheid bereikt kan worden in het automatisch bepalen of een vorm afkomstig is van een gezonde vrijwilliger of een patiënt. Zelfs bij een klein aantal vormen kunnen SSM's al zinvol worden gebruikt. Dit maakt de technologie bij uitstek geschikt in zeldzame aangeboren aandoeningen.

Hoofdstuk 8 beschrijft de vroege resultaten van een nieuwe chirurgische benadering van Madelung deformiteit. In deze case series studie vergeleken wij de resultaten na een radioscapholunate (RSL) arthrodese en constructie van een nieuw distaal radioulnair gewricht (n=6), met resultaten na de 'klassieke' reverse wedge osteotomie (n=7). Deze eerstgenoemde techniek bestaat uit twee fases: (1) gemodificeerde RSL arthrodese en triquetrectomie; en (2) distale scaphoidectomie. In overeenstemming met het ontwikkelde protocol uit hoofdstuk 2, hebben wij zowel functionele uitkomstmaten (PROMs) en klinische uitkomstmaten (pijn, ROM, en grijpkracht) geëvalueerd. De resultaten na osteotomie en reconstructie waren vergelijkbaar, behalve voor de extensiebeweging van de pols. Dit is niet ongebruikelijk na een fusie van het RSL-gewricht. Als studies met een langere follow-up de duurzaamheid van de nieuwe procedure kunnen bevestigen, zou dit een geschikte behandeloptie kunnen zijn voor een subgroep van symptomatische patiënten met een abnormale sigmoid notch, waarbij een osteotomie niet voldoet.

Alleen toekomstige studies zullen de vraag 'Wat is Madelung deformiteit?' kunnen beantwoorden door het gebruik van een geprotocolleerde aanpak van prospectief geïncludeerde patiënten. Wij hebben verschillende aanbevelingen gedaan over hoe een volledige workup zou moeten gaan, inclusief het gebruik van klinisch, genetisch, en beeldvormend onderzoek. Om patiëntbeleving te evalueren zou het geschikt zijn om het Patient Reported Outcomes Measurement Information System (PROMIS) te gebruiken. Totdat er grote multicenter onderzoeken zijn, kunnen de bevindingen van ons surveyonderzoek als uitgangspunt worden gebruikt om de ernstige functionele, mentale en sociale gezondheidseffecten van Madelung deformiteit aan te tonen.

Door onze innovaties op het gebied van beeldvorming toe te passen, kunnen automatische en objectieve beoordelingen van de pols in 3D worden uitgevoerd. Ook kunnen we nu de biomechanische effecten van anatomische veranderingen zien door het gebruik van 4D beeldvorming. Kwantificering van de volledige vorm via een SSM kan het diagnostisch proces verbeteren en statistische vormvariaties bepalen. Toekomstige implementaties van SSM's kunnen zelfs worden gebruikt om een virtuele chirurgische reconstructieplanning te ontwikkelen.

Door het combineren van onze 3D, 4D, en SSM-bevindingen, is het duidelijk dat de sigmoid notch bij sommige patiënten ernstig vervormd is. De voorlopige resultaten van onze nieuwe chirurgische aanpak lijken toereikend. Als deze resultaten op de lange termijn standhouden, zou dit een oplossing kunnen bieden voor een subgroep van patiënten.

ADDENDUM

FOUR-DIMENSIONAL ROTATIONAL RADIOGRAPHIC SCANNING OF THE WRIST IN PATIENTS AFTER PROXIMAL ROW CARPECTOMY

A. Peymani [1], M. Foumani [1], J.G.G. Dobbe [2],
S.D. Strackee [1], G.J. Streekstra [2]

[1] Department of Plastic, Reconstructive and Hand Surgery, Amsterdam UMC, University of Amsterdam, Amsterdam, The Netherlands.
[2] Department of Biomedical Engineering and Physics, Amsterdam UMC, University of Amsterdam, Amsterdam, The Netherlands.

J Hand Surg Eur Vol. 2017 Oct;42(8):846-851.

ABSTRACT

We measured cartilage thickness, contact surface area, volume of the capitate and shape of the capitate during motion in the operated and unaffected wrists of eleven patients with a mean follow-up of 7.3 years after proximal row carpectomy. Radiocapitate cartilage thickness in the operated wrists did not differ significantly from radiolunate cartilage thickness in the unaffected wrists. The radiolunate surface area was significantly less than the radiocapitate surface area. The volume of the capitate was significantly increased in the operated wrists. The shape of the capitate changed significantly in two of three orthogonal directions. The combination of remodeling of the capitate, increase in its surface area and intact cartilage thickness could help to explain the clinical success of proximal row carpectomy.

INTRODUCTION

Proximal row carpectomy (PRC) is used in the treatment of various post-traumatic and degenerative disorders of the wrist.[1] In many patients, it provides good long-term results, including maintenance of function and pain relief.[2,3]

The biomechanics of the wrist after PRC may provide information about the mechanisms whereby these results are attained. Until now they have been studied almost exclusively in static cadaveric models; this has several disadvantages, including the need to artificially load tendons and the disruption of ligaments.[4-7] It is also not possible to investigate the changes that occur after soft tissue healing, scar tissue formation, capsular scarring, and bone remodeling over time.[6-8]

The purpose of our study was to investigate the effects of PRC on wrist joint kinematics in patients.

METHODS

Setting and study population

A total of 64 individuals who had undergone a unilateral PRC between 1998 and 2007 were invited to take part in the study. Patients were invited if they had normal non-operated contralateral wrists without any history of trauma or systemic diseases. Eleven patients agreed to participate. The mean post-operative follow-up was 7.3±3.4 years (range 1.9-10.7). The participants underwent computed tomography (CT) and four-dimensional rotational radiographic (4D-RX) scanning[9] of both wrists.

Additionally, to investigate any anatomical differences between the carpal bones of the left and right hand, twelve healthy participants (four men, eight women; mean age of 24±2.4 years, range 22-31) were studied. These participants had no history of congenital wrist abnormalities or wrist injuries and underwent CT-scans of both wrists. The local medical ethics committee approved this study.

Assessment and measurement of carpal bone kinematics

To record wrist bone positions during motion we used 4D-RX imaging.[9] This method uses a static CT scan to obtain virtual three-dimensional (3D) models of the radius, ulna, and carpal bones through segmentation (Figure 1) by the use of a previously described algorithm.[10] Using a regular 3D rotational X-ray system (BV Pulsera, Philips Healthcare, The Netherlands), the static CT scans are combined with dynamic scans made during three motions: flexion-extension motion, radio-ulnar deviation, and dart-throwing motion. Finally, virtual bone models are aligned with dynamic scans by registration, thereby quantifying motion patterns of wrist bones in vivo.[11,12]

A motorized hand-shaker device[10] was used to move the wrist with an imposed range of motion (ROM) set for each patient individually to avoid any pain or discomfort. During each of the three motions, the X-ray source was rotated around the wrist to acquire 20 volume reconstructions, each reconstruction corresponding to a unique wrist position. Assessment of 4D-RX imaging data in a previous study demonstrated a precision of 0.02±0.005 mm for translation and 0.12±0.07 degrees for rotation.[10]

Figure 1. 3D reconstruction of the radius, ulna and carpal bones after segmentation.

Computation of joint space thickness and articular surface area

Individual articular cartilage layers could not be visualized owing to limitations of CT imaging; however, subchondral bone just below the cartilage layer was clearly definable. Total cartilage thickness could therefore be approximated by determining the distance between opposing subchondral bones. In this study, the joint space thickness was defined as the thickness of articular cartilage between the lunate and radius (unaffected wrists), or between the capitate and radius (operated wrists).

For each wrist position, joint space thickness was calculated using a previously specified method.[12] To this end, for each point on a bone, the nearest point to the opposite bone was determined using a k-Nearest Neighbors algorithm (Supplementary Video 1). To filter points contributing to the articular surface, two constraints were applied. First, the distance between a point on a bone and a point on an opposite bone should be less than 4 mm.

The second constraint was a maximum angle difference of 15 degrees between the normal vector of a point (vector perpendicular to the bone surface) and the normal vector of an opposite point. Thresholds of 4 mm and 15 degrees were chosen pragmatically.[12] Joining all these points during motion provided the articular surface area defined as the area on the radius with which the lunate or capitate articulates (Figure 2).

The minimum distance to the opposite bone during motion was determined for each point, representing a situation where articular cartilage layers were minimal. The mean of these distances for all points in the articular surface area provided the joint space thickness. The mean joint space thickness was calculated by taking the mean of the radius-to-lunate and lunate-to-radius distances (unaffected wrists) or the mean of the radius-to-capitate and capitate-to-radius distances (operated wrists). The joint space thickness and articular surface areas were recalculated for the combination of all three motions (60 wrist positions in all).

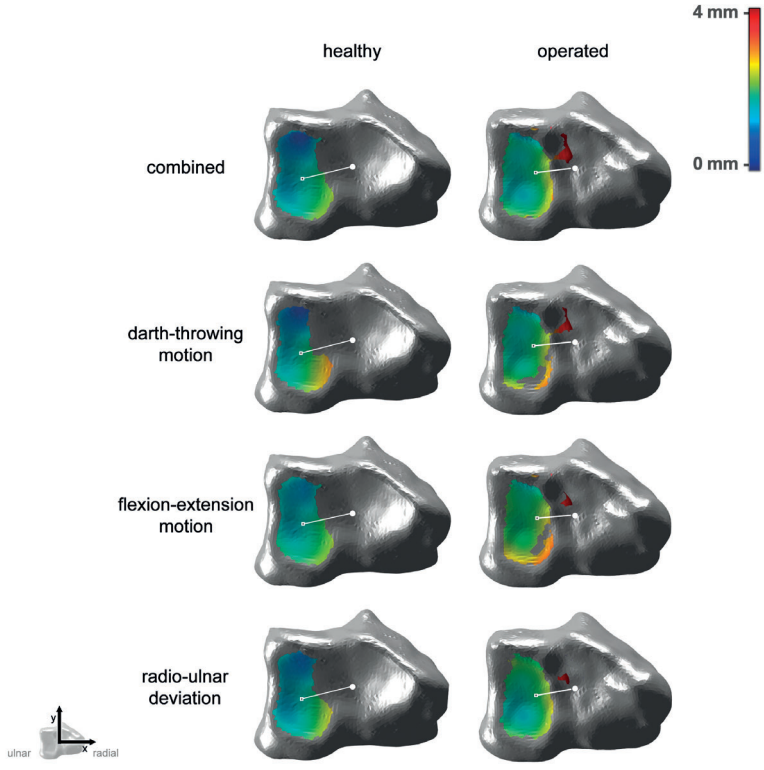

Figure 2. Articular surface areas of the radius with the lunate (left) and capitate (right). The colour map indicates the shortest distance to the neighbouring bone during the entire motion.

Assessment of the volume and shape of the capitate

The volume of the capitate was calculated from its virtual model. To enable shape comparisons, each capitate was described as an ellipsoid with three gravitational axes[13] of lengths (ranked in order, from largest to smallest) A, B and C (Figure 3).

To determine whether any differences between capitates were due to naturally occurring anatomical differences, we repeated our assessment comparing healthy left and right wrists using CT imaging data from twelve healthy volunteers.

Statistical analysis

All variables followed a normal distribution, confirmed by Shapiro–Wilk tests. Paired samples t-tests were used to investigate the differences between unaffected wrists and operated wrists for joint space thickness, articular surface area, volume and shape parameters (lengths of ellipsoid axes) of the capitate.

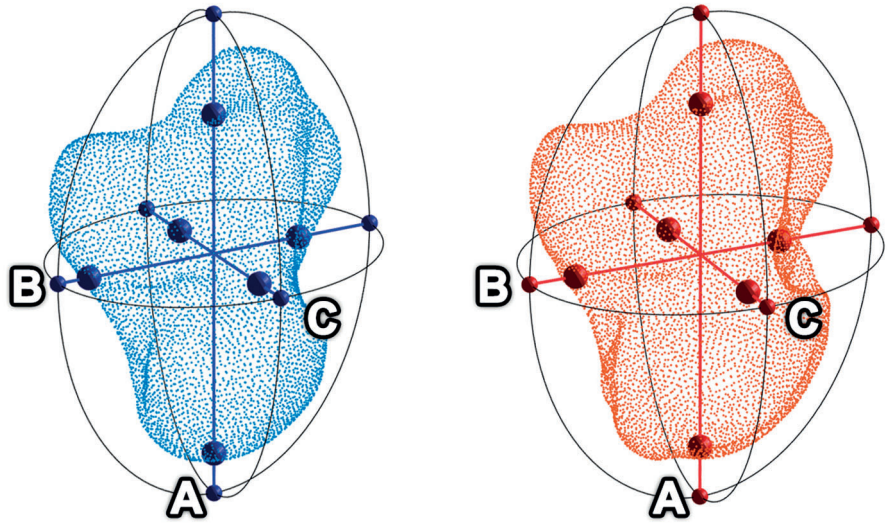

Figure 3. The capitate bone represented as an ellipsoid in the healthy (blue) and the operated wrist (red) with axes A, B and C.

RESULTS

The characteristics of the eleven patients in the study are described in Table 1.

The biomechanical comparison between operated and unaffected wrists is presented in Table 2. There were no significant differences in mean joint space thickness between operated and unaffected wrists. However, the articular surface area in operated wrists was significantly larger compared with unaffected wrists. When comparing the area of the articular surface for different motions, the difference was only significant for flexion-extension motion.

In Table 3 the differences in volume and shape of the capitate are shown. The volume of the capitate was significantly larger in operated wrists than in unaffected wrists. Shape comparisons displayed significantly longer B and C axes in the capitate after PRC. The volume and shape of the capitate did not differ significantly between the left and right wrists of twelve healthy volunteers.

DISCUSSION

In this case-series study, it was shown that after PRC the mean joint space thickness stays intact and the articular surface area slightly increases. The capitate undergoes anatomical changes after PRC, its volume and size increasing significantly.

A major strength of this study was that features were investigated in patients instead of cadavers, allowing the natural processes of soft tissue healing and capsule scarring to occur.[4,8] Another strength was that we investigated the wrist joint parameters in 3D space and in a dynamic setup covering the entire ROM. In contrast, previous studies have measured radiocapitate space in static configurations using two-dimensional imaging,[14-16] ignoring changes in orientation and

Table 1. Characteristics of the study group.

	Proximal row carpectomy patients (n=11)
Women	6
Mean age at surgery, y (range)	43±11 (19-59)
Mean age at follow-up, y (range)	50±10 (30-63)
Indication for surgery	
Kienböck's diesease	4
SNAC	2
SLAC	1
Other	4
Mean imposed range of motion, degrees (range)	
Unaffected wrist	
Dart-throwing motion	53±10 (37-73)
Flexion-extension motion	79±12 (55-93)
Radio-ulnar deviation	49±10 (34-64)
Operated wrist	
Dart-throwing motion	43±11 (23-60)
Flexion-extension motion	59±15 (37-79)
Radio-ulnar deviation	33±10 (19-44)

SNAC: Scaphoid Nonunion Advanced Collapse; SLAC: Scapholunate Advanced Collapse.

Table 2. Joint space thickness and articular surface area.

	Unaffected wrists (n=11)	Operated wrists (n=11)	P
Mean joint space thickness, mm (range)			
Dart-throwing motion	1.5±0.4 (0.8-2.2)	1.5±0.6 (0.8-3.0)	0.797
Flexion-extension motion	1.4±0.3 (1.0-1.9)	1.5±0.5 (1.0-2.4)	0.864
Radio-ulnar deviation	1.4±0.4 (0.8-1.9)	1.4±0.4 (0.9-2.0)	0.982
Combined[a]	1.3±0.3 (0.8-1.9)	1.3±0.5 (0.7-2.4)	0.963
Mean articular surface area, cm^2 (range)			
Dart-throwing motion	1.2±0.3 (0.7-1.6)	1.3±0.3 (0.8-2.0)	0.252
Flexion-extension motion	1.2±0.3 (0.8-1.7)	1.5±0.3 (1.0-2.0)	**0.029**
Radio-ulnar deviation	1.3±0.3 (0.8-1.6)	1.2±0.3 (0.8-1.9)	0.724
Combined[b]	1.4±0.3 (0.9-1.8)	1.7±0.4 (1.1-2.3)	**0.014**

[a]Joint space thickness (mm) combined for all three motions.
[b]Articular surface (cm^2) combined for all three motions.

the positions of carpal bones during movement.[9] A limitation of this study was the potential for selection bias. Out of the 64 invited persons, eleven persons agreed to participate. It is possible that patients with good results from surgery might have been more likely to participate.

We compared the operated and unaffected wrists in individual patients. It might be suggested that the differences found are due to anatomical differences between the left and right wrists. However, previous research showed no significant differences between the wrists of healthy

Table 3. Volume and shape of the capitate.

	Proximal row carpectomy patients			Healthy volunteers		
	Unaffected wrists (n=11)	**Operated wrists (n=11)**	**P**	**Left wrists (n=12)**	**Right wrists (n=12)**	**P**
Mean volume, cm^3 (range)	3.5±0.8 (1.9-4.7)	3.7±0.9 (2.1-5.0)	**0.010**	3.2±0.9 (2.0-4.8)	3.2±0.9 (2.0-4.8)	0.828
Mean axis length, mm (range)						
Ellipsoid axis A	34.0±3.0 (27.5-37.0)	34.1±3.2 (27.2-37.5)	0.389	32.3±3.2 (27.2-37.2)	32.2±3.0 (27.5-36.9)	0.240
Ellipsoid axis B	23.8±2.4 (19.3-28.0)	24.6±2.5 (20.7-27.9)	**0.003**	23.9±2.3 (20.6-27.4)	23.8±2.2 (20.7-27.0)	0.721
Ellipsoid axis C	19.0±1.5 (16.3-21.3)	19.7±1.7 (16.9-22.5)	**0.005**	18.7±1.7 (16.6-21.3)	18.7±1.8 (16.3-21.6)	0.308

volunteers and the unaffected wrists of patients.[17] We showed that there were no significant anatomical differences in the size and shape of the capitate in each wrist in healthy volunteers, supporting our belief that the differences found in patients are indeed effects of the PRC procedure itself.

In this study, we were able to witness the biomechanical effects after PRC on the wrist joint. The cartilage-containing areas of the lunate fossa and capitate remain intact even though a new articular surface has been established. Previous cadaveric studies have investigated biomechanical changes in the radiocapitate joint using low-pressure-sensitive contact film.[5-7] These studies showed a significant increase of contact pressure in the radiocapitate joint. These increased forces could possibly cause capitate remodeling as shown in our study. Two of these cadaveric studies reported a decrease in the contact area of the lunate fossa.[6,7] In contrast, we found an increased surface area after PRC, which is not surprising as we measured surface area after years of capitate remodelling under the influence of increased contact pressure. Taken together, increased radiocapitate forces could provide a credible explanation for the remodeling and increased surface area of the capitate that were seen several years after surgery, highlighting the adaptive capacity of the wrist after major anatomical changes.

The mean follow-up of 7.3 years gives a relatively limited insight into the long-term effects of anatomical changes in the wrist joint, especially since degenerative changes have been documented mainly in studies with a long-term follow-up.[15,18,19] Furthermore, all measurements in this study were done at a single time point. It would be valuable to investigate the changes using repeated measurements over longer periods.

In conclusion, the combination of remodeling of the capitate, the corresponding increase in the articular surface area and the unaltered joint space thickness could help to explain the clinical success of PRC.

REFERENCES

1. Inglis AE, Jones EC. Proximal-row carpectomy for diseases of the proximal row. ***J Bone Joint Surg Am.*** 1977;59(4):460-463.
2. Berkhout MJ, Bachour Y, Zheng KH, Mullender MG, Strackee SD, Ritt MJ. Four-Corner Arthrodesis Versus Proximal Row Carpectomy: A Retrospective Study With a Mean Follow-Up of 17 Years. ***J Hand Surg Am.*** 2015;40(7):1349-1354.
3. Richou J, Chuinard C, Moineau G, Hanouz N, Hu W, Le Nen D. Proximal row carpectomy: long-term results. ***Chir Main.*** 2010;29(1):10-15.
4. Blankenhorn BD, Pfaeffle HJ, Tang P, Robertson D, Imbriglia J, Goitz RJ. Carpal kinematics after proximal row carpectomy. ***J Hand Surg Am.*** 2007;32(1):37-46.
5. Hogan CJ, McKay PL, Degnan GG. Changes in radiocarpal loading characteristics after proximal row carpectomy. ***J Hand Surg Am.*** 2004;29(6):1109-1113.
6. Tang P, Gauvin J, Muriuki M, Pfaeffle JH, Imbriglia JE, Goitz RJ. Comparison of the "contact biomechanics" of the intact and proximal row carpectomy wrist. ***J Hand Surg Am.*** 2009;34(4):660-670.
7. Zhu YL, Xu YQ, Ding J, Li J, Chen B, Ouyang YF. Biomechanics of the wrist after proximal row carpectomy in cadavers. ***J Hand Surg Eur Vol.*** 2010;35(1):43-45.
8. Debottis DP, Werner FW, Sutton LG, Harley BJ. 4-corner arthrodesis and proximal row carpectomy: a biomechanical comparison of wrist motion and tendon forces. ***J Hand Surg Am.*** 2013;38(5):893-898.
9. Carelsen B, Bakker NH, Strackee SD, et al. 4D rotational x-ray imaging of wrist joint dynamic motion. ***Med Phys.*** 2005;32(9):2771-2776.
10. Carelsen B, Jonges R, Strackee SD, et al. Detection of in vivo dynamic 3-D motion patterns in the wrist joint. ***IEEE Trans Biomed Eng.*** 2009;56(4):1236-1244.
11. Foumani M, Strackee SD, Jonges R, et al. In-vivo three-dimensional carpal bone kinematics during flexion-extension and radio-ulnar deviation of the wrist: Dynamic motion versus step-wise static wrist positions. ***J Biomech.*** 2009;42(16):2664-2671.
12. Foumani M, Strackee SD, van de Giessen M, Jonges R, Blankevoort L, Streekstra GJ. In-vivo dynamic and static three-dimensional joint space distance maps for assessment of cartilage thickness in the radiocarpal joint. ***Clin Biomech (Bristol, Avon).*** 2013;28(2):151-156.
13. Goldstein H, Poole C, Safko J. Classical mechanics. 3rd. In: Addison Wesley; 2002.
14. Croog AS, Stern PJ. Proximal row carpectomy for advanced Kienbock's disease: average 10-year follow-up. ***J Hand Surg Am.*** 2008;33(7):1122-1130.
15. DiDonna ML, Kiefhaber TR, Stern PJ. Proximal row carpectomy: study with a minimum of ten years of follow-up. ***J Bone Joint Surg Am.*** 2004;86(11):2359-2365.
16. Wall LB, Didonna ML, Kiefhaber TR, Stern PJ. Proximal row carpectomy: minimum 20-year follow-up. ***J Hand Surg Am.*** 2013;38(8):1498-1504.
17. Foumani M, Strackee SD, Stekelenburg CM, Blankevoort L, Streekstra GJ. Dynamic in vivo evaluation of radiocarpal contact after a 4-corner arthrodesis. ***J Hand Surg Am.*** 2015;40(4):759-766.
18. Ali MH, Rizzo M, Shin AY, Moran SL. Long-term outcomes of proximal row carpectomy: a minimum of 15-year follow-up. ***Hand (N Y).*** 2012;7(1):72-78.
19. Lumsden BC, Stone A, Engber WD. Treatment of advanced-stage Kienbock's disease with proximal row carpectomy: an average 15-year follow-up. ***J Hand Surg Am.*** 2008;33(4):493-502.

SUPPLEMENTAL DATA

Supplementary Video 1. Scan the QR code to view the video.

EPILOGUE

I am pleased to write this epilogue to Dr. Abbas Peymani's thesis, Madelung Deformity. Because it is very uncommon, Madelung Deformity is difficult to study and our knowledge is seriously deficient in multiple areas. Not only has Abbas approached multiple facets of the problem, but he has also done so with remarkable success. His thesis advances our knowledge in several areas.

In the 20th century, manuscripts on Madelung deformity included only qualitative assessment of deformity severity and surgical results. In the early 21st century, quantitative measurements became possible but were based on 2-dimensional imaging. Abbas has single-handedly dragged the study of Madelung Deformity well into the 21st century by defining and demonstrating 3-dimensional measurements that build on the 2-dimensional past and pursuing 4-dimensional imaging that better defines the altered motion of the wrist. Applying his engineering prowess to the medical problem, he has defined new 3-dimensional measurements that supplement the older measurements, written software extensions to automate the measurements, thus eliminating any problems with reliability and reproducibility, and advanced measurement techniques by defining a statistical model of the deformity.

The use of social media to gain insight into the functional and social cost to the individuals with Madelung Deformity opens the door and turns on the light in a room previously dark and devoid of knowledge. He has led the way not only in using this technique to study Madelung Deformity but also to explore many other uncommon and rare diseases.

Abbas is a young man. Let us hope the hours of work to complete this thesis have not depleted his enthusiasm for his chosen topic. Our insight into Madelung Deformity can benefit from his intelligence, perceptiveness, perspicacity, diligence, and achievements for many decades to come.

H. Relton McCarroll, M.D.
Consultant
Shriners Hospital for Children Northern California

ACKNOWLEDGEMENTS

The original research in this dissertation would not have been possible without the fantastic support from all the patients participating in the various projects.

Prof. dr. C.M.A.M. van der Horst. Beste professor, bedankt voor de kans die ik heb gekregen om onderzoek te doen en om als semi-arts binnen uw team te kunnen functioneren. Er zijn weinig mensen die ik heb ontmoet met zoveel charisma en passie voor het vak en de patiënten.

Dr. S.D. Strackee. Beste Simon, het was een waar genoegen om onder jouw supervisie de projecten in dit proefschrift te bedenken en uit te voeren. Door onze samenwerking hebben de afgelopen jaren niet als werk aangevoeld, maar als een welkome en plezierige uitdaging. Bedankt voor het delen van je genialiteit, je humor, en je mentorschap.

Dr. ir. G.J. Streekstra. Beste Geert, jouw visie en ideeën voor de verschillende projecten hebben ons werk naar een hoger niveau getild; jouw rust en kalmte waarborgden de haalbaarheid.

Dr. J.G.G. Dobbe. Beste Iwan, dit proefschrift was niet mogelijk geweest zonder jouw expertise en support. Jouw deur stond altijd open en onze "vijf minuten" eindigden vaak in oneindige brainstormsessies over rotatiematrices, coördinatenstelsels, en het fitten van cirkels in 3D.

Dr. M. Foumani. Mahyar, er zijn zoveel mijlpalen die ik nooit had gehaald zonder jouw onvoorwaardelijke hulp: onderzoek in het AMC, mijn avontuur in Boston, en de klinische ervaring in Groningen. Jij hebt een sleutelrol gespeeld in mijn groei, en ik hoop ooit deze rol voor een ander te kunnen vervullen.

Aan de overige leden van mijn promotiecommissie, prof. dr. M. Maas, prof. dr. G.M.M.J. Kerkhoffs, dr. M.H.M. van Doesburg, prof. dr. F. Nollet, prof. dr. H.E.J. Veeger, en dr. J.W. Colaris, hartelijk dank dat u zitting heeft willen nemen in mijn promotiecommissie.

Dr. J. Upton. I remember you giving me your unlocked MacBook and telling me to use all the data I needed for my research. Observing your surgeries was one of the highlights during my research fellowship in Boston. Thank you for sharing both your knowledge and all your data on Madelung Deformity.

Dr. H.R. McCarroll. I was extremely excited when I received a response from you after my initial e-mail. Thank you for all your inspiring thoughts and feedback; I still remember us getting breakfast in Las Vegas, brainstorming about Madelung Deformity before the ASSH annual meeting started. I still can't believe you agreed to collaborate on several of the projects in this thesis.

Prof. dr. D. Vickers. Thank you; your handwritten letter inspired a young researcher to continue his quest to understand Madelung Deformity.

Prof. dr. M.A. Ikram. Arfan, it is at your department, and under your supervision, I learned the value of critical thinking in research. I will never forget working among some of the most brilliant minds in medical research.

Prof. dr. M. Frens. Maarten, bedankt voor je vertrouwen in mij toen ik net startte met de geneeskunde opleiding. Jouw mentorschap heeft mijn ervaring als student naar een hoger niveau getild door de participatie in de Erasmus MC Honours Class.

Dr. S.J. Lin. I genuinely appreciate the chance to work under your supervision at the Beth Israel Deaconess Medical Center; balancing the different projects helped my growth immensely.

Dr. B.T. Lee. Thank you for all your time, advice, and Facetime calls; your positive energy and wisdom have inspired me to work for the career I want.

V. van Vuure. Vera bedankt voor alle gezelligheid en hulp, jij hebt mijn ervaring aan het AMC als onderzoeksstudent, semi-arts, en uiteindelijk promovendus nog plezieriger gemaakt dan het al was.

M. Montes Klaver. Mario, bedankt voor de altijd goede sfeer, je humor, en oprechtheid.

G. Brahmer. Geoffrey, thank you for your friendship, wisdom, creativity, coffee sessions, authenticity, kindness, and road trips.

AMC collega's, Melanie, Marieke, Max, Anne, Pieter, Elisa, Hans Smit, Kenneth, Sybren, en Annelinde; bedankt voor een ziek mooie tijd op G4.

BIDMC research team, Masoud, Austin, Sabine, ARJ, Sebastian, Jose, Andres, Rodrigo, David, Anne, Winona, Parisa, Alex, Anmol, Faris, and Ahmed; thank you for an unforgettable experience in Boston.

Dr. W. Kelder, drs. E.A. Boonstra, dr. E. Bosma, dr. J.P. Deroose, drs. G.J. Glade, dr. B.P.J.A. Keller, dr. A.F.T. Olieman, dr. I.C.J.H. Post, dr. B.B. Pultrum, dr. ir. S.G.J. Rödel, drs. A.P.M. Stael, dr. C.G. Vos, drs. H.H. Zwaving; bedankt voor alle begeleiding en geduld tijdens mijn eerste klinische stappen als arts-assistent chirurgie.

Martini collega's, Allard, Arthur, Bas, Berber, Carine, Charlotte, Deborah, Edwin, Ewoud, Jael, Joost, Laura, Maartje, Marjolein, Merel, Mirjam, Nienke, Patrick, Paul, Rianne, Robert, Sofie, Tom; dank voor een geweldige en leerzame tijd in het hoge Noorden.

My parents, Nami, Nickoe, and Vedad; thank you for always staying positive and inspiring, and your continuous support.

PORTFOLIO

PhD student:	Abbas Peymani
PhD period:	2017-2021
PhD supervisor:	prof. dr. C.M.A.M. van der Horst

		ECTS
ORAL PRESENTATIONS		
2018	Biomechanics After Proximal Row Carpectomy. Robert M. Goldwyn Visiting Professor Research Symposium, Boston, MA, USA.	0.5
2018	Effect of Obesity and Its Associated Cost in Autologous Breast Reconstruction. Plastic Surgery Research Council, Birmingham, AL, USA.	0.5
2019	Carpal kinematics in Madelung Deformity. Nederlandse Vereniging voor Plastische Chirurgie Congres, Amsterdam, The Netherlands.	0.5
2020	Carpal kinematics in Madelung Deformity. American Association for Hand Surgery Annual Meeting, Fort Lauderdale, FL, USA.	0.5
2020	#MadelungDeformity: Insights into a Rare Congenital Difference Utilizing Social Media. Plastic Surgery The Meeting, San Francisco, CA, USA.	0.5
2020	3D Shape Modeling the Distal Radius: Applications in Madelung Deformity. Plastic Surgery The Meeting; San Francisco (Virtual), CA, USA.	0.5
POSTER PRESENTATIONS		
2017	Indocyanine Green Angiography in Immediate Breast Reconstruction. Massachusetts Chapter of the American College of Surgeons, Boston, MA, USA.	0.5
2017	The NSQIP 30-Day Challenge: Reliability of Outcomes in Breast Reconstruction. Massachusetts Chapter of the American College of Surgeons, Boston, MA, USA.	0.5
2017	Is There a Weekend Effect in Orbital Fracture Management? Massachusetts Chapter of the American College of Surgeons, Boston, MA, USA.	0.5
2018	A Comparison of Complication Rates after Autologous and Alloplastic Breast Reconstruction in Patients undergoing Therapeutic and Prophylactic Mastectomies. American Society for Reconstructive Microsurgery, Phoenix, AZ, USA.	0.5
2018	Hand Surgery Outcomes In Orthopedic And Plastic Surgery. Plastic Surgery Research Council, Birmingham, AL, USA.	0.5
2018	Biomechanics After Proximal Row Carpectomy. Federation of European Societies for Surgery of the Hand, Copenhagen, Denmark.	0.5
2018	Surgical Management of Madelung Deformity: A Systematic Review. Federation of European Societies for Surgery of the Hand, Copenhagen, Denmark.	0.5
2018	Hand Surgery Outcomes In Orthopedic And Plastic Surgery. Federation of European Societies for Surgery of the Hand, Copenhagen, Denmark.	0.5
2018	Disparities in Treatment of Traumatic Nerve Injuries of the Upper Extremity. Federation of European Societies for Surgery of the Hand, Copenhagen, Denmark.	0.5
2019	Quantitative Assessment of Madelung Deformity in 3D Space. American Society for Surgery of the Hand Annual Meeting, Las Vegas, NV, USA.	0.5
2019	Carpal kinematics in Madelung Deformity. American Society for Surgery of the Hand Annual Meeting, Las Vegas, NV, USA.	0.5
2020	Quantitative Assessment of Madelung Deformity in 3D Space. American Association for Hand Surgery Annual Meeting, Fort Lauderdale, FL, USA.	0.5

PhD Portfolio (continued)

		ECTS
2020	#MadelungDeformity: Insights into a Rare Congenital Difference Utilizing Social Media. American Society for Surgery of the Hand, San Antonio (Virtual), TX, USA.	0.5
2020	A 3D Statistical Shape Model of the Distal Radius in Madelung Deformity. American Society for Surgery of the Hand, San Antonio (Virtual), TX, USA.	0.5
CONFERENCES		
2017	Massachusetts Chapter of the American College of Surgeons, Boston, MA, USA	0.5
2018	American Society for Reconstructive Microsurgery, Phoenix, AZ, USA	1.0
2018	Federation of European Societies for Surgery of the Hand, Copenhagen, Denmark	1.0
2018	Plastic Surgery Research Council, Birmingham, AL, USA	1.0
2019	Nederlandse Vereniging voor Plastische Chirurgie, Amsterdam, The Netherlands	0.25
2019	American Society for Surgery of the Hand, Las Vegas, NV, USA	0.5
2020	American Association for Hand Surgery , Fort Lauderdale, FL, USA	1.0
2020	American Society for Peripheral Nerve, Fort Lauderdale, FL, USA	0.5
2020	American Society for Reconstructive Microsurgery, Fort Lauderdale, FL, USA	1.0
2020	American Society for Surgery of the Hand, San Antonio (Virtual), TX, USA	1.0
2020	Plastic Surgery The Meeting, San Francisco (Virtual), CA, USA	1.0
SUPERVISION		
2018-2019	Research student: Sybren van Rijn, Medicine	1
2019-2020	Research student: Annelinde Piek, Medicine	4
COURSES		
2019	Kortjakje Zondagsschool voor Plastische Chirurgie, Zeist, The Netherlands	0.25
2019	Probabilistic Morphable Models, University of Basel, Basel, Switzerland	2
OTHER		
2017-2020	Weekly Department Research Meeting	4

LIST OF PUBLICATIONS

Peymani A, Adams HH, Cremers LG, Krestin G, Hofman A, van Duijn CM, Uitterlinden AG, van der Lugt A, Vernooij MW, Ikram MA. ***Genetic Determinants of Unruptured Intracranial Aneurysms in the General Population.*** Stroke. 2015 Oct;46(10):2961-4. doi: 10.1161/STROKEAHA.115.010414. Epub 2015 Aug 18.

Bos D, Poels MM, Adams HH, Akoudad S, Cremers LG, Zonneveld HI, Hoogendam YY, Verhaaren BF, Verlinden VJ, Verbruggen JG, **Peymani A**, Hofman A, Krestin GP, Vincent AJ, Feelders RA, Koudstaal PJ, Van Der Lugt A, Ikram MA, Vernooij MW. ***Prevalence, Clinical Management, and Natural Course of Incidental Findings on Brain MR Images: The Population-based Rotterdam Scan Study.*** Radiology. 2016 Nov;281(2):507-515. doi: 10.1148/radiol.2016160218. Epub 2016 Jun 23.

Peymani A, Foumani M, Dobbe JGG, Strackee SD, Streekstra GJ. ***Four-dimensional rotational radiographic scanning of the wrist in patients after proximal row carpectomy.*** J Hand Surg Eur Vol. 2017 Oct;42(8):846-851. doi: 10.1177/1753193417718427. Epub 2017 Jul 6.

Chi D, Curiel D, Bucknor A, **Peymani A**, Chattha AS, Bletsis PP, Kamali P, Lin SJ. ***Institutional Collaboration in Plastic Surgery Research: A Solution to Resource Limitations.*** Plast Reconstr Surg Glob Open. 2018 Jun 6;6(6):e1822. doi: 10.1097/GOX.0000000000001822. eCollection 2018 Jun.

Peymani A, Johnson AR, Dowlatshahi AS, Dobbe JGG, Lin SJ, Upton J, Streekstra GJ, Strackee SD. ***Surgical Management of Madelung Deformity: A Systematic Review.*** Hand (N Y). 2019 Nov;14(6):725-734. doi: 10.1177/1558944718793179. Epub 2018 Aug 13.

Peymani A, Malyar M, Johnson AR, Chen AD, Van Der Hulst RWJ, Lin SJ. ***The Impact of Resident Post Graduate Year Involvement in Body Contouring Procedures: A Comprehensive Analysis of 9,638 patients.*** Ann Plast Surg. 2019 Mar;82(3):310-315. doi: 10.1097/SAP.0000000000001714.

Cuccolo NG, Zwierstra MJ, Ibrahim AM, **Peymani A**, Afshar S, Lin SJ. ***Reconstruction of Congenital Microtia and Anotia: Analysis of Practitioner Epidemiology and Postoperative Outcomes.*** Plast Reconstr Surg Glob Open. 2019 Jun 19;7(6):e2318. doi: 10.1097/GOX.0000000000002318. eCollection 2019 Jun.

Sparenberg S, Blankensteijn LL, Ibrahim AM, **Peymani A**, Lin SJ. ***Risk factors associated with the development of sepsis after reconstructive flap surgery.*** J Plast Surg Hand Surg. 2019 Dec;53(6):328-334. doi: 10.1080/2000656X.2019.1626738. Epub 2019 Jun 17.

Peymani A, Dobbe JGG, Streekstra GJ, McCarroll HR, Strackee SD. ***Quantitative Three-Dimensional Assessment of Madelung Deformity.*** J Hand Surg Eur. 2019 Dec;44(10):1041-1048. doi: 10.1177/1753193419876203. Epub 2019 Sep 24.

Bucknor A, **Peymani A**, Kamali P, Epstein S, Chen AD, Bletsis PP, Chattha AS, Mathijssen I, Rakhorst H, Lin SJ. ***International and Geographic Trends in Gender Authorship within Plastic Surgery.*** 2018. Plast Reconstr Surg. 2019 Oct;144(4):1010-1016. doi: 10.1097/PRS.0000000000006076.

Egeler SA, Huang A, Johnson AR, Ibrahim AM, Bucknor A, **Peymani A**, Mureau MAM, Lin SJ. ***Regional Incidence of and Reconstructive Management Patterns in Melanoma and Non-melanoma Skin Cancer of the Head and Neck: a 3 Year Analysis in the Inpatient Setting.*** J Plast Reconstr Aesthet Surg. 2020 Mar;73(3):507-515. doi: 10.1016/j.bjps.2019.10.017. Epub 2019 Nov 9.

De Roo MGA, Dobbe JGG, **Peymani A**, van der Made AD, Strackee SD, Streekstra GJ. ***Accuracy of Manual and Automatic Placement of an Anatomical Coordinate System for the Full or Partial Radius in 3D Space.*** Sci Rep. 2020 May 15;10(1):8114. doi: 10.1038/s41598-020-65060-7.

Dobbe JGG, **Peymani A**, Roos HAL, Beerens M, Streekstra GJ, Strackee SD. ***Patient-specific plate for navigation and fixation of the distal radius: a case series. Int J Comput Assist Radiol Surg. 2021 Feb 11. doi: 10.1007/s11548-021-02320-5.***

ABOUT THE AUTHOR

Abbas Peymani was born on April 2nd, 1987 in Gouda, the Netherlands, the city world famous for its cheese. After finishing his computer science degree at Leiden Institute of Advanced Computer Science, Leiden University in 2009, he worked as a software developer in Amsterdam, before deciding to switch careers to medicine. He was rejected from medical school three years in a row and was rejected again in 2010 after participating in a local selection procedure. In 2017 he double graduated as a medical doctor and epidemiologist from Erasmus University, University of Rotterdam. He was awarded the AMC PhD Scholarship to conduct research on congenital hand anomalies at the Academic Medical Center, University of Amsterdam, under the supervision of prof. dr. Chantal M.A.M. van der Horst. Soon after starting his PhD, he was accepted for a 1-year research fellowship at the Beth Israel Deaconess Medical Center, Harvard Medical School in Boston, under the supervision of dr. Samuel J. Lin. This collaboration allowed him to present his research both nationally and internationally, for which he was awarded the 2020 American Association of Hand Surgery Resident Award. In November 2020 he started working as a general surgery resident at the Martini Hospital in Groningen under the supervision of dr. Wendy Kelder.